Craig Donald Nicolson
BEng (Hons)

April 2004

‘Development of a Ducted Wind Turbine’

Faculty of Engineering
Energy Systems Division
University of Strathclyde
Glasgow

Thesis in partial fulfilment of the degree of Master of Science in:
Energy Systems and the Environment.

By

Craig Donald Nicolson
BEng (Hons)

Faculty of Engineering
Energy Systems Division
University of Strathclyde
Glasgow

2004

Acknowledgements

Throughout the duration of this project many people were available to lend a helping hand that in turn helped to make the project run smoothly. I would like to take this opportunity to acknowledge the help received from these various people.

I would like to thank Dr Andrew Grant who was always available to provide information and direction. Also Mr Cameron Johnstone who helped whenever he could. I would also like to thank all the staff in ESRU and SEEF who provided invaluable information at various stages of the project.

Thank you to Eric Duncan and all the staff in laboratory M2 who provided assistance in the construction of various test rigs.

Thanks also goes out to all the staff at W K McMillan Steel Fabricators especially Mr William McMillan who provided me with the platform to carry out this project.

This project was carried out over the duration of a TCS (Teaching Company Scheme) and therefore thanks goes to the TCD for providing funding for the project.

“Engineering is the science of economy, of conserving the energy, kinetic and potential, provided and stored up by nature for the use of man. It is the business of engineering to utilize this energy to the best advantage, so that there may be the least possible waste.”

William A. Smith, 1908

Abstract

The energy demands of today are vast and require generation of large quantities of electrical power. This demand has typically been met with use of fossil fuels but the World and UK government have set aspirations and targets to reduce emissions from power generation and increase the role of renewable energy technologies. Renewables have typically been utilised on large scale developments to address this situation but this raises problems. The intermittent nature of renewables on the grid, the remote locations far from points of utilisation and public opposition to developments of wind farms especially.

This thesis investigates the development of a novel ducted wind turbine that could be introduced into an urban environment and address the problems associated with the large scale devices by being integrated into the building fabric and generating on-site. The requirement to produce the most efficient device possible is essential so work has been carried out to characterise various generators available that will enable pairing with a rotor exhibiting similar characteristics to ensure optimal performance from the device.

Contents

List of Figures

List of Symbols

a	acceleration	[]
A	Area	[m^2]
B	Magnetic Flux Density	[T]
c	constant	[]
C	Performance Coefficient	[]
d	distance	[m]
e	induced voltage	[V]
E	Back EMF	[V]
f	frequency	[Hz]
F	Force	[N]
I	Current	[A]
K	Constant	[]
L	Length	[m]
m	Mass	[kg]
$\dot{m}$	mass flowrate	[kg/s]
n	Number of Poles	[]
N	Number of turns in winding	[]
p	Power	[W]
P	Pressure	[N/m^2]
q	Volumetric flowrate	[m^3/s]
r	Radius	[m]
R	Resistance	[Ω]
t	Period	[s]
T	Torque	[Nm]
v	velocity	[m/s]
V	Voltage	[V]
w	Windspeed	[knots]
Y	Annual Energy Yield	[kWh]
Z	Number of parallel paths in winding	[]
α	angle of attack	[^{o}]
δ	Differential pressure coefficient	[]
ϕ	Magnetic Flux	[Wb]
γ	Axial reduction factor	[]
η	efficiency	[]
λ	Tip Speed Ratio	[]
θ	Angle of Wind	[^{o}]
ρ	density	[kg/m^3]
ω	angular velocity	[rad/s]

Subscripts

A	Armature	LZ	Lorentz
C	Single loop	O	No Load
D	Drag	P	Power
E	External	t	terminals
F	Field	T	Terminal
L	Lift	V	Velocity

1.0 Introduction

Throughout the ages the demand for energy has risen from primitive man requiring very little daily energy consumption to today, where the need for energy is vast. As this need for energy production increased the demand was met through the use of relevant technologies. These technologies tended to utilise known fossil fuels like coal, oil and natural gas. It is commonly known that these fossil fuels are producers of greenhouse gases and pollute the atmosphere by contributing to the greenhouse effect. The greenhouse effect is causing global warming and this has been particularly evident since the industrial revolution. During the past 100 years there has been an increase of approximately 0.5^{o}C of the average air temperature. Since 1860 the four warmest years have been in the 1990's. Since the 1800's a rise in sea level of approximately 10-25cm has been observed, there has been shrinkage of mountain glaciers and a reduction in Northern Hemisphere snow cover. The world is warmer now than at any time in the last 600 years and recent warming stands out against a record of stable temperatures over the past 10,000 years.

Therefore the generation of energy from fossil fuels that create greenhouse gases is not environmentally friendly but the production of energy is still heavily dependant upon these sources. It is also known that the reserves of these fossil fuels are diminishing and therefore alternative means of energy production are required.

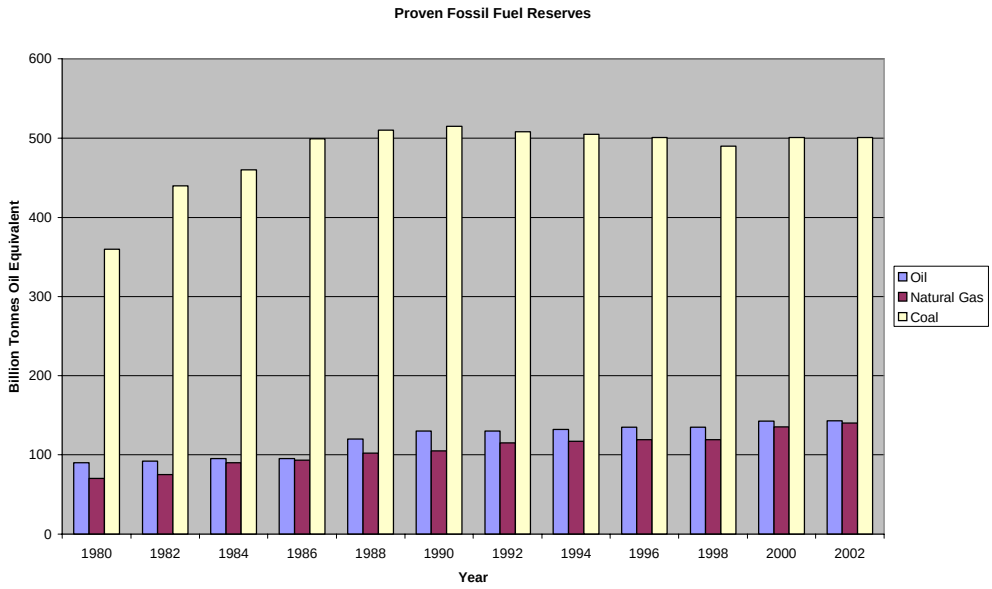

FIGURE 1
FOSSIL FUEL RESERVES

Figure 1 shows the proven fossil fuel reserves from 1980 till 2002. These figures were sourced from the 'BP Statistical Review of World Energy.'

One alternative approach to the use of fossil fuel is the production of nuclear energy using fission from uranium. Nuclear power generation is a very environmentally friendly source of generation when considering greenhouse gas pollution, with nuclear producing either none or very little of SO_2, NO_2 or CO_2. The main area of concern regarding nuclear generation is the environmental impact that it has. There is a lot of public concern over nuclear power stations due to radiation and nuclear waste. The past shows that accidents can and will happen with incidents at Windscale (now Sellafield), Three Mile Island and the major disaster at Chernobyl in 1986. The other major issue regarding nuclear power is nuclear waste. There is still no effective way of disposing radioactive waste other than storing it in metal casks. From this, the public perception of nuclear power generation is very low and it appears that it will never be widely accepted as an appropriate means of energy generation.

The only feasible approach is the use of renewable energy technologies that will produce no harmful emissions when generating. Renewable energy technologies consist of wind energy conversion, wave energy, tidal stream energy, Ocean Thermal Energy Conversion (OTEC), solar energy (photovoltaics for electrical generation) and biomass.

The worlds leaders have recognised this energy generation problem and have begun to address it with developments like the Kyoto agreement of 1997 and more local policies like the Renewables Obligation and the Renewables Obligation Scotland. The Kyoto agreement of 1997 was a global step towards the reduction of emissions of greenhouse gases. Each country that signed up to the agreement has to fulfil its individual commitment to help achieve the global target of a 5.2% reduction in greenhouse gases by 2012 compared to 1990 levels, The EU has the overall target of reducing greenhouse gas emissions by 10% in 2010 and the UK has signed commitments to reduce its greenhouse gas pollution by 12.5% from the level in 1990 by the year 2012. The UK as a whole has set at target of 10% of all energy to be supplied form renewable sources. This target is realistic but requires more than just

development of renewables. The current setup of the national grid is for one-way flow of energy. Centralised power stations transmit the energy through the transmission network, down through the distribution network to consumers. The introduction of renewables will see energy generation in remote locations to maximise favourable conditions for generating. These remote locations tend to be far away from where the generated energy is required in urbanised and industrial areas. This requires energy flows in the opposite direction from which the grid was intended to work and gives rise to energy losses in transmission over great distances. Upgrading of the grid is therefore essential. The government has highlighted this problem and stated that there is a need for local or embedded (distributed) generation where energy is generated on-site and used as required and any excess generation may be sold back to the grid. The government also states that innovation is fundamental to the future of energy generation, as we require new and sustainable ways of satisfying energy needs.

The aim of this report is to investigate and progress the design and production of a novel building integrated Ducted Wind Turbine module (DWT) towards a commercial product. The DWT utilises wind flow patterns in highly urbanised areas to produce power on-site for building services and hence negates any transmission and distribution losses.

2.0 History of Wind Power

The human race has been harnessing the energy of the wind as far back as 5000 BC, where the earliest known use was in Egypt where the wind propelled boats along the River Nile. The utilisation of wind has been the primary form of power for transportation of vehicles across water until recent times. The Vikings were using the wind to power their fleet of longboats when exploring and conquering the Northern Atlantic around 1000 AD.

China is often regarded as the 'birth' place of the windmill with simple windmills in use around 200 BC. These first windmills were used and designed to automate relatively simple tasks like gain grinding and water pumping. The earliest documentation of a Chinese windmill was in 1219 AD by Yehlu Chhu-Tshai. In 1100 AD windmills were used extensively in the Middle East for food production and merchants and crusaders returning to the western world carried this technology back to Europe. Around 1400 AD the Dutch refined the windmill and used it extensively to drain flooded fields and marshland in the river Rhine area. Settlers who utilised the power for similar applications such as water pumping transferred this technology to the 'new world' around 1850.

The first use of a large windmill for electricity generation was in Cleveland, Ohio in 1888 by a Charles F. Brush. The 'Brush' machine had a multi-bladed rotor with a diameter of 17 metres and a large hinged tail to rotate the rotor out of the wind. This was the first use of a step-up gearbox in a windmill used to rotate the generator at the required rotational speed. This machine had a successful operating period of 20 years but demonstrated the limitations of low speed, high solidity rotors for electricity generation.

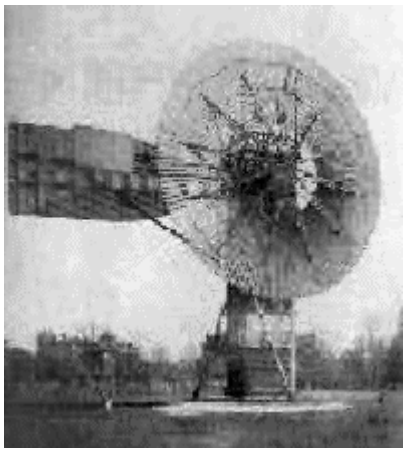

FIGURE 2 [1]
BRUSH WINDMILL

The pioneer of modern day wind turbines was the Danish meteorologist Poul La Cour (1846–1908). La Cour was one of the pioneers of modern aerodynamics and used these principles in the design of his wind turbines; low solidity and four bladed rotors incorporating primitive aerofoil shapes. The first of these new design wind turbines was built in 1891. The technology spread and was widely utilised throughout Denmark, with 120 utilities incorporating a wind turbine in their system by 1918.

A Frenchman G. J. M. Darrieus designed a windmill in the shape of an eggbeater in the 1930s. This was utilising a vertical axis for the shaft rather than a conventional horizontal shaft. This device was not widely adopted and the La Coeur design became established throughout the world.

Industrialisation in Europe, then later in America led to a gradual decline in wind generation. The steam engine and use of cheap fossil fuels led to this decline. There was however some interest in the development of larger devices and in the 1940s the largest wind turbine of the time was located on a hilltop in Vermont. The turbine was rated at 1.25 MW for a wind speed of 30mph (13.4m/s) and was used to power the local utility during World War II.

The end of World War II saw the prices of fossil fuel drop and also the interest in wind turbines. It was not until this OPEC oil embargo of 1973 that the interest resurfaced. The rising energy prices and the questionable availability of fossil fuels led to the realisation that alternative means of power generation were required.

The development and the refinement of the wind turbine continued but it was not until the development of machines rated at 55kW in 1980 that the market for wind turbines took off. The great Californian wind rush of the early eighties saw thousands of these devices installed and because the Danish had a track record in wind turbine construction about half of the Californian wind turbines are from Danish origin.

FIGURE 3 [2]
CALIFORNIAN WIND FARM

The development since has brought very little radical changes to the designs but the ratings of the turbines have been ever increasing with Enercon in Germany producing 4.5MW devices.

3.0 The Wind Resource

Effectively all renewable forms of energy (with the exceptions of geothermal and tidal) are types of solar energy. It is the power that radiates from the sun that enables renewable energy technologies to exist. In a single hour the sun radiates approximately 175 billion kWh of energy and approximately 1 - 2 percent of this is converted into wind energy. This is an enormous resource to be utilised. But how does the sun create wind and what is wind?

The earth orbits the sun and receives light and heat from the sun daily. It is the heat that the earth receives that creates wind. Figure 4 shows that the surface of the earth has a temperature gradient. The majority of the heat from the sun is received at the equator and it gradually reduces towards both poles.

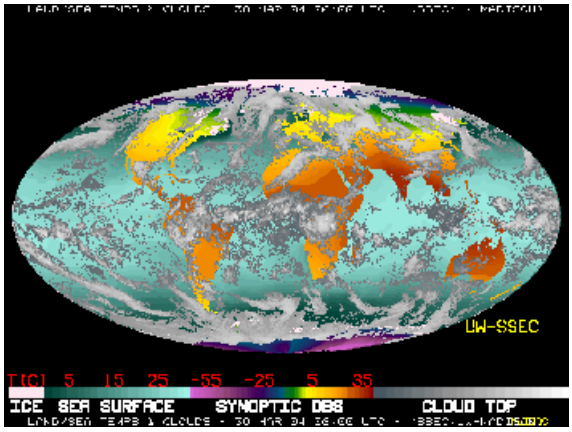

FIGURE 4 [3]
SATELLITE IMAGE SHOWING EARTH SURFACE TEMPERATURE VARIATIONS

This temperature gradient creates wind. In the warmer regions of the earth the air is hot and is therefore at a high pressure, conversely at the colder regions the air is at a low pressure. Wind is the movement of air from areas of high pressure to low pressure. Hot air is lighter than cold air and will rise until it reaches an altitude of approximately 10km, it will then spread to the North and South poles. However the wind flow is not as simple as that, if this was just the case the wind would always flow from the equator in the direction of either pole. The reason the wind does not just flow to either pole is due to the rotation of the earth. As the earth is spinning it creates a force known as the Coriolis force.

3.1 Coriolis Force

The Coriolis force was discovered in 1835 by a French mathematician: Gustave Gaspard Coriolis (1792-1843). It is a known visible phenomenon where the rotation of the earth causes any moving object in the northern hemisphere to be deflected to the right and any moving object in the southern hemisphere to be deflected to the left. Visual impacts of the Coriolis force can be seen on railroad tracks where the rail on one side wears faster than the other; depending upon which hemisphere. The Coriolis force does not create wind but affects its flow.

The winds primarily affected by these temperature gradients and Coriolis force occur on a large scale and are found at high altitudes above the earth. They are known as geostrophic winds. These geostrophic winds produce predominant wind directions for different regions of the earth.

Latitude	*90^o – 60^o N*	*60^o – 30^oN*	*30^o – 0^o N*	*0^o – 30^o S*	*30^o – 60^o S*	*60^o – 90^o S*
Direction	*NE*	*SW*	*NE*	*SE*	*NW*	*SE*

FIGURE 5
PREDOMINANT WIND DIRECTIONS

Figure 6 shows a generalised pattern of the global winds and indicates regions of predominantly high and low pressures.

These generalised patterns of wind directions represent the wind flows at high altitudes (geostrophic winds). The winds that affect us in every day life, although ultimately controlled by the geostrophic winds, are largely affected by the surface of the earth. As is commonly known, the earths surface is neither uniform nor smooth. The earth has large flat plains (desert regions), areas covered with plant life (rainforests), very uneven regions (mountain ranges) and very smooth regions (seas and oceans). All these different types of land can affect the wind near the surface of the earth to a large degree.

These areas of the earth all have different values of roughness, which can impede the flow of air. Obviously the lower the value of roughness the less the air is impeded.

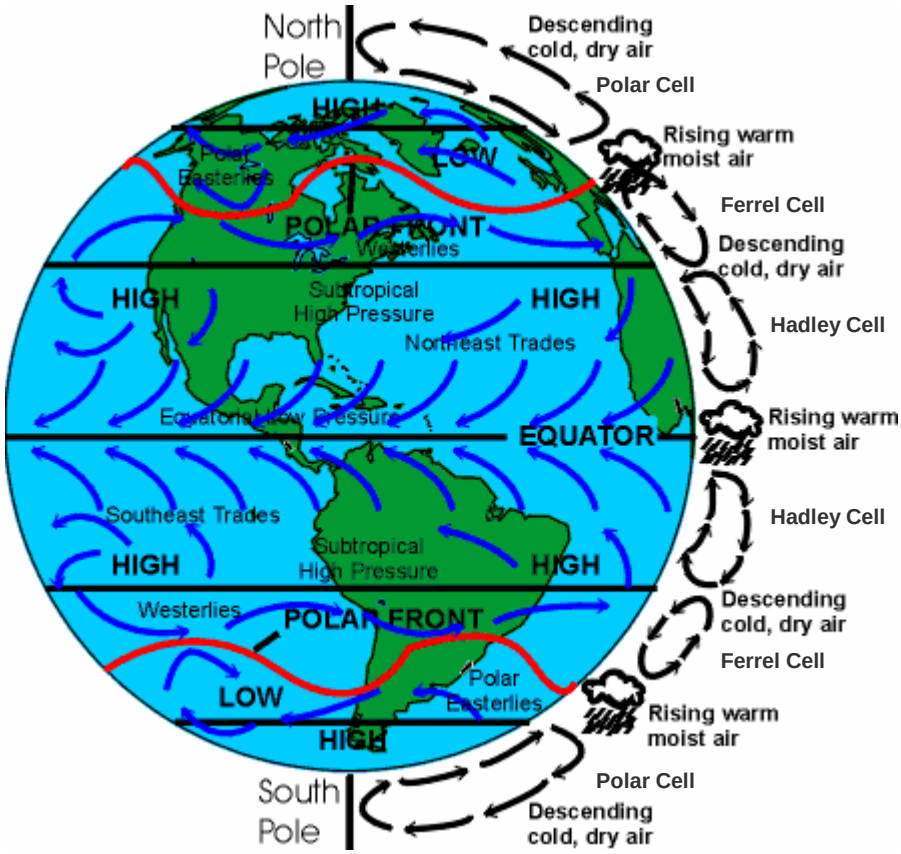

FIGURE 6 [4]
GLOBAL WIND PATTERNS

3.2 Roughness and Wind Shear

As mentioned previously the earth has varying roughness values depending upon where on the surface you look. These roughness values can be classified into various classes ranging in scale from 0 to 4. Figure 7 shows a table of the varying roughness classes.

Roughness Class	Description of Roughness
0	Water Surface
0.5	Open terrain with smooth surface – airport runways
1.0	Open agricultural area, no fences/hedges, smooth rounded hills.
1.5	Agricultural land with some buildings and fences/hedges of height 26ft(8m) separated by a distance of approximately 1.25km.
2.0	Agricultural land with some buildings and fences/hedges of height 26ft(8m) separated by a distance of approximately 0.5km.
2.5	Agricultural land containing many buildings with many plants or shrubs or fences/hedges of height 26ft(8m) separated by a distance of approximately 0.25km.
3.0	Villages and small towns, agricultural land containing many sheltering fences/hedges or forest areas and very rough and uneven terrain
3.5	Large cities with tall buildings.
4.0	Very large cities with many tall buildings and skyscrapers.

FIGURE 7
SURFACE ROUGHNESS CLASSES

Any free stream of air is affected by the roughness nearer the surface of the earth. This effect of the roughness creates a velocity profile of the wind flow over the surface. This effect is known as wind shear and is shown in figure 8.

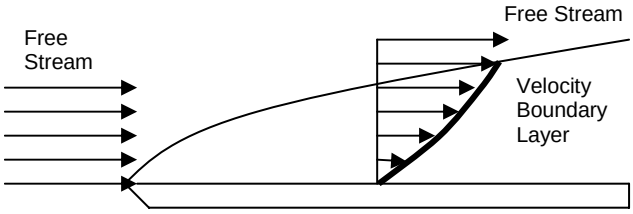

FIGURE 8
WIND SHEAR DIAGRAM

In figure 8 the arrows represent the velocity of the airflow, it shows that the velocity is slowest nearest the surface and increases as the altitude increases. Figure 8 also shows that a Velocity Boundary Layer exists and any airflow below this layer is affected by the surface and anything above is not affected by the surface. (The velocity of the air above the boundary layer is the same as that of the free stream of air.) The greater the value of surface roughness, the greater the wind shear and hence the thicker the velocity boundary layer, which effects the free flow of air. Wind shear is a very important factor in determining turbine location.

3.3 Wind Shade

If an object with a large roughness class impedes the flow of air it can also create what is known as wind shade. If such an object is impedes the flow of air it will slow the air and deflect its path. The object will in turn create turbulence in the airflow and the turbulence will vary depending upon the shape of the object.

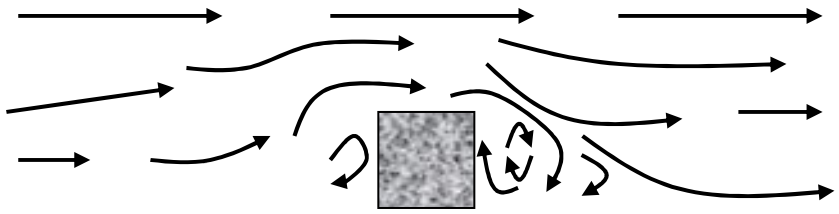

FIGURE 9
WIND SHADE DIAGRAM

Figure 9 shows the airflow is diverted up and over the object but there are regions of turbulence before and after the object .The region of turbulence after the object is much greater than the area before it. When the air flows over the object it travels at a high velocity whereas the area behind the object has been sheltered and has very slow moving air at low pressure. This causes some of the high pressure air to flow abruptly downwards and backwards to try to equalize the pressures. This can happen behind any obstacle and the turbulent region can stretch to large distances behind the object but obviously the severity of the effect decreases with distance. This region behind the object is known as the shade, as the object is effectively shading the land from the airflow.

The effects discussed in the previous sections can occur on global scales with roughness and shading occurring over large mountain ranges or open desert regions. The can also occur on more local scales with housing, and even fencing creating shade, but there are some more localised occurrences that can effect the flow of the wind.

3.4 Sea Breezes

Sea breezes are one of these local phenomena, which are caused by a temperature gradient created by the sun. Land is heated quicker than the sea / ocean, so during any day the land will become hotter than the sea. The hot air over the land rises and flows out to sea and leaves an area of low pressure behind. This then paves the way from the cooler air from the sea to move inshore and creates a sea breeze. Figure 10 illustrates the formation of a sea breeze.

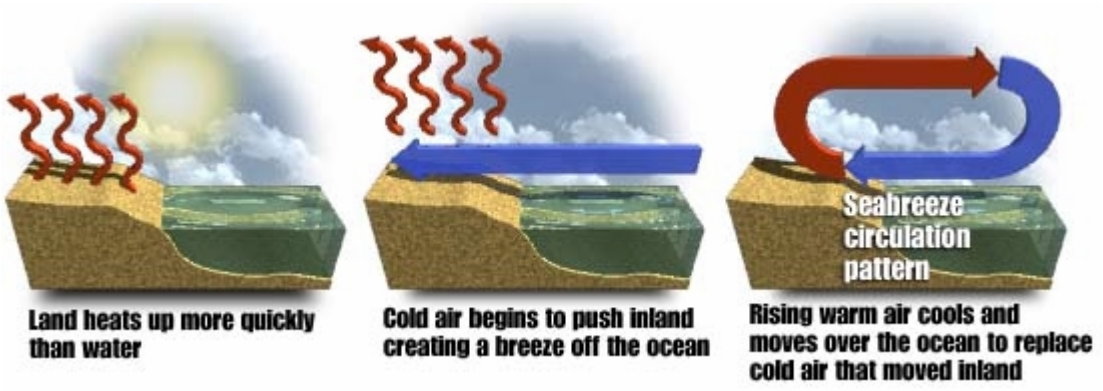

FIGURE 10 [5]
SEA BREEZE FORMATION

The opposite effect that creates the sea breeze happens at night and is known as a land breeze. As the sun goes down the sea / ocean has a larger thermal store than the land therefore, the land cools quicker than the water. As this happens the cooler air from the land begins to flow to the sea and there is the formation of a land breeze circulation pattern in which the direction opposes that shown in Figure 10.

3.5 Mountain and Valley Winds

Mountain and valley winds often occur when the sun radiates heat onto one face of the valley. (south-facing in northern hemisphere, north-facing in southern hemisphere) The warm air on the exposed face begins to rise and flow up the valley allowing cooler neighbouring air fill the void left. At night the slopes cool very quickly and the air begins to flow downwards.

3.6 Tunnel Effect

Utilising the laws of fluid mechanics, if a fluid of certain velocity is through a pipe of area A_1 and then that fluid is passed through a pipe of smaller area A_2 then the velocity of the fluid will increase. (Continuity Equation) Equation 1 identifies the theory.

$$\rho A_1 v_1 = \rho A_2 v_2$$

EQUATION 1

It is this law that shows the tunnel effect on the wind. If an air stream is flowing in the open countryside then suddenly approaches a hilly area, the wind is compressed and forced to travel between the hills (natural occurring tunnels) and therefore increases the velocity of the wind. This effect can be seen in urban environments also where the wind velocity is greater between two buildings than out in the open.

Wind in urban environments differs from wind in rural environments this is due to the texture and shape of the landscape. As mentioned previously in section 3.2 an urban environment exhibits a greater value of surface roughness than a rural environment, so has a greater amount of turbulence in the air stream. Buildings will also create wind shade as described in section 3.3, so urban wind differs vastly from rural wind. When wind approaches then hits a building or tall structure it basically has two options of where to go; it can either deflect to a side and try to go around the building or deflect upwards and try to go over the building. It is this upwards path that the ducted wind turbine utilises but this will be discussed in detail later.

4.0 Wind Measurement and Instrumentation

It is necessary to be able to measure and record the speed and direction of the wind to be able to predict and monitor performance of a wind turbine. Nowadays humans are provided with data from the met office regarding the weather and readings such as wind speed, wind direction, temperature and pressure are all widely available but just how are these values measured and how were they measured years ago?

4.1 The Beaufort Scale

The Beaufort Scale was devised in 1805 and revised in 1807 by Sir Francis Beaufort (1774 – 1857) as a system for estimating the strength of the wind without the aid of instruments. The scale was devised by Beaufort while serving upon HMS Woolwich and was used to describe wind effects on a fully rigged man-of-war sailing vessel; the scale was later extended to include descriptions of land effects also. The first official use of the scale was during the voyage of the Beagle (1831 – 1836) and the Beagle's commander, Robert Fitzroy, went on to become the first director of what is now known as the Met Office in 1854.

A representation of the Beaufort Scale with descriptions of both land and sea effects is shown in Figure 12.

FIGURE II [6]
SIR FRANCIS BEAUFORT

Beaufort Number	Description	Wind	Speed	Observations
		mph	Knots	
0	Calm	0	0	Tree leaves don't move; smoke rises vertically; sea is calm, mirror like.
1	Light Air	1-3	1-3	Tree leaves don't move; smoke drifts slowly; Direction of wind shown by smoke, not by vane; sea is lightly rippled.
2	Slight Breeze	4-7	4-6	Tree leaves rustle; flags wave slightly; Vanes show wind direction; small wavelets or scale waves.
3	Gentle Breeze	8-11	7-10	Leaves and twigs in constant motion; small flags extended; long un-breaking waves.
4	Moderate Breeze	13-18	11-16	Small branches move; flags flap; waves with whitecaps.
5	Fresh Breeze	19-24	17-27	Small trees sway; flags flap and ripple; moderate waves with many whitecaps.
6	Strong Breeze	25-31	22-27	Large branches sway; umbrellas used with difficulty; flags beat and pop; larger waves with regular whitecaps.
7	Moderate Gale	32-38	28-33	Sea heaps up, white foam streaks; whole trees sway; difficult to walk; large waves.
8	Fresh Gale	39-46	34-40	Twigs break off trees; moderately high sea with blowing foam.
9	Strong Gale	47-54	41-47	Branches break off trees; tiles blown from roofs; high crested waves.
10	Whole Gale	55-63	48-55	Some trees blown down; damage to buildings; high churning white seas and exceptionally high waves hiding ships from view.
11	Storm	64-74	56-63	Widespread damage to trees and buildings; mountainous waves. Sea covered in white foam.
12	Hurricane	75+	64+	Severe and extensive damage.

FIGURE 12
THE BEAUFORT SCALE

4.2 Modern Day Instruments

Nowadays there are many instruments used to measure various aspects of climate and these in turn are utilised in wind energy systems. In order to measure wind speed anemometers are utilised, wind vanes measure the wind direction, thermometers measure ambient air temperature and barometers measure the atmospheric pressure. It is the first two devices that will de described here.

4.2.1 Anemometers

Wind speed measurement is commonly done using a cup anemometer. The most common design utilised is to have 3 cups mounted on a vertical shaft. The wind

speed is recorded by measuring the rate of rotation of the shaft. There are a number of methods of measuring the rate of rotation and these are:

- Mechanical counter registering number of rotations
- A photoelectric switch
- Electrical voltage changes

The mechanical counter indicates the wind flow in distance, where the average wind speed is obtained by dividing the wind flow by time. The photoelectric anemometer contains a disc that has many slots and a photoelectric cell. The rotation of the cups causes the rotation of the disc and as the slots periodically pass the photoelectric cell, pulses are produced representing the wind speed. The last type and the type utilised in this project is the electrical voltage change type. Inside the body of the anemometer the vertical shaft is attached to the rotor of a small generator whose output gives an instantaneous measurement of wind speed.

The response and accuracy of a cup anemometer are determined by the physical properties that it exhibits. The weight, dimensions and internal friction are all key components in the design.

FIGURE 13 [7]
CUP ANEMOMETER

The anemometer utilised in this project is an A100L2 Anemometer produced by Vector Instruments. It is an electrical voltage change type with an output of 0-2.5V DC for a wind range of 0-150 knots. The data sheet for this can be found in the Appendix.

4.2.2 Wind Vanes

The direction of wind is normally measured using a wind vane. Conventional wind vanes consist of a large tail that keeps on the downwind side of a vertical shaft and a counterweight at the upwind side to maintain balance of the vane on the shaft. Early versions of wind vanes were commonly seen on the spires of churches and other buildings but were more commonly known as weathervanes. These vanes did not record the direction of the wind but merely gave a visual indication.

FIGURE 14 [8]
WEATHERVANE

Modern day devices are not as aesthetic in appearance but do provide a method of recording the direction of the wind. Most wind vanes nowadays utilise potentiometers inside the housing where the resistance of the potentiometer changes depending upon the wind direction. By measuring the resistance of this, or by measuring a voltage across the potentiometer the direction of the wind can be recorded.

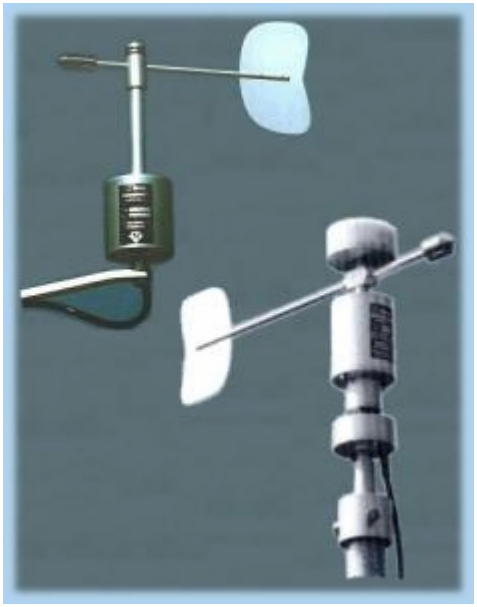

FIGURE 15 [7]
WIND VANES

It should be noted that wind direction is measured from the direction that it flows from and not the direction in which it is heading. For example a South Westerly wind is blowing from the South West and going in the direction of North East.

The wind vane utilised in this project is a W200P wind vane produced by Vector Instruments. It is potentiometer type with a 1kΩ resistance. The data sheet for this can be found the Appendix.

4.3 The UK Wind Resource

The United Kingdom has a vast wind resource; Scotland is recognised as having the best wind resource in Europe and therefore the best opportunity for developing and utilising wind power.

Figure 17 is a map produced by the British Wind Energy Association (BWEA), which indicates the annual average wind speed in the UK. The map provides the wind speeds in the standard S.I. units of metres per second (m/s) but in order to make a reference to speeds that may be more understandable, figure 16 shows the relationships between miles per hour (mph), knots and metres per second (m/s).

1m/s = 2.24mph = 1.94knots

1mph = 0.447m/s = 0.87knots

1knots = 0.514m/s = 1.15mph

FIGURE 16
VELOCITY RELATIONSHIPS

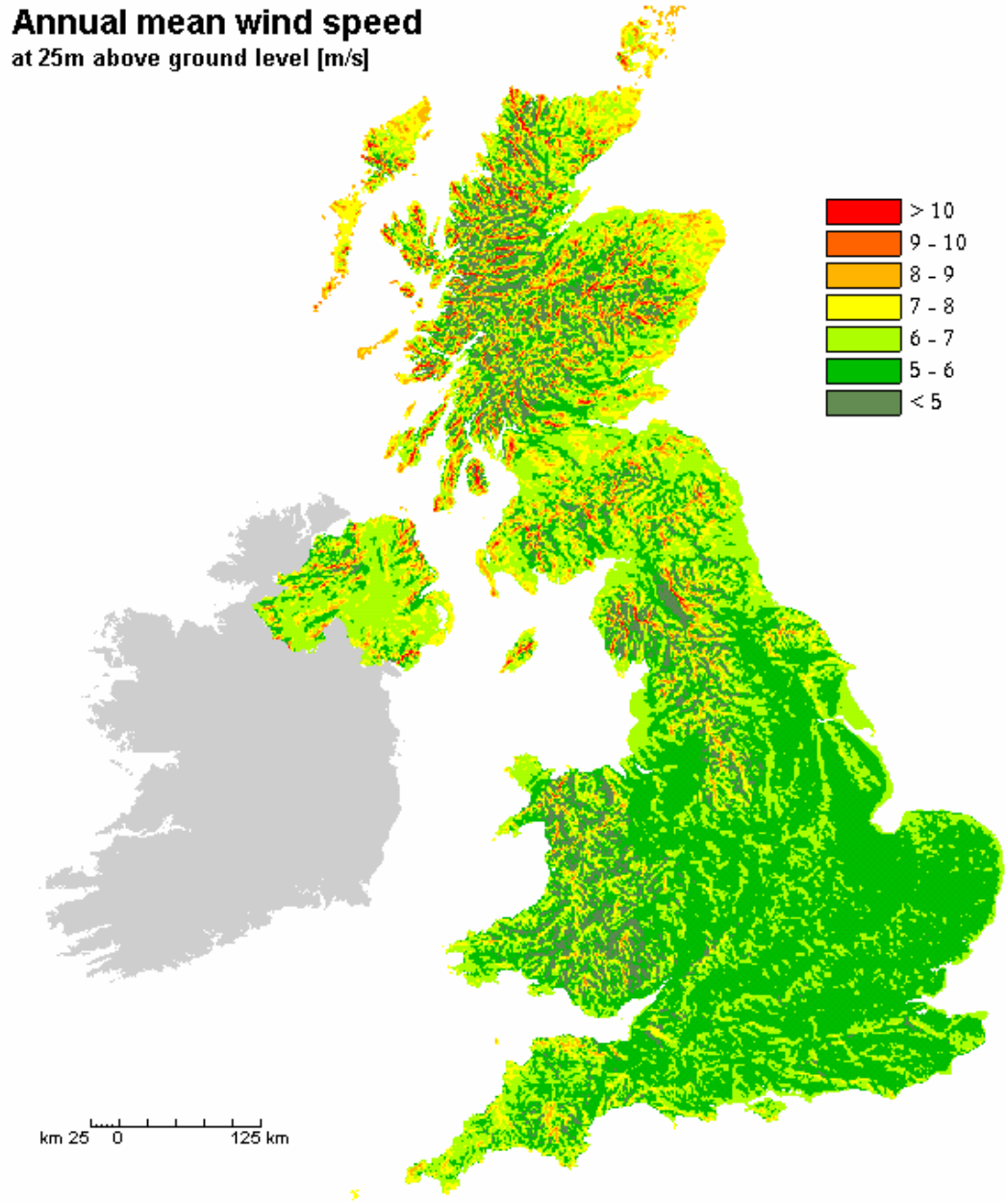

FIGURE 17 [9]
UK WIND RESOURCE

Figure 17 indicates that Scotland does indeed have the greatest wind resource in the UK.

5.0 Wind Turbine Design

The wind turbines in existence today fall into two main categories. The first is Horizontal Axis Wind Turbines (HAWT) and are so called because the rotating shaft of the turbine is on the horizontal axis. The other main category is Vertical Axis Wind Turbines (VAWT) and the rotating shaft is on the vertical axis.

5.1 Vertical Axis Wind Turbines

Vertical Axis Wind Turbines (VAWT) are not a common sight on the landscape of the world, as was explained earlier the Darrieus design was not widely adopted. VAWT are still the subject of research and development, and may become established in niche applications.

VAWT can be subdivided into two categories:

1. **Savonius** This type of turbine utilises drag forces to force rotation of the shaft.
2. **Darrieus** This type of turbine utilises lift forces to force rotation of the shaft.

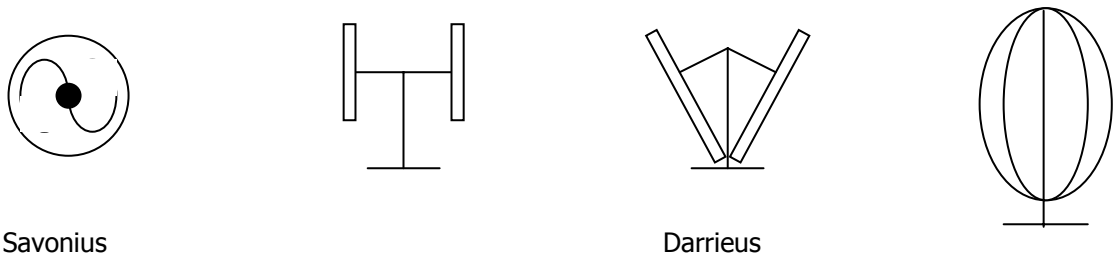

FIGURE 18
VERTICAL AXIS WIND TURBINE TYPES

The advantage of VAWT is that they do not have to be faced in any particular direction with respect to the wind.

5.2 Horizontal Axis Wind Turbines

Horizontal Axis Wind Turbines (HAWT) are common place throughout the world and are easily recognisable. Although the basic fundamental principle behind every design of a HAWT is the same there are many characteristics than can be changed.

5.2.1 Number of Blades

Examining different types of wind turbines and windmills throughout the ages it can be noticed that they do not all have the same number of blades. Older wind turbines and windmills have many blades on the rotor. These older machines used drag forces rather than lift forces to turn the rotor so the more blades that the drag force affected the better. Modern machines use aerofoil designs for the blades and hence utilise lift forces to turn the rotor, so don't require as many blades. Numerous blades could still be utilised but this raises the cost of the machines in blade manufacturing and structure reinforcing to cope with the additional weight. The most common used number of blades is three. The reason that three blades are used is because of stability. If a minimum of three blades is used the system can be modelled as a disc when dynamically balancing the machine. Using an equal number of blades can cause stability problems, when one blade is in the maximum power location the opposite blade is entering the wind shade in front of the tower.

In spite of this stability problem two bladed machines are manufactured as they have the cost saving of having one less blade. The machines need a higher wind speed than three bladed machines to produce the same power output. This property also adds to the problem of noise produced from a turbine. The problem with stability mentioned above can be helped by allowing the rotor to effectively rock back and forth which reduces any 'shock' to the system.

One bladed machines are also manufactured but are not widely used due to the enhancement of the problems associated with the two bladed machines. One bladed machines do however save on the cost of producing blades, but they do require the position of a counterweight on the opposite side of the hub.

5.2.2 Location of Blades

Another deciding factor is whether to put the blades upwind or downwind of the rotor. Most machines in use today are upwind machines. An upwind machine has the blades in front of the nacelle with respect to the wind flow. Upwind machines have the advantage of avoiding any wind shade created by the tower but do require a yawing mechanism to keep the blades perpendicular to the wind flow.

Downwind machines have the blades placed after the nacelle with respect to the wind flow. The advantage of this design is that the machine does not need a yawing mechanism present, as the machine will automatically yaw into the wind. The downside of a downwind machine is that the power output may fluctuate due to the wind shade created by the tower.

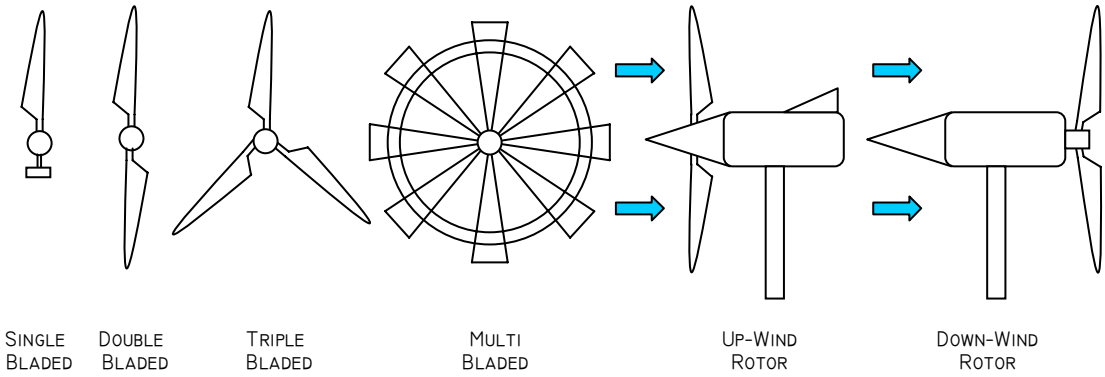

FIGURE 19
HORIZONTAL AXIS WIND TURBINE TYPES

Other than size and rating of the turbine, the design for turbines to be located on a wind farm is virtually the same, but when planning a wind farm the planners have to be aware of the effects that the turbines themselves will have on other turbines nearby.

5.2.3 Turbine Wake

A wind turbine works by extracting energy from the wind and converting it into a rotational movement then into electrical current. As energy cannot be created or destroyed (it can only change form) and some energy has been extracted from the wind, the wind after the turbine is now travelling at a slower speed and in a turbulent

fashion. This region of slower - turbulent airflow after the turbine is called the wake of the turbine.

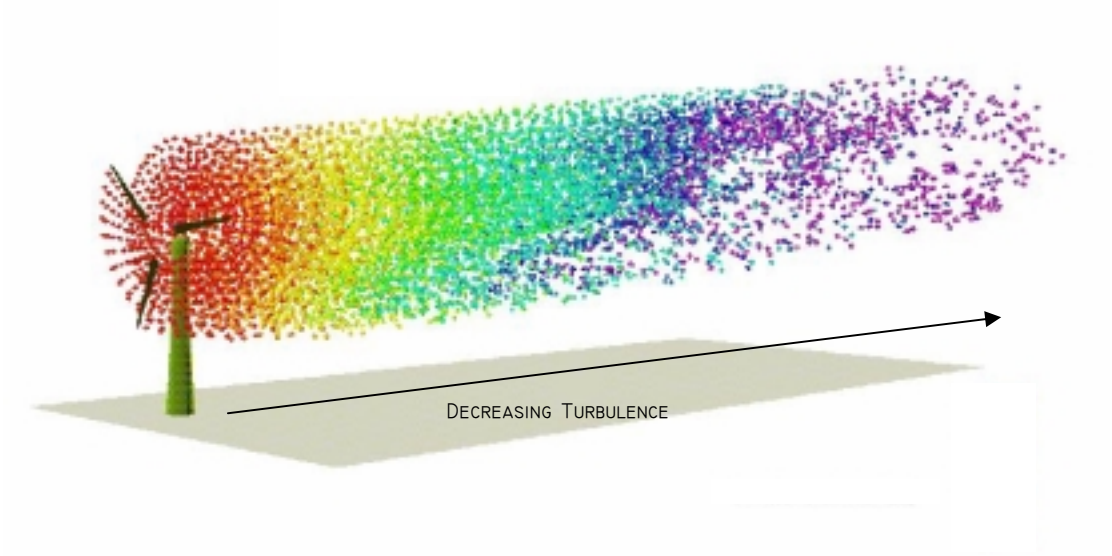

FIGURE 20 [10]
TURBINE WAKE

5.2.4 Park Effect

When planning a wind farm it would appear obvious to put as many turbines on the area of land as possible, to get the most power output due to more turbines operating. However as explained in the previous sections the airflow is affected by objects in the path of the wind. Using this theory it would seem obvious to put the turbines as far apart as possible to get the highest 'quality' of air passing through the turbine.

The standard theory for placing wind turbines in a wind farm is to place them 5-9 rotor diameters apart in the predominant direction of the wind flow and 3-5 rotor diameters apart in the direction perpendicular to the wind flow.

5.3 Environmental Effects

The various sub-sections in section 5.2 relate to properties and effects that have an impact on the performance of the operation of the wind turbine. The planning of a wind farm also has to consider the environmental impacts that the wind farm will cause.

5.3.1 Visual Impact

Wind turbines are physical machines that have to be situated somewhere to generate power. In most cases the location of wind farms are in rural or isolated areas. This leads to a visual impact on the landscape. The visual impact that is created can be a very subjective point of view, with people varying in opinion if they add to the landscape or 'destroy' the landscape.

5.3.2 Noise

Noise is a key concern to the public when the proposition of a wind farm to be located near then arises. Noise can come from various aspects of a wind turbine. Mechanical noise can come from the mechanical workings of the turbine. The gearbox, drive train and generator can all create noise that will be emitted from the overall turbine. The noise from these devices has been greatly reduced from previous years due to improved engineering practices. The gearboxes used in modern wind turbines are specifically designed for use in wind turbines to reduce the noise emission from them.

When wind 'hits' any surface a noise is created. Noise will be created when the wind hits items like trees or shrubs but the wind can also create vibration in some surface, which will then also emit their own noise. From this theory it can be seen that a wind turbine will generate some noise when the blades are rotating. This is generally not a problem anymore as most turbines are located in rural areas – away from people and careful design of the blades has reduced the noise emission from turbines.

5.3.3 Shadow

As turbines are generally large vertical structures they will cast a shadow when the sun is out. The shadow created by a wind turbine can be predicted before the actual turbine is built as data about the height of the turbine and where the sun rises and falls can be used to calculate the regions where a shadow is going to be cast.

5.3.4 Flicker

This is another effect from the shadow cast from a wind turbine. If the blades are rotating and the sun is shining a flicker effect may be induced. This flickering of light could be annoying but again careful planning can ensure that any flicker effect that occurs will not disturb any neighbours of the wind turbine.

5.3.5 Animals

Concern over the impact that wind turbines may have on animals, particularly birds, arise from wildlife groups and the public. The wind turbines will create no obstacle to having wildlife grazing on the same land as the turbine. Birds are a greater concern where they could be killed if they flew into the tower or rotating blades. Birds are killed every year due to collisions with overhead power lines, poles and even flying into windows. The impact of wind farms on birds is not as great as would be expected, but paths have to be considered before locating a wind farm.

5.3.6 Electro-Magnetic Interference

Early wind turbines caused problems and interference in the transmission of radio waves. The turbines were predominantly constructed using metal, with the metallic structure and rotation of the blades causing electro-magnetic interference. Nowadays there is little or no interference as the blades are now made from a non-metallic composite although the towers are still steel structures.

6.0 Wind Power Theory

Wind turbines and windmills work by extracting some of the energy from the wind. The wind causes rotation of a shaft, which drives a generator and produces electricity.

In order to understand the workings of a wind turbine the various components must be investigated.

6.1 Wind Turbine Components

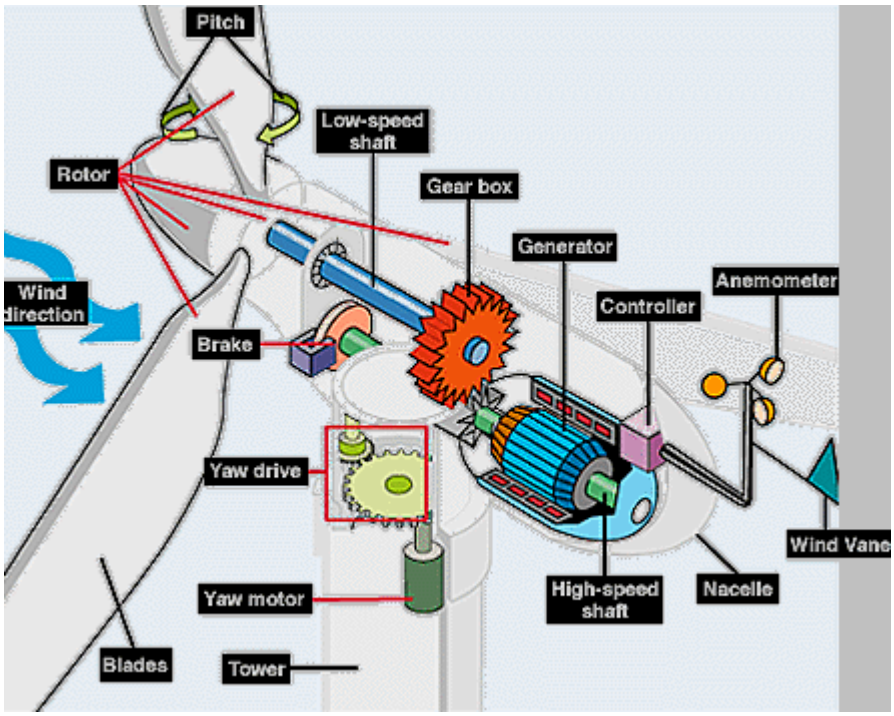

FIGURE 21 [11]
WIND TURBINE COMPONENTS

Blades - The rotor blades are the elements of the turbine that capture the wind energy and convert it into a rotational form. The pitch of the blades can often be altered to optimise wind capture.

Hub - The hub is the connection point for the rotor blades and the low speed shaft. (not identified in figure 21.)

Gearbox - The gearbox takes the rotational speed from the low speed shaft and transforms it into a faster rotation on the high-speed shaft.

Brake - The brake is a physical brake, similar to a disc brake on the wheel of a car, connected to the high-speed shaft. It is used in servicing the equipment to ensure that no components start to rotate, endangering the repair worker. In large turbines there is the requirement for 2 independent systems.

Generator - The generator is connected to the high-speed shaft and is the component of the system that converts the rotational energy of the shaft into an electrical output.

Anemometer & Wind Vane - The anemometer is used to measure the wind speed and the wind vane is used to note the wind direction.

Yaw drive - The yaw drive is used to ensure that the rotor blades are perpendicular to the flow of the wind.

Controller - The controller is a computer system that monitors and controls various aspects of the turbine – like the yaw mechanism. It has the ability to shut down the turbine if a fault occurs.

Tower - The tower is used to support the nacelle and rotor blades.

Nacelle - The nacelle is the unit located at the top of the tower that encapsulates the drive chain and generator.

All these components are found in typical wind turbines that are located in wind farms all over the world. In the following section, the way in which the rotor extracts energy from the wind is explained.

6.2 Lift and Drag forces

Any body in a moving stream will experience a force acting upon it. This force can be resolved into two components. The force acting in the direction of the flow in known as the 'drag' force and the force acting perpendicular to the flow is known as the 'lift' force.

The drag force can be sub-categorized into two further components pressure drag and friction drag. Pressure drag is where the force on the front of the body is large and tries to 'push' the body along with the flow. Friction drag occurs when the fluid passes along the sides of the body and fiction effects try to pull the body along with it. All bodies will experience a combination of these two drag forces but depending upon the shape of the body one will be more prominent than the other. A body designed to produce large quantities of lift is an aerofoil.

The total drag force F_D can be found from equation 2.

$$F_D = C_D \frac{1}{2} \rho v^2 A$$

EQUATION 2

where: C_D is the drag coefficient
ρ is the fluid density (kg/m^3)
v is the fluid velocity (m/s)
A is the frontal area of the body (m^2)

The value of C_D depends primarily on the shape of the body.

The total lift force on a body can also be found using equation 3.

$$F_L = C_L \frac{1}{2} \rho v^2 A$$

EQUATION 3

Where C_L is the lift coefficient and all other quantities are as above except for the frontal area (A). As an aerofoil is a complex shape it would be difficult to define and calculate the frontal area of it so it is convention to use the area normal to the fluid flow.

As is the case for C_D the value of C_L depends upon the shape of the body and the flow conditions. For aerofoils it is normal to plot graphs of C_L and C_D as a function of the angle of attack (α).

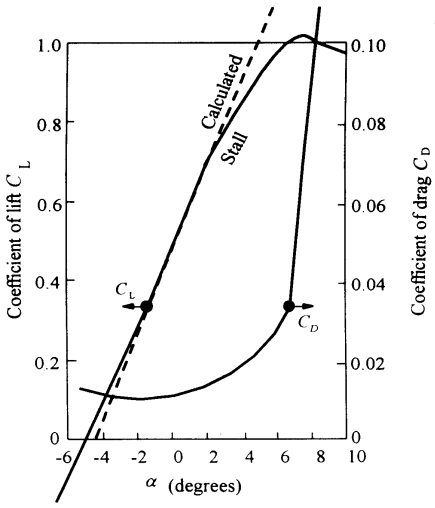

FIGURE 22 [12]
LIFT AND DRAG FORCES

The values of C_L and C_D can be calculated using equations with factors such as blade chord length and number of blades on rotor. These calculations can be carried out manually but it requires an iterative procedure so it is more common to use computer based packages for these calculations.

Figure 23 illustrates how an aerofoil develops lift: the wind approaches the aerofoil from the right and is split into two portions, one over the top and one under the bottom. The airflow over the top moves at high velocity and has low pressure whereas the airflow under the aerofoil is moving at a slower velocity and has a high pressure.

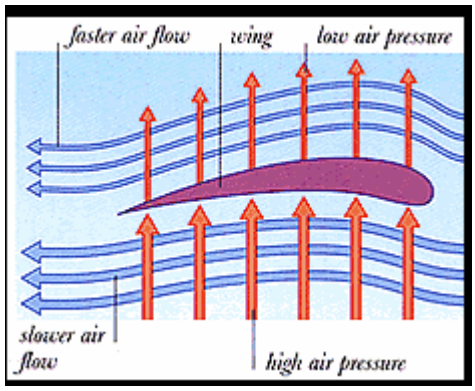

FIGURE 23 [13]
AEROFOIL THEORY

The aerofoil in figure 23 has created a pressure difference between the top and bottom of the wing. The low-pressure above the aerofoil therefore tries to suck the wing upwards with the high-pressure air beneath the aerofoil trying to push the wing upwards. This resulting action creates lift force.

The blades of a wind turbine are aerofoils. Since they are attached to the central hub of the machine, the blades spin round in response to lift forces.

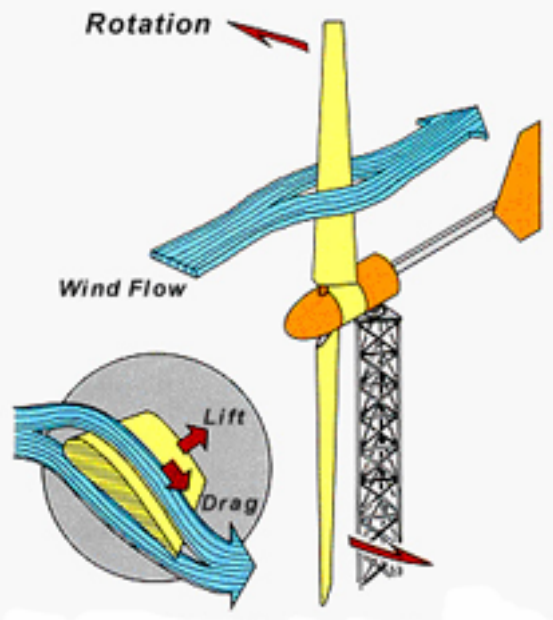

FIGURE 24 [14]
PRINCIPLES OF WIND TURBINE AERODYNAMIC LIFT

Figure 24 shows the principle of lift being used to create the rotation for a wind turbine. It also shows the drag force mentioned in Section 6.2. As the air flows over the aerofoil there is some friction between the flow of the air and the surface of the aerofoil. The air effectively tries to drag the aerofoil back with the flow of the wind. This is obviously an unwanted effect but it cannot be completely removed.

The blades of the turbine are pitched at a certain angle to obtain the maximum amount of lift from the wind. This is impossible to do for all wind speeds. In the design of turbines the manufacturer usually develops two strategies for this problem:

Strategy 1: Information about the siting of the turbine is extensively researched and the blades are pitched at a fixed angle to maximize efficiency at the average speed found on the site. This method obviously loses out on generation capacity at higher and lower wind speeds but will be at the optimal pitch for the largest portion of the year.

Strategy 2: This strategy uses variable pitch blades where the controller can vary the pitch of the blades as the wind changes to ensure the optimal lift from the wind. This method gives greater performance over the duration of the year but comes at an increased cost.

Wind is a very unpredictable commodity and can become very strong, causing vast amounts of damage to structures. Most wind turbines are designed to have a working range of ~ 4m/s to ~ 25m/s but recently, Scotland (January 2002) experienced wind speeds of up to 90mph (40.23m/s). This wind speed was almost double of the maximum working range of the turbine. If the turbine was allowed to utilize this wind it would at the very least damage itself and possibly tear itself apart. Some control aspects need to be introduced to shut down the turbine if the wind speed exceeds 25m/s.

By enabling control of the pitch of the turbine blades the controller can pitch the blades of the turbine into a stall position (no lift is generated) so that the machine will cease to turn in the extreme weather conditions and hence will not damage itself.

This section has shown how wind turbines extract energy from the wind to create a rotational movement to generate power. The quantity of power that is extracted from the wind can now be calculated.

6.3 Wind Turbine Calculations

6.3.1 Power in the Wind

To calculate the power available in the wind equation 4 is used.

$$p = \frac{1}{2}\rho A v^3$$

EQUATION 4

where: p is the power (W)
ρ is the air density (kg/m^3)
v is the air velocity (m/s)
A is the swept area of the rotor (m^2)

The value calculated from equation 4 is only the theoretical maximum power available and in practice the value extracted from a wind turbine will be significantly less.

A value known as the power coefficient (C_p) is the ratio of the actual power output compared to the theoretical available.

$$C_p = \frac{Actual\ Power}{Available\ Power}$$

EQUATION 5

Therefore equation 4 is amended to include the power coefficient to show the power available from a wind turbine.

$$p = C_p \frac{1}{2}\rho A v^3$$

EQUATION 6

An analysis from Betz states that the value of C_p is very unlikely to exceed the value of 0.593. (See section 6.3.3 on Betz Theory)

Equation 6 shows that the wind speed has an important effect on the power output from the turbine. The power in the wind is proportional to the cube of the wind speed. (If the wind speed doubles – the power output increases by **eight** times)

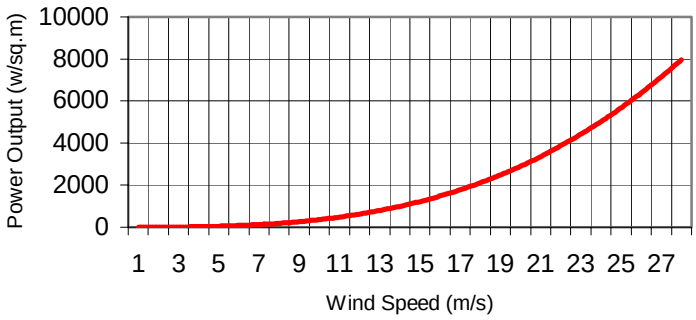

FIGURE 25
BETZ THEORY POWER OUTPUT

The chart shown in figure 25 represents the Betz Theory power output for a turbine using air density as 1.225 kg/m^3.

6.3.2 Tip Speed Ratio

The tip speed ratio of a turbine is defined as:

$$\lambda = \frac{\omega r}{v}$$

EQUATION 7

where: λ is the Tip Speed Ratio ( )
ω is the rotor angular velocity (rad/s)
w is the radius at the blade tip (m)
v is the air velocity (m/s)

The tip speed ratio (λ) and the coefficient of performance (C_p) are often plotted against each other to the relationship that exists between the two. Figure 26 shows the relationships between the two characteristics for various types and designs of wind turbine.

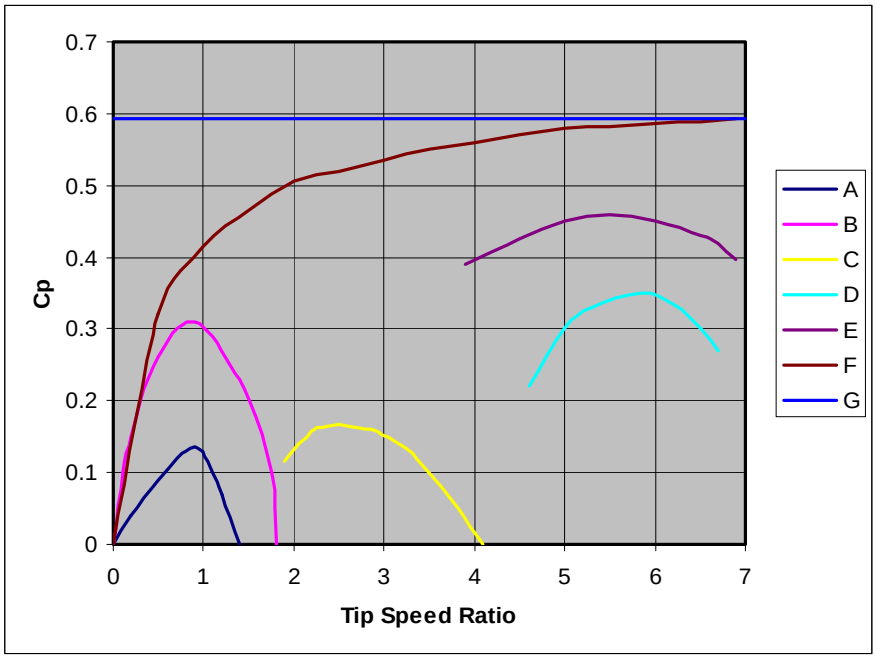

A: Savonius Rotor

B: American Multi Blade Rotor Type

C: Dutch 4 Arm Rotor Type

D: Darrieus rotor

E: High Speed 2 Blade HAWT

F: Ideal Propeller

G: Betz limit

FIGURE 26
TIP SPEED RATIO VS CP RELATIONSHIPS

6.3.3 Betz Theory

Figure 27 shows the rotor of a turbine and the characteristics of the airflow about this rotor.

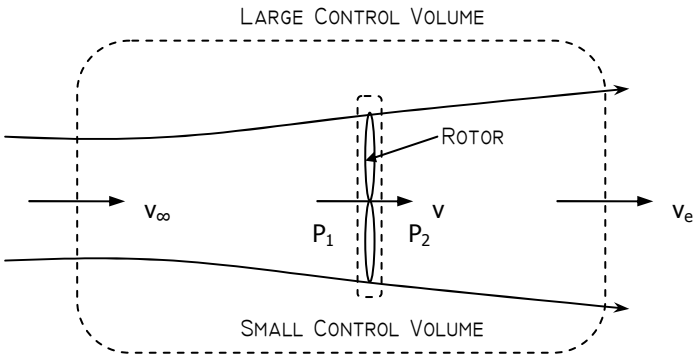

FIGURE 27
BETZ THEORY

It is assumed that the air is travelling at a velocity that is perpendicular to the rotor only. V_∞ is the velocity at the entrance to the large control volume, V is the velocity at the rotor and V_e is the velocity at the exit of the large control volume. Pressures P_1 (upstream of rotor) and P_2 (downstream of rotor) also feature in the calculations.

The energy equation for the large control volume is:

$$\frac{P_\infty}{\rho}+\frac{v_\infty^2}{2}=\frac{P_e}{\rho}+\frac{v_e^2}{2}+\frac{W}{kg}$$

EQUATION 8

where $P_\infty = P_e = P_{atmospheric}$

Therefore the work extracted at the rotor

$$\frac{W}{kg}=\frac{v_\infty^2-v_e^2}{2}$$

EQUATION 9

Across the rotor disc

$$\frac{P_1}{\rho}+\frac{v^2}{2}=\frac{P_2}{\rho}+\frac{v^2}{2}+\frac{W}{kg}$$

EQUATION 10

Therefore again

$$\frac{W}{kg}=\frac{P_1-P_2}{\rho}=\frac{v_\infty^2-v_e^2}{2}$$

EQUATION 11

The momentum equation for the large control volume is

$$\dot{m}[v_e-v_\infty]=F_E \text{ (external force)}$$

EQUATION 12

And for the small control volume the equation is

$$0=A[P_1-P_2]+F_E$$

EQUATION 13

This external force exerted on the control volume is a retarding force that reduces the momentum of the air flowing through the system. The rotor and its supporting structure exert this retarding force. Obviously the rotor has an equal and opposite force in the direction of the flow due to the wind.

It then follows that

$$\dot{m}[v_\infty-v_e]=A[P_1-P_2]$$
$$\rho AV[v_\infty-v_e]=A[P_1-P_2]$$

EQUATION 14

From equation 11

$$\rho A v[v_\infty - v_e] = \frac{1}{2}\rho A[v_\infty^2 - v_e^2]$$

$$\rho A v[v_\infty - v_e] = \frac{1}{2}\rho A(v_\infty + v_e)(v_\infty - v_e)$$

EQUATION 15

Which gives

$$V = \frac{v_\infty + v_e}{2}$$

EQUATION 16

The power extracted from the rotor is

$$p = \dot{m}\frac{v_\infty^2 - v_e^2}{2}$$

$$p = \rho A v \frac{v_\infty^2 - v_e^2}{2}$$

$$p = \frac{\rho A}{4}(v_\infty + v_e)(v_\infty^2 - v_e^2)$$

EQUATION 17

If a term called the axial reduction factor (γ) is introduced, it can be written

$$v = v_\infty(1 - \gamma)$$

EQUATION 18

Using this axial reduction factor the exit velocity can be written as

$$v_e = v_\infty(1 - 2\gamma)$$

EQUATION 19

Substituting v_e into equation 17 gives

$$p = \frac{\rho A v_\infty^3}{4}(2 - 2\gamma)(2 - 2\gamma)2\gamma$$

$$p = 2\rho A v_\infty^3[\gamma - 2\gamma^2 + \gamma^3]$$

EQUATION 20

For maximum power conditions

$$\frac{dp}{d\gamma} = 0$$

$$1 - 4\gamma + 3\gamma^2 = 0$$

EQUATION 21

Solving for γ

$$0 = (1-\gamma)(1-3\gamma)$$

therefore

$$\gamma = 1 \; or \; \frac{1}{3}$$

γ=1 is the minimum power condition.

Therefore for maximum power output $\gamma = \frac{1}{3}$

Substituting for γ in equation 20

$$\hat{p} = 2\rho A v_\infty^3 \left(1 - \frac{1}{3}\right)^2 \times \frac{1}{3}$$

$$\hat{p} = \frac{8}{27}\rho A v_\infty^3$$

EQUATION 22

The power coefficient has previously been defined in equation 5 and can be found by rearranging equation 6

$$C_p = \frac{p}{\frac{1}{2}\rho A v_\infty^3}$$

The maximum value that C_p can achieve can be found by substituting equation 22 for p.

$$\hat{C}_p = \frac{\hat{p}}{\frac{1}{2}\rho A v_\infty^3}$$

$$\hat{C}_p = \frac{16}{27}$$

$$\hat{C}_p = 0.593$$

This value of 0.593 is known as 'Betz Limit'. This is the value normally regarded as the absolute upper limit for performance of a wind turbine.

It is important to realize that this is not a measure of efficiency as the energy is not captured and dissipated but rather just not captured.

This theory is applicable to and can be used for all Horizontal Axis Wind Turbines (HAWT).

7.0 Ducted Wind Turbines

The theory and application of all aspects discussed until now relate to traditional wind turbines. The purpose of this project is to promote and develop the use of innovative new devices: Ducted Wind Turbines.

7.1 Progression of the DWT

The development of these devices dates back to an original idea by a Glaswegian engineer that was patented in 1979 (Webster). After the death of Webster, the family contacted the University of Strathclyde and development of the idea has continued ever since.

The Energy Systems Research Unit (ESRU) within the Mechanical Engineering Department has been responsible for the continued development, and has spawned various undergraduate and postgraduate projects. The pinnacle of the development stage so far has been the construction of prototype devices for a demonstration scheme on the Lighthouse Building in the centre of Glasgow. Devices exist on the roof of the James Weir Building of the University and are used to gather information for various student projects.

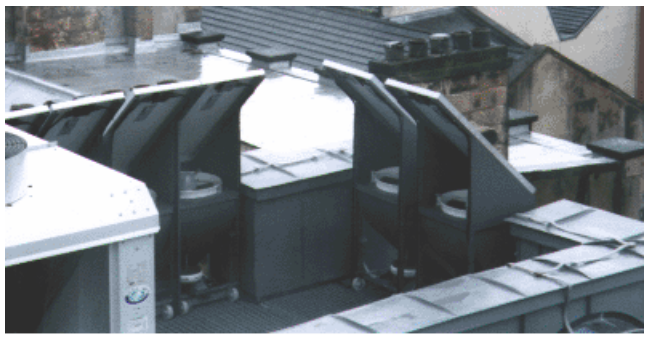

FIGURE 28 [15]
DWTS ON LIGHTHOUSE BUILDING ROOF

This theory of operation is that the device is located at the edge of the roof of a building and utilises the updraft of the airflow along a building façade. The air flows upwards; hugging the building wall then enters the front of the duct. The arrows in figures 29 and 30 show the flow over the building and through the turbine. (Note: only a portion of the wind will be deflected upwards and over the building as some

will be deflected downwards and around the sides of the building.) A spoiler is also utilised at the top of the device to enhance the flow due to pressure differential through the turbine. The spoiler is optimised for the pressure differential across the duct and an integrated PV panel can be mounted on the spoiler to enhance the generation from the device, but the PV will not be at its optimal operating inclination.

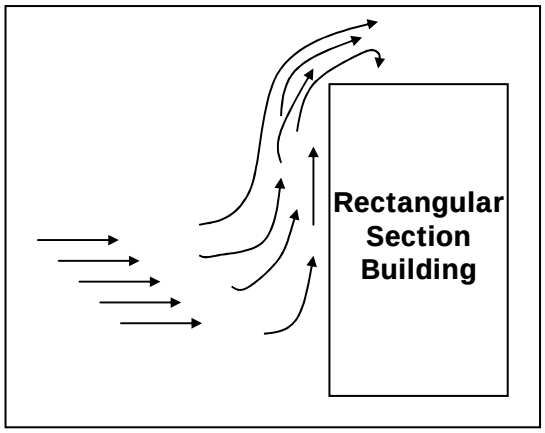

FIGURE 29
WIND FLOW OVER BUILDING

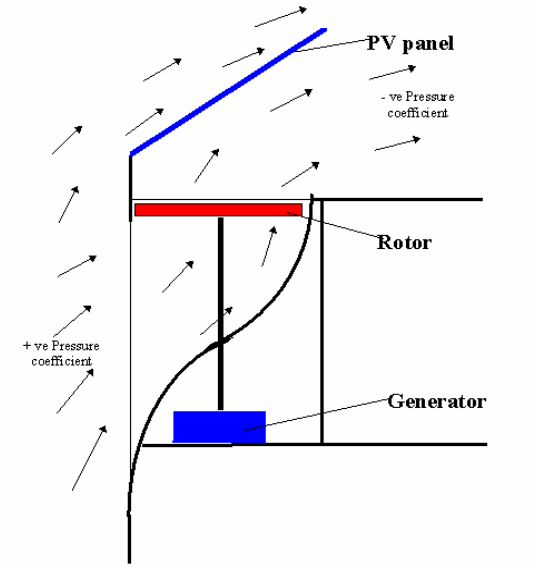

FIGURE 30 [15]
WIND FLOW THROUGH DWT

These DWTs are designed for urban environments but are suited to office buildings and high rise buildings rather than a small household. These devices are unlike most other common wind turbines in the fact that they are uni-directional. Most turbines will position themselves perpendicular to the flow of the wind. A Horizontal Axis Wind Turbine (HAWT) will yaw into position and a Vertical Axis Wind Turbine (VAWT) is always in the correct position.

The DWTs are fixed into position on one or more edge of a building façade, therefore are dependant upon the wind blowing in the correct direction. Previous testing performed in the university has indicated that the DWT will perform favourably to a wind direction variability of 120 degrees (60 degrees to each side of perpendicular) without significant power reduction.

Figure 30 shows that the shaft connected to the rotor is mounted in the vertical direction, which would indicate a VAWT but the theory behind these devices is similar to HAWT theory.

7.2 DWT Theory

To illustrate the potential for these DWTs, a simple mathematical model for one-dimensional flow can be established.

If a simple duct, with no turbine is considered (Figure 31).

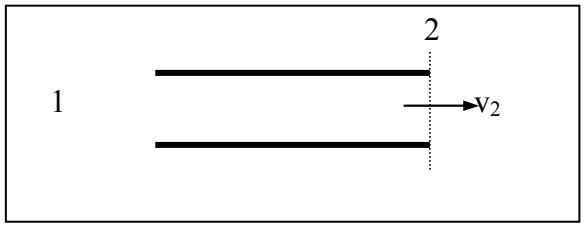

FIGURE 31
SIMPLE DUCT

$$\frac{P_1}{\rho}+\frac{0^2}{2}=\frac{P_2}{\rho}+\frac{v_2^2}{2}$$

EQUATION 23

Re-arranging:

$$v_2=\sqrt{\frac{2(P_1-P_2)}{\rho}}$$

EQUATION 24

This is only the ideal situation; a velocity coefficient (C_V) must be introduced.

$$v_2=C_v\sqrt{\frac{2(P_1-P_2)}{\rho}}$$

EQUATION 25

If a differential pressure coefficient (δ) is introduced. (difference in pressure coefficients between ends of duct)

$$(P_1-P_2)=\delta\frac{1}{2}\rho v_\infty^2$$

EQUATION 26

Then:

$$v_2 = C_v \sqrt{\delta}\ v_\infty$$

EQUATION 27

A turbine is now introduced into the duct that creates a pressure drop ΔP_T and changes the above theory.

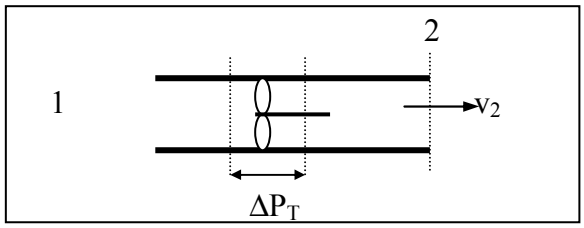

FIGURE 32
SIMPLE DUCT WITH TURBINE

$$\frac{P_1}{\rho} + \frac{0^2}{2} = \frac{P_2}{\rho} + \frac{v_2^2}{2} + \frac{\Delta P_T}{\rho}$$

EQUATION 28

Therefore:

$$v_2 = C_V \sqrt{\frac{2(P_1 - P_2 - \Delta P_T)}{\rho}} = C_V \sqrt{\delta v_\infty^2 - \frac{2\Delta P_T}{\rho}}$$

(allowing for losses in the duct)

EQUATION 29

Re-arranging equation 29:

$$\frac{\Delta P_T}{\rho} = \frac{\delta v_\infty^2}{2} - \frac{v_2^2}{2C_V}$$

EQUATION 30

The power extracted by the turbine is:

$$\Delta P_T \cdot q = A v_2 \Delta P_T = A v_2 \left[\frac{\delta \rho v_\infty^2}{2} - \frac{\rho v_2^2}{2C_V^2} \right]$$

EQUATION 31

where: A is the duct cross sectional area (m^2)
q is the volumetric flowrate of the air (m^3/s)

The maximum power condition is achieved when:

$$\frac{d}{dv_2} = 0$$

EQUATION 32

therefore:

$$\frac{\delta \rho v_\infty^2}{2} - \frac{3\rho v_2^2}{2C_V^2} = 0$$

EQUATION 33

Since δ is also a function of v_2, equation 33 becomes:

$$\frac{3v_2^2}{C_V^2} = \delta v_\infty^2$$

or

$$v_2 = C_V \sqrt{\frac{\delta}{3}} v_\infty$$

EQUATION 34

A table can now be established for the velocity ratio v_2/v_∞ for various values of C_V and δ.

Duct velocity coefficient	**0.5**	**0.75**	**1.0**
δ **= 1.0**	0.289	0.433	0.578
δ **= 1.5**	0.354	0.530	0.707
δ **= 2.0**	0.408	0.612	0.816

Relating back to equation 29:

$$\Delta P_T = \frac{1}{2}\rho\left[\delta v_\infty^2 - \frac{v_2^2}{C_V^2}\right]$$

EQUATION 35

For Maximum Power:

$$\Delta P_T = \frac{1}{2}\rho\left[\delta v_\infty^2 - \frac{\delta}{3} v_\infty^2\right] = \frac{1}{3}\rho\delta v_\infty^2$$

EQUATION 36

and the power extracted from the airstream by the turbine:

$$\Delta P_T \cdot Av_2 = \frac{1}{3}\rho\delta v_\infty^2 \cdot AC_V\sqrt{\frac{\delta}{3}}v_\infty = \frac{1}{3\sqrt{3}}\rho A\delta^{\frac{3}{2}}v_\infty^3 C_V$$

EQUATION 37

The Power Coefficient C_P:

$$C_P = \frac{p}{\frac{1}{2}\rho A v_\infty^3} = \frac{2}{3\sqrt{3}} \cdot C_V\delta^{\frac{3}{2}}$$

EQUATION 38

The table below shows the values of C_P for the maximum power condition.

Duct velocity coefficient	0.5	0.75	1.0
δ = 1.0	0.192	0.289	0.385
δ = 1.5	0.354	0.530	0.707
δ = 2.0	0.544	0.817	1.09

The C_P values quoted here are gross ones (as in the Betz analysis for free wind turbines). The actual C_P for any system must incorporate corrections for the rotor and generator efficiencies. In applying this theoretical model, there is also the assumption that values of the differential pressure coefficient δ are unaffected by the presence of the turbine duct: reasonably accurate for a single unit, more questionable for several grouped along the roof edge.

Experimental conditions approximate to: δ = 1.5, C_V = 0.5 in the table, giving C_P ~ 0.35 for the rotor. This is however reduced by generator losses to ~ 0.20 – 0.25.

The scope for improvement is:

- Reduce the losses from the generator
- Maximise δ
- Reduce losses in duct to move C_V towards 1

7.3 Size and Power

The installation on the Lighthouse building had restrictions placed upon the design as the architect did not want the appearance of the building to be altered or destroyed. The architects restrictions limited the size of the turbine rotor to 0.6m diameter. Utilising this diameter of 0.6m calculations using the theory in section 6.3 can be performed to determine the power outputs of these devices.

Assumptions have to be made regarding the turbine operation.

Air Density (ρ):	1.225kg/m^3
Wind Speed (V):	10m/s
Rotor Diameter (r):	0.3m

Section 7.2 shows that present experimental work shows a Cp value of 0.35.

In order to calculate the power in the wind the swept area of the turbine has to be calculated using equation 39.

$$A = \Pi r^2$$
$$A = \Pi \times 0.3^2$$
$$A = 0.2827 m^2$$

EQUATION 39

Using equation 6 the power available from the turbine can be calculated.

$$p = C_p \frac{1}{2} \rho A v^3$$
$$p = 0.35 \times \frac{1}{2} \times 1.225 \times 0.2827 \times 10^3$$
$$p = 60.61 W$$

The value of power calculated assumes that there are no losses from the generator, and obviously this would never be the case but in order to make predictions on the performance the assumption of no losses is made.
In order to calculate the annual energy yield from a single turbine unit, equation 40 is used.

$$Y = p \times 8760$$

EQUATION 40

where p is the turbine power rating (kW)

$$Y = \frac{60.61}{1000} \times 8760$$
$$Y = 531kWh$$

The value of 531kWh assumes that the wind is constantly blowing at the rated turbine speed (10m/s) for the entire duration of the year. This is clearly never going to be the case. A capacity coefficient is required to estimate the percentage of the time that the wind will be at the rated speed. The capacity coefficient for Scotland is usually taken as 0.35 but since the ducted units are direction dependant, a value of 0.25 is assumed.

A realistic annual energy yield from a single unit would be:

$$Y = 531 \times 0.25$$
$$Y = 132.75kWh$$

This value is not great but the units would not be installed individually and instead would be installed in banks of multiple units. If a bank of 10 units are installed then the energy yield for the year rises to 1327.5kWh.

The calculated values are for a rotor diameter of 0.6m and that value was chosen because of restrictions placed by the architect of the building. In order to retrofit a DWT to a building a rotor diameter of 1m should be possible without too many problems relating to the installation. The calculated values would then increase.

For a 1m diameter rotor, based on the same assumptions as before:

$$p = 168.37W$$
$$Y = 368.72kWh$$

The increase in diameter has led to a 3 times increase of energy yield.
The power output and annual energy yield of the DWTs is small in the scale of the whole electricity system. The layout of the national grid in the UK and most other

grids is based upon centralized generation where large multi-megawatt power stations generate the power and it is then transmitted through the transmission network then distributed through the distribution network at reducing voltage levels until it arrives at the wall socket at 230Vac. The introduction of renewables in remote locations opposes the hierarchical structure of the network by generation at lower voltage levels and trying to transmit and distribute in the 'wrong' direction. This introduction of generators on the distribution network is known as embedded generation (distributed generation).

7.4 Embedded Generation (Distributed Generation)

Distributed generation is an electricity generation source that is connected to the distribution network rather than the high voltage transmission network. Distributed generation projects are generally smaller scale generation projects and renewable energy generation. Obviously large scale renewable generation occurs but commonly the renewable generation is on a smaller scale.

As previously mentioned the network of power lines throughout the UK operate so that the power is transferred down from the high voltage transmission network through the distribution network to the consumers. Embedded generation alters the topology of the network as generation capacity is introduced into the distribution network and flows can be to and from consumers.

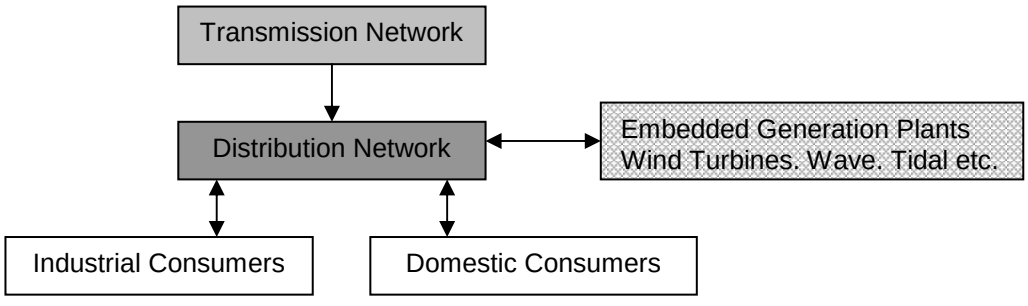

FIGURE 33
UK GRID SETUP + EMBEDDED GENERATION

Figure 33 shows that the distribution network must deal with bi-directional flow, both to and from the network. The industrial and domestic customers must also be able to send and receive from the network as more and more customers are

generating their own power using PV facades or wind turbines, where any excess generation can be sold back to their local public electricity supplier.

7.4.1 Benefits of Embedded Generation

As embedded generation is connected to the distribution network rather than the transmission network it will be located closer to the consumers than large scale generation connected to the transmission network. Therefore the electricity is delivered in a more direct fashion than through the hierarchy of the network. This direct delivery implies that the power has to travel a shorter distance and so it will incur fewer losses through transmission. The power is also transmitted at a lower voltage level than on the transmission network so the cost of large transformers and equipment is gone. By generation closer to the consumers can also effect the environment because the higher percentage of power transmitted (and not 'lost' through transmission) will reduce the overall production of electricity required to be generated. In the event of a power cut in either the transmission network or distribution network, distributed generation could effectively supply the power demand for the local customers on the network.

7.4.2 Embedded Generators

The use of a bank of DWTs on a building would obviously be a source of embedded generation. If a bank of DWTs is installed there are options on what type of system to deploy to utilise the energy produced.

7.4.2.1 DC System

This type of system is generally not deployed unless for specific small supplies. PV systems provide a DC electricity output so can be connected easily, but most wind turbines use AC generators. The AC output from the turbine will have to put through a rectifier to convert it to DC. (A rectifier is a power electronics component used to convert AC into DC.) The typical use of this system is to store the power in a battery or battery bank. In order to do this a charge controller is required. This device controls the charge into the battery so that it does not overload and at worst

'explode'. Once the devices are connected to the battery the DC devices that require the power can be connected and the system is complete.

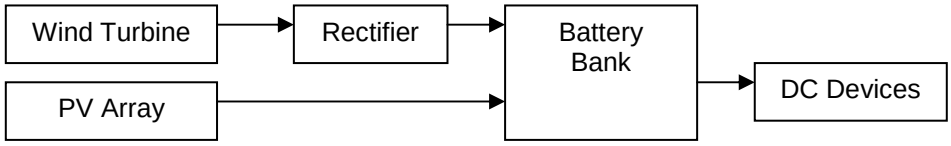

FIGURE 34
DC EMBEDDED GENERATION SYSTEM

7.4.2.2 AC / DC System

This type of system employs the same technology as the DC system but also has the advantage of being able to power AC devices. There are two outputs from the battery bank in this system, the DC output and the AC output. The AC output is initially a DC output but it is then put through an inverter to convert it into AC. (An inverter is a power electronics component that converts DC into AC – there are many different types of inverter available but an inverter that provides an output of 230V @ 50Hz is required) Once the DC output is inverted to AC it is ready to supply any devices.

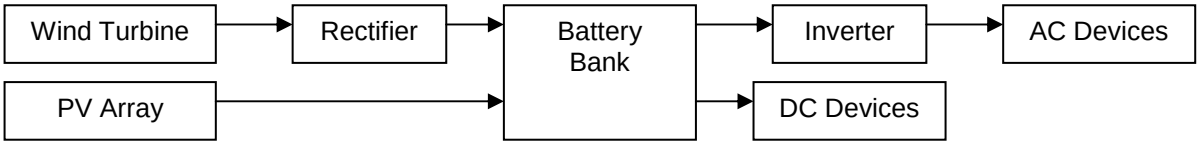

FIGURE 35
AC/DC EMBEDDED GENERATION SYSTEM

7.4.2.3 AC System

This type of system is the same as the AC / DC system except we remove the straight DC output from the battery bank and supply everything through the inverted output.

7.4.2.4 Grid Interfaced System

This is an incremental step forward from the AC system. If the AC system is used to supply the power to all or part of a consumers demand it could become unreliable. Under certain conditions there may be a power deficiency from the AC system. By

having a grid interface system the power supply can be switched from the embedded AC system to the grid.

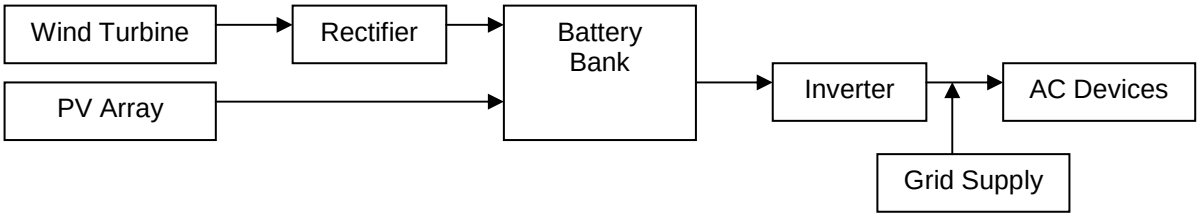

FIGURE 36
GRID INTERFACED SYSTEM

7.4.2.5 Grid Connected Systems

In this system the power form the grid is available at all times. Instead of using a battery bank to store the generated power the excess power generated is 'sold' back to the grid. In this case the public electricity supplier will connect some metering arrangement to measure the quantity of power that is sent into the network. Generally the price paid for power generated by a consumer will be a lot less than the price the consumer will pay for power supplied. Typically the public electricity supplier will use a two meter system, where one meter will measure power imported and the other meter will measure power exported.

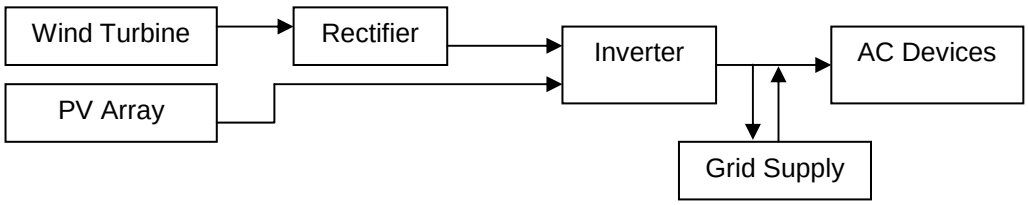

FIGURE 37
GRID CONNECTED SYSTEM

In figure 36 the output from the wind turbine is still rectified to DC and then inverted to AC as the inverter will ensure that the output is 230V @ 50 Hz. The inverter acts as a device for controlling the power quality of the system.

If a variable speed wind turbine is used the power output and frequency of that output are completely dependant upon the wind speed. So the frequency can vary constantly – not good for a power network. This is where the rectifier and inverter come into play where the output is controlled to provide 230 V @50Hz.

If consideration is given to use a grid connected system, engineering recommendations exist that have the governing rules that must be employed when using embedded generation.

Engineering Recommendation G59 – RECOMMENDATIONS FOR THE CONNECTION OF EMBEDDED GENERATING PLANT TO THE REGIONAL ELECTRICITY COMPANIES' DISTRIBUTION SYSTEM.

Engineering Recommendation G77 – UK TECHNICAL GUIDELINES FOR INVERTER CONNECTED SINGLE PHASE PHOTOVOLTAIC (PV) GENERATORS UP TO 5KVA.

The installation of DWTs has to follow one of the systems available to use for small scale users. As the installation will be in many cases a retrofit to an existing building the grid will already be connected and the DWTs would not be able to supply all the power for a building. A grid interfaced system is the preferred option where a shortage of generation is met with the grid but excess is stored in a battery bank rather than sold back to the local utility, because of poor prices paid for generation and the extra requirements to meet the engineering recommendations.

The battery bank is obviously a key component in an installation so proper care and maintenance must be taken of these batteries.

8.0 Storage

Storage is a key component in any small-scale renewable energy installation due to the intermittent nature of renewable energy. The most common choice of storage is the battery but it is not the only option available. Other storage options available are flywheels, compressed air and hydrogen fuel cells. The use of these other options are not common although a lot of research and development into the use of fuel cells may make them a viable option in the near future. The energy stored in the batteries is required to power any monitoring equipment and any loads that are connected. In order to ensure an effective renewable installation it is essential to properly maintain the batteries.

8.1 Composition of a Battery

All batteries contain one or more electrochemical cells. A cell is the basic building block from which a battery is made; a battery will consist of one or more cells that are electrically connected.

For storage of electrical energy the lead acid battery is the most common type used. It is a very rugged type of battery and used for many applications including cars, boats and submarines.

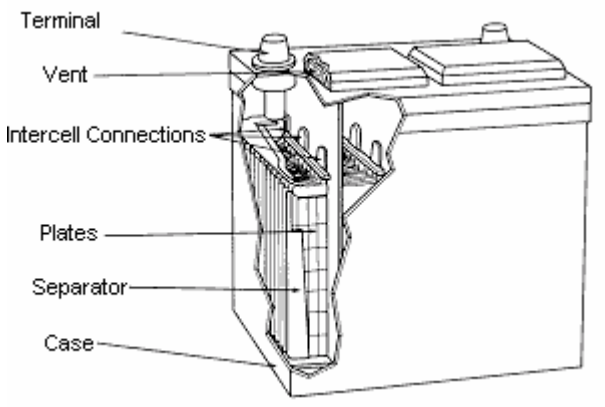

FIGURE 38 [16]
FLOODED LEAD ACID BATTERY

A 12V lead acid battery consists of six cells electrically connected. These cells have a nominal voltage of 2V so summate to provide the 12V. All lead acid batteries are based upon the same set of chemical reactions and utilise the same materials. The materials utilised inside the battery are lead dioxide (PbO_2), lead (Pb), sulphuric acid (H_2SO_4) and water (H_2O).

The negative electrode of the lead acid battery is made of lead (Pb) and the positive electrode is made of lead dioxide (PbO_2). The electrolyte solution is dilute sulphuric acid ($H_2SO_4 + H_2O$). If the electrodes of the cell are connected to a load, providing electrons a path to flow from one electrode to the other, negatively charged oxygen ions (O^-) from the positive electrode (PbO_2) bond with positively charged hydrogen ions (H^+) to form water (H_2O) molecules. The lead dioxide (PbO_2) electrode is therefore left with an electron deficiency giving it a positive electrical charge. The sulphate ions (SO_4) left over from the disassociation of the hydrogen ions (H) from the sulphuric acid (H_2SO_4) will join with the lead (Pb) in each electrode to form lead sulphate ($PbSO_4$). This reaction leads to the discharging of the battery and in theory; the result would be two electrodes of lead sulphate ($PbSO_4$) and an electrolyte solution of pure water (H_2O). When charging a lead acid battery the chemical reactions experienced during discharge are reversed.

$$PbO_2 + H_2SO_4 \rightarrow PbSO_4 + H_2O + O$$
$$Pb + H_2SO_4 \rightarrow PbSO_4 + 2H$$

EQUATION 41
DISCHARGING CHEMICAL REACTIONS

$$PbSO_4 + H_2O + O \rightarrow PbO_2 + H_2SO_4$$
$$PbSO_4 + 2H \rightarrow Pb + H_2SO_4$$

EQUATION 42
CHARGING CHEMICAL REACTIONS

The physical construction of lead batteries does change. A standard lead acid car battery uses lead sponge as the lead plates. A car battery is designed to provide a high level of current for a short period of time (ignition) and then is constantly charged, when the vehicle is used, by the alternator. This is termed a shallow cycle. For use in renewable energy installations deep cycle batteries are required. The recharging of the battery is completely dependant upon nature and therefore it cannot be relied upon to constantly provide a charging current. The battery can therefore become highly discharged, this type of use is termed a deep cycle. The construction of a typical lead acid car battery uses the spongy lead, which makes it able to supply high currents but they are still cheap and light. Repeated deep cycling of a car battery will cause the spongy plates to crumble and reduce the battery effectiveness then

eventually destroy it. A purpose constructed deep cycle battery uses scored sheets of lead as the plates. The plates are many times thicker than the ones used in car batteries and are constructed of solid lead. Due to the construction of the deep cycle lead acid battery it is more expensive and often larger than a car battery.

Deep Cycle Lead Acid Batteries should always be used in renewable energy installations.

Batteries are rated in terms of their voltage and their storage capacity. A battery will be provided with a voltage rating and a capacity value, typically measured in amp-hours (Ah). A battery with a rating of 100Ah will be able to supply a current of 100A for 1 hour or a current of 1A for 100 hours. (Or any combination of current and time summating to 100Ah.)

8.2 Battery Connections

As previously discussed, batteries are constructed from the electrical connection of individual cells. Batteries can also be electrically connected to make a battery bank. In the use of a battery bank there are a number of possible connections available to provide different outputs. It is essential that the correct connection technique is utilised to provide the desired output.
The batteries shown are rated a 12V and have a capacity of 75Ah.

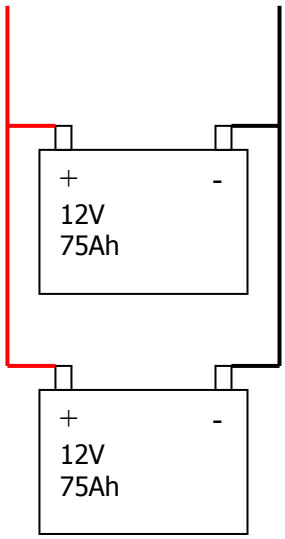

The connection shown has two batteries connected in parallel. The parallel connection provides a voltage level of 12V and a total capacity of 150Ah. In order to increase the capacity further, batteries can be added using the same connection method.

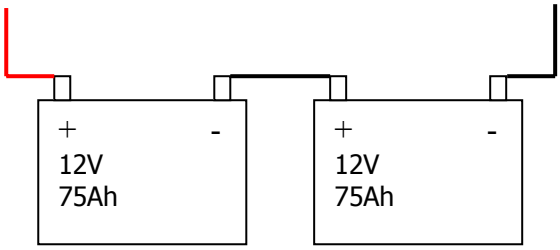

The connection shown has two batteries connected in series. The series connection provides a voltage level of 24V and a total capacity of 75Ah. In order to increase the voltage further, batteries can be added using the same connection method.

It is essential that the battery connections are made for the desired voltage output.

Parallel Connection = Increased Capacity

Series Connection = Increased Voltage

8.3 Battery Maintenance

Batteries and any storage medium used are a key component in any installation and therefore it is essential to safely and adequately maintain the batteries to ensure optimal efficiency and lifespan.

Visual inspections are a simple way to check for any problems that may be easily corrected or may require the battery to be recycled and replaced. Simple wear and tear or damage to the casing can be found.

The State of Charge of a battery can be checked by checking the chemical condition of the electrolyte. Using a hydrometer the specific gravity (weight of object compared to that of water) of the electrolyte can be measured to indicate the level of charge. As mentioned previously the battery electrolyte solution is dilute sulphuric acid, which is a mixture of sulphuric acid (H_2SO_4) and water (H_2O). The ratio of mixture is 36% sulphuric acid to 64% water. A fully charged battery will have a specific gravity reading of 1.270, as the battery becomes discharged the electrolyte turns to water (indicated in equation 41), which lowers the specific gravity closer to 1.000. Therefore by measuring the specific gravity, the level of charge of the battery can found.

The state of charge test indicates the amount of charge available in the battery but it does not measure its ability to supply current. A load test measures the ability of the battery to adequately deliver current. A load test places a heavy load on the battery to draw a high current and the voltage drop seen by the battery determines its ability to deliver current.

These simple maintenance checks and tests can help to ensure that the most is being achieved from the battery storage and that the installation is working efficiently.

With the theory and storage options relating to the design of the DWTs covered it is time to move on to the development of the devices.

Section 7.2 indicated that scope for improvement in the design of the DWTs was to reduce the losses from the generator. One method of reducing the losses is to utilise a generator that exhibits similar torque / speed characteristics to the blades in order to ensure an optimal system. In order to construct this optimal system the available generators have to be characterised.

9.0 Generator Characterisation

The aim of this series of experiments was to produce a set of characteristics on a range of generators available that could be potentially used as the generation unit on a Ducted Wind Turbine.

By gaining an understanding of the characteristics and the expected performance of the generators will enable the best and most efficient device be produced when coupled with the range of available turbine rotors.

The experimental work consisted of two types of characterisation:

- Characterisation of a variable speed DC motor.
- Performance of generators when driven by DC motor.

Each experiment and theory will be explained individually then the results will be combined for the full characterisation of the generators.

9.1 Characterisation of DC Motor

This experimentation involved the use of an eddy-current dynamometer to characterise a shunt connected DC Motor. In order to understand the process of characterisation; the theory, experimental procedure and the processing of the results will be explained.

9.1.1 DC Motors

The principal behind all electric motors is magnetism. A motor uses magnetism to create motion. Some motors are permanent magnet machines where the magnetic field used to create the rotational movement is created by actual magnets that permanently exert a magnetic field. More commonly used are electro-magnets where the magnetic field is created by passing current through a coil of wire.

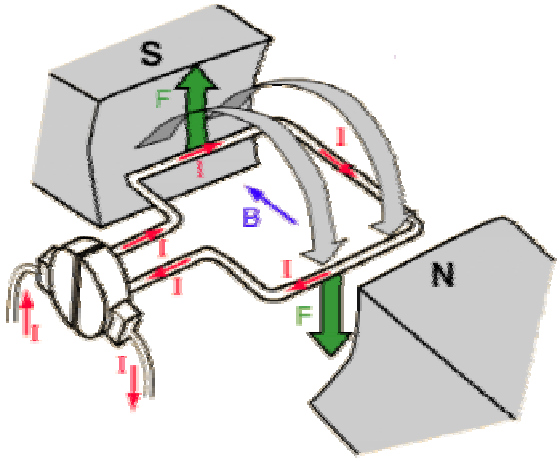

FIGURE 39 [17]
DC MOTOR PRINCIPLE OF ROTATION

Figure 39 shows the basic set up of a DC motor, the image shows permanent magnets to create the magnetic field. The blue arrow shows the direction of the magnetic field from the north to the south pole, the red arrows show the direction of the current flow and the green arrows represent the force on the conductor wire. The image above can be used to represent either a motor or generator. If current is supplied to the conductor wire we will induce movement and create the force, but if the conductor is rotated in the direction shown there will be a current induced in the conductor and this will be a generator.

A relationship exists between the magnetic field, the current and the force. The force is more commonly known as Lorentz Force.

$$F_{LZ} = BLI$$

EQUATION 43

where F_{LZ} = Lorentz Force (Nm)
B = Average Magnetic flux density (T)
L = Length of conductor (m)
I = Current through conductor (A)

An electrical machine consists of two parts: the rotor and the stator. Normally the stator is the outer part and is fixed in position with the inner component, the rotor free to rotate inside the stator. Conductors can be placed on both the rotor and stator and these form the windings of the machine. There are two types of windings, the field and the armature windings. The field windings are used to create the magnetic

field and are the primary source of the flux, whereas the armature windings are where the induced current will flow. In a DC motor the field windings are located on the stator and the armature windings are located on the rotor.

The driving force behind a DC motor is the current supplied to the armature windings (Armature Current – I_A). These windings on the rotor are located inside the stator, which has the field windings setting up the magnetic field by means of supplying a current (Field Current – I_F) to the windings to produce an electromagnet. The interaction of the armature and field windings creates the Lorentz force and rotates the rotor.

The total power input to a DC Motor is the summation of the power supplied to the armature and the field.

$$p_{IN} = V_A I_A + V_F I_F$$

EQUATION 44

This theory represents the basic workings of a DC motor but there are different types, depending upon the connections of the armature and field windings.

9.1.1.1 DC Motor Types

There are two categories of DC motor: self-excited and separately excited.

- Separately excited: The field and armature circuits are totally separate. The field current is supplied from a secondary source (or by permanent magnets).
- Self-excited: The field and armature currents are provided by the same source. These are usually smaller motors and the field and armature may be connected in three different ways:

    1. **Shunt Motor**: The field and armature windings are in parallel.
    2. **Series Motor**: The field and armature windings are in series.
    3. **Compound Motor**: Both shunt and series windings are used.

9.1.1.2 Torque in DC Motors

Consider a single loop of wiring around a rotor, with length 2L (L is the length of the rotor, therefore the total length of the wire crossing the stator field lines is 2L) and current I_C flowing through the loop.

The average force (or Lorentz Force) on the loop will be:

$$F_{LZ-C} = BLI_C$$

EQUATION 45

If instead of a single loop in the armature winding, there are 'z' parallel paths and the total armature current is I_A, the current in the single loop (I_C) will be:

$$I_C = \frac{I_A}{z}$$

EQUATION 46

The torque developed by the single loop will be:

$$T_C = F_{LZ-C} r$$

EQUATION 47

where: r = radius of rotor (m)

Substituting I_C into F_{LZ-C} gives:

$$T_C = \frac{BLI_A r}{z}$$

EQUATION 48

The magnetic flux density (B) is given by:

$$B = \frac{\phi}{A}$$

EQUATION 49

where ϕ = Flux per pole (Wb)
A = Area per pole (m^2)

If there are 'n' poles on the stator, the area per pole is calculated from:

$$A = 2\frac{\pi rL}{n}$$

EQUATION 50

By substituting 'A' back into the magnetic flux density equation the following is obtained:

$$B = \frac{\phi n}{2\pi rL}$$

EQUATION 51

This can then be substituted back into the torque equation to obtain:

$$T_C = \frac{\phi n I_A}{2\pi z}$$

EQUATION 52

This equation represents the torque generated only on one side of the single loop. The total rotor torque is calculated by multiplying by 2 (the loop has 2 sides) and multiplying by the number of turns in the armature winding (N).

Total rotor Torque:

$$T = \frac{N\phi n I_A}{\pi z}$$

EQUATION 53

By defining a constant 'K' as:

$$K = \frac{nN}{\pi z}$$

EQUATION 54

The total rotor torque becomes:

$$T = K\phi I_A$$

EQUATION 55

And if the rotor is rotating at speed ω (rad/s), the mechanical power out is:

$$p_{OUT} = \omega T$$

EQUATION 56

Therefore if the input power (equation 44) and the output power (equation 56) are known, the efficiency of the motor can be calculated.

$$\eta_{MOT} = \frac{P_{OUT}}{P_{IN}}$$

EQUATION 57

9.1.1.3 Armature Voltage

During rotation within the stator field a voltage is induced upon the armature windings. In a generator this is the generated voltage but in a motor this is the 'back emf'. This voltage can be calculated using the principle of Faradays Law.

Faradays Law states that a voltage 'e' will be induced when a conductor of length 'L', moves at a velocity 'v' in a magnetic field with flux 'B'.

$$e = BLv$$

EQUATION 58

Referring to the single loop on the rotor, which represents one turn on the armature, the induced voltage across the terminals of the turn (e_t) is:

$$e_t = 2BL\omega r$$

EQUATION 59

Substituting the equation for B so we get the average voltage across the turn:

$$e_t = \frac{n\phi\omega}{\pi}$$

EQUATION 60

For every parallel path around the rotor there will be a number of turns connected in series. The number of turns in each parallel path is be given by N/z.

Therefore:

$$E_A = \frac{N\phi n\omega}{\pi z}$$

EQUATION 61

And substituting in constant 'K' the voltage induced in the armature is:

$$E_A = K\phi\omega$$

EQUATION 62

The magnetic flux (ϕ) in a DC machine is dependent upon the field current (I_F) and is almost proportional to it. (This is only true for low values of field current, for high values magnetic saturation takes place and there is a nonlinear relationship with the field current and the flux.) The relationship between the flux and the field current is called the 'magnetisation characteristic' and it can be easily shown that for a constant speed the open circuit characteristic of induced voltage (E_A) against field current (I_F) is the same as the magnetisation characteristic, except for a constant factor.

$$E_A = K\phi\omega = K'\omega I_F$$

EQUATION 63

The theory described is consistent for all DC motors. The motor used in this experiment was a shunt motor.

9.1.1.4 DC Shunt Motor

In a shunt motor the field and armature windings are in 2 parallel paths, as shown in figure 40.

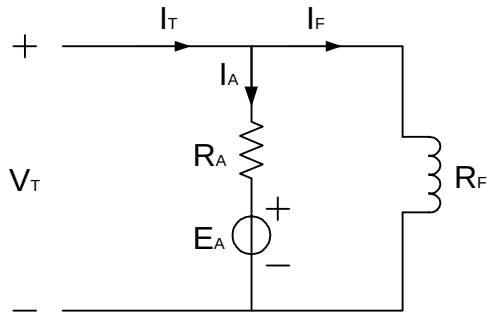

FIGURE 40
DC SHUNT MOTOR CONFIGURATION.

The voltage across the armature is:

$$V_T = I_A R_A + E_A$$

EQUATION 64

where: $I_A R_A$ = voltage drop across armature
E_A = back emf

Re-arranging to give the back emf:

$$E_A = V_T - I_A R_A$$

EQUATION 65

By substituting for E_A (equation 61) and rearranging equation 55 to give I_A.

$$E_A = K\phi\omega$$
$$I_A = \frac{T}{K\phi}$$

EQUATIONS 66 & 67

A torque-speed relationship can be derived:

$$\omega = \frac{V_T}{K\phi} - \frac{R_A}{(K\phi)^2} T$$

EQUATION 68

9.1.2 Dynamometer

A dynamometer is a piece of equipment that measures mechanical force, speed, or power. For a typical motor-dynamometer test cell, the motor shaft is directly coupled to the dynamometer. The dynamometer can exert a braking force on the engine when the engine is running. Many dynamometers have sensors that measure engine speed and torque. Knowing these values, the dynamometer can calculate engine-power output. Dynamometers allow us to reproduce a desired speed or torque for a test under controlled conditions.

Dynamometers use different methods to induce a braking force on the device under test. The various types of dynamometer available are water brake, Eddy Current, AC and DC dynamometers.

In this experiment an Eddy Current dynamometer was utilised

9.1.2.1 Eddy Current Dynamometer

The construction of an eddy current dynamometer is based upon the theory of eddy currents.

When metal moves through a varying magnetic field (or is located in a changing magnetic field) currents are induced within the metal. These induced currents are called 'eddy currents'. The eddy current brake works on the principal of Lenz Law (Heinrich Lenz 1804 – 1865): An electric current induced by a changing magnetic field will flow such that it will create its own magnetic field that opposes the magnetic field that created it. These opposing fields occupying the same space at the same time result in a pair of forces. Therefore by inducing eddy currents within the metal, an electromagnetic force is created that opposes the electromagnetic force that created it and effectively acts as a brake to slow the motion of the metal through the original magnetic field.

The construction of an eddy current brake (figure 41) includes a toothed disc (rotor) that is driven by a motor, magnetic poles (stators) that are located each side of the disc and an excitation coil (wound in circumference direction). Passing current through the exciting coil forms a magnetic flux loop around the coil through the stators and rotor. The rotation of rotor produces a density difference; this induces eddy currents within the stator. The electromagnetic force created by the eddy currents is applied in opposition to the rotational direction and acts as a braking device. The higher the current applied to the excitation coil, the larger the eddy current electromagnetic force and the stronger the braking action.

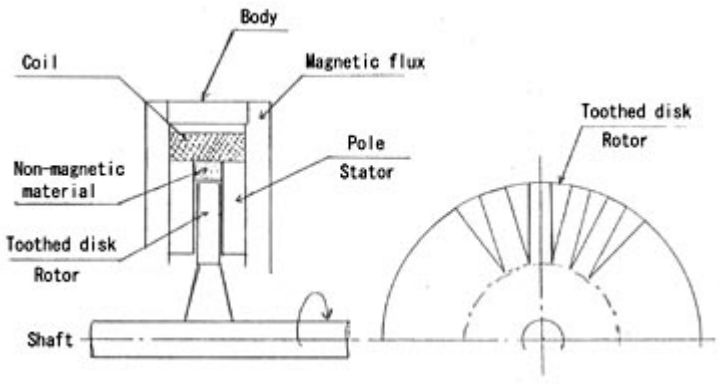

FIGURE 41 [18]
EDDY CURRENT DYNAMOMETER.

In order to characterise the DC Motor the eddy current dynamometer and motor are coupled together.

9.1.3 Motor Testing

9.1.3.1 Test Equipment

The equipment required for this test procedure is as follows.

Equipment	Quantity
DC motor (shunt)	1
Eddy current dynamometer	1
Multimeter	5

The DC motor has a tachometer attached to the shaft and produces a voltage output that varies linearly with the rotational speed. The tachometer output is rated at 20.8V/1000RPM. A controller unit is supplied with the DC motor that allows speed control by varying the current supplied to the armature.

The readings from the data plate on the motor.

SERIAL NO: C.151608.A
FRAME: 7B
H.P.: 1.5 (1118.55W)
TORQUE: (7.12 Nm)
VOLTS: 180A, 210F
Ph:
~: DC
AMPS: 7.6
RPM: 1500 (157.079 rad/s)
RATING: CONT
TYPE: SHUNT

The values indicated in red are calculated values.

1 H.P. = 745.6999 W
rad/s = RPM x $2\pi/60$
$P=\omega T$

The eddy current dynamometer is supplied with a controller that allows a varying current to be supplied to the excitation coil and vary the braking action. The torque from the dynamometer is measured using a spring balance.

The dynamometer casing has a spigot attached with a chain that pulls down on the spring balance to indicate the force. The torque is calculated as follows:

Outer diameter of dynamometer casing: 220mm
Distance from casing to centre of chain clip: 25.2mm

Distance from shaft centre to point of force = (220/2) + 25.2
135.2mm

The chain is attached to the chain clip on the dynamometer casing and the spring balance to indicate mass. The torque exerted on the dynamometer is calculated by multiplying the mass indicated by gravity and then by the distance from where the load is applied to the pivot point.

$$F = m \times a$$
$$T = F \times d$$
$$T = m \times 9.81 \times 0.1352$$

EQUATIONS 69, 70 & 71

where F = Force (N)
m = mass (kg)
d = distance (m)
a = acceleration (ms^{-2}) (here 9.81 for gravity)
T = Torque (Nm)

The setup of the required equipment is shown in figure 42.

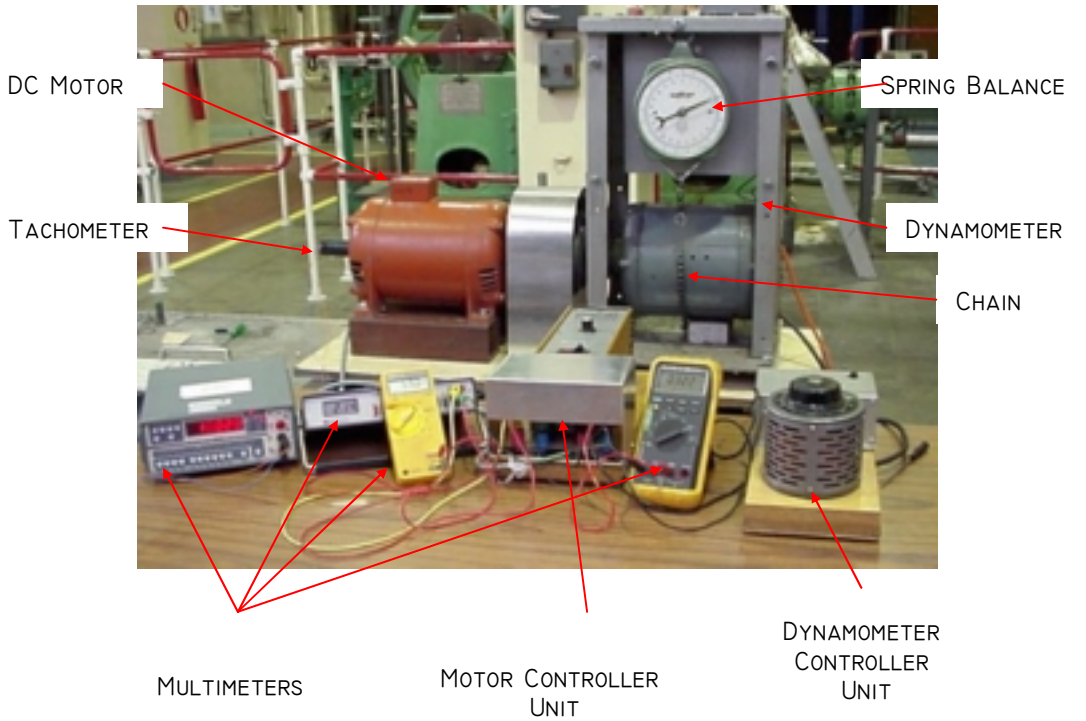

FIGURE 42
TEST SETUP

The five multimeters are used to measure:
- Armature Voltage (V_A)
- Armature Current (I_A)
- Field Voltage (V_F)
- Field Current (I_F)
- Tachometer Voltage (V_{TACH})

9.1.3.2 Test Procedure

9.1.3.2.1 No Load

Under no-load condition the motor runs up to the no-load speed (ω_o). As armature current is very small under no-load condition, the armature voltage drop can be neglected making E_A almost equal to the applied armature voltage V_T.

Therefore:

$$V_T \approx E_A = K\phi\omega_0 = K'\omega_0 I_F$$

EQUATION 72

Switch on all equipment and run DC Motor up to the no load speed. Let the motor settle for approximately 1 minute then note down values on all multimeters.
Reduce speed of motor and turn off all equipment.

9.1.3.2.2 Constant Speed

Switch on all equipment and run the DC motor at a speed of 100 RPM.

Note down values on all multimeters.

Apply load to the dc motor by braking the dynamometer. Apply a load of approximately 0.5kg.

Adjust the motor speed control to 100 RPM.

Let the motor run for at least 1 minute to settle down to steady state.

Note down values on all multimeters.

Increase the load in increments of 0.5kg until the armature current is at rated value. (I_A = 7.6A value from data plate)

Repeat procedure for different values of RPM (100-1000 RPM)

Speed (RPM)	**Voltage** (V_{TACH}) (V)
100	2.08
200	4.16
300	6.24
400	8.32
500	10.4
600	12.48
700	14.56
800	16.64
900	18.72
1000	20.8
1100	22.88
1200	24.96
1300	27.04
1400	29.12
1500	31.2

FIGURE 43
TACHOMETER SPEED/VOLTAGE TABLE

9.1.4 Results

The results from both test procedures will be analysed.

9.1.4.1 Results from No Load Testing

The results from section 9.1.3.2.1 are shown in the table below with the test repeated on numerous occasions to produce an average value and to check for consistency in results.

No Load Test Results

DC Motor				Tach	Vspeed / 0.0208	Speed (RPM) * 2π/60	Va / (No*If)	k' * If	k'If
Vf	**If**	**Va**	**Ia**	**Vspeed**	**Speed**	**No**	**k'**	**k'If**	**kϕ**
V	A	V	A	V	RPM	rad/s			
220	0.34	155.7	0.42	27.44	1319.23	138.1495	3.31482	1.12704	1.12704
220	0.31	157.6	0.39	28.6	1375	143.9897	3.53072	1.09452	1.09452
221	0.32	156.4	0.39	27.9	1341.35	140.4654	3.4795	1.11344	1.11344
221	0.3	157.9	0.39	28.9	1389.42	145.5	3.61741	1.08522	1.08522
221	0.3	157.8	0.38	28.8	1384.62	144.9966	3.62767	1.0883	1.0883
221	0.3	158.4	0.38	29	1394.23	146.0035	3.61635	1.08491	1.08491
221	0.3	158.6	0.36	29.1	1399.04	146.507	3.60847	1.08254	1.08254
220	0.32	156.3	0.37	27.95	1343.75	140.7172	3.47106	1.11074	1.11074
221	0.3	156.8	0.37	28.62	1375.96	144.0904	3.62735	1.08821	1.08821
220	0.3	157.8	0.38	29	1394.23	146.0035	3.60265	1.0808	1.0808
221	0.29	158.3	0.38	29.13	1400.48	146.658	3.72201	1.07938	1.07938
221	0.29	158.6	0.37	29.19	1403.37	146.9601	3.7214	1.0792	1.0792
221	0.29	158.7	0.36	29.23	1405.29	147.1615	3.71865	1.07841	1.07841
							Average		1.09175

FIGURE 44
NO LOAD TEST RESULTS

The results show that all the recorded values are pretty consistent over the range of testing and can therefore be considered to be accurate and provide an average value for kϕ as 1.09175.

This value for kϕ can now be used against the value of Armature current (I_A) recorded when testing under different loads using the constant speed test to calculate the torque, then the power output from the motor.

9.1.4.2 Results from Constant Speed Testing

The results obtained from the testing of the motor under constant speed operation whilst varying the load can be seen in the table below. The testing was performed on 2 separate occasions and provided almost identical results. The results from the second test are used and results from the first test can be seen in Appendix 2. (NOTE: The table only shows the results for 100RPM)

Ra (Ω) 2.4
Rf (Ω) 639

DC Motor				Tach	Dyno	Fric	(Vf*If) + (Va*Ia)	(Load + Fric Load)* 9.81 * 0.1352	Vspeed / 0.0208	Torque (Nm) * ω (rad/s)	Pout / Pin
Vf	If	Va	Ia	Vspeed	Load	Load	Pin	Torque	Speed	Pout	η
V	A	V	A	V	Kg	Kg	W	Nm	RPM	W	%
220	0.31	11.7	0.25	2.06	0	0.1	71.125	0.1326	99.038	1.3756	1.93%
219	0.3	13.7	1.5	2.06	0.6		86.25	0.9284	99.038	9.6289	11.16%
219	0.3	14.2	1.83	2.04	1		91.686	1.4589	98.077	14.984	16.34%
219	0.3	16.4	2.64	2.09	1.6		109	2.2547	100.48	23.725	21.77%
219	0.3	19.3	3.12	2.08	2.1		125.92	2.9179	100	30.556	24.27%
219	0.3	23.8	3.61	2.05	2.6		151.62	3.581	98.558	36.96	24.38%
219	0.3	24.5	4.2	2.06	3.1		168.6	4.2442	99.038	44.018	26.11%
219	0.3	24.3	4.59	2.07	3.5		177.24	4.7747	99.519	49.76	28.08%
218	0.3	24.6	5.25	2.09	4.1		194.55	5.5705	100.48	58.615	30.13%
218	0.3	25.6	5.75	2.08	4.6		212.6	6.2337	100	65.279	30.70%
219	0.29	27.2	6.59	2.06	5.4		242.76	7.2947	99.038	75.656	31.17%
222	0.29	28.7	7.44	2.1	5.9		277.91	7.9579	100.96	84.136	30.27%

FIGURE 45
CONSTANT SPEED TEST RESULTS (100RPM)

The table in figure 45 shows the results obtained from the testing of the DC Motor with the dynamometer. The electrical power input to the motor is calculated using equation 44, torque is calculated using equation 71, rotational speed is calculated using the voltage speed correlation of the tachometer (20.8V per 1000RPM), the mechanical power output is calculated using equation 56 and the efficiency of the motor is calculated using equation 57. The value of torque is altered slightly from that of equation 71 because of a small frictional loading effect on the motor of 0.1kg.

As shown by equation 55 the torque of any DC motor is dependant upon the value of the armature current (I_A) so a relationship of the armature current versus the efficiency of the motor at each rotational speed is plotted.

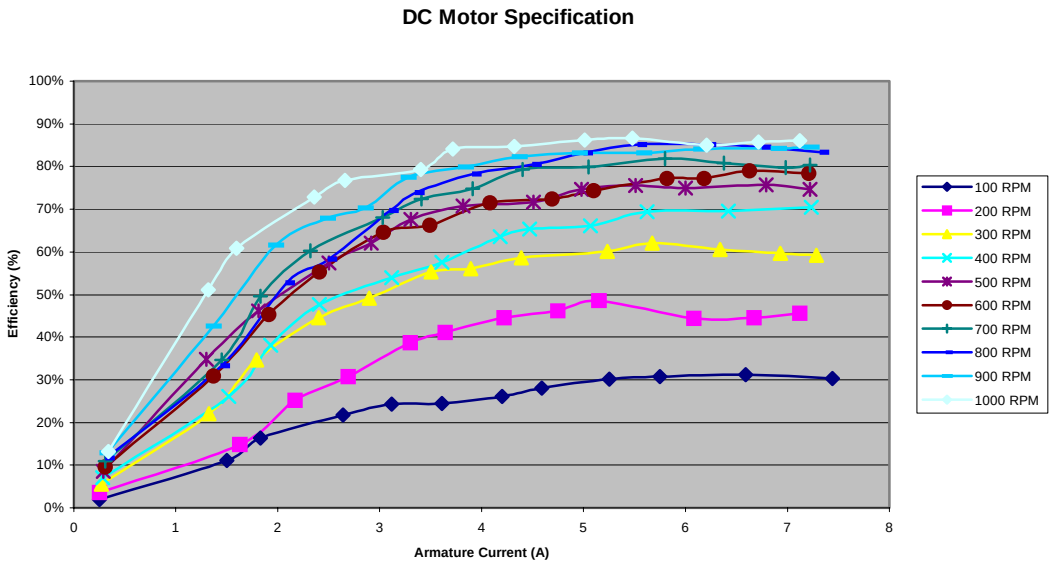

FIGURE 46
DC MOTOR I_A VS η CURVES

Figure 46 shows the relationship that exists between the armature current and motor efficiency for the speed range 100 – 100 RPM and for the full range of the armature current (0-7.6A).

From the chart it can be seen that the motor operates most efficiently at high speeds and that the speed of 1000 RPM provides the greatest efficiency. The efficiencies seem to increase following a polynomial relationship until approximately 4.5A (Armature Current (I_A)), which is approximately 63% of full load current, and then level out to a constant efficiency. A prediction can be made that the efficiency will stay constant until a certain value above rated current then decrease rapidly, at this point the motor would either stall or the wiring would begin to fail from over-current. If the motor is overloaded and started to draw too much current the fuse should blow and cut off the power altogether. In order to represent the information provided by the testing, a trendline can be added for each set of data points.

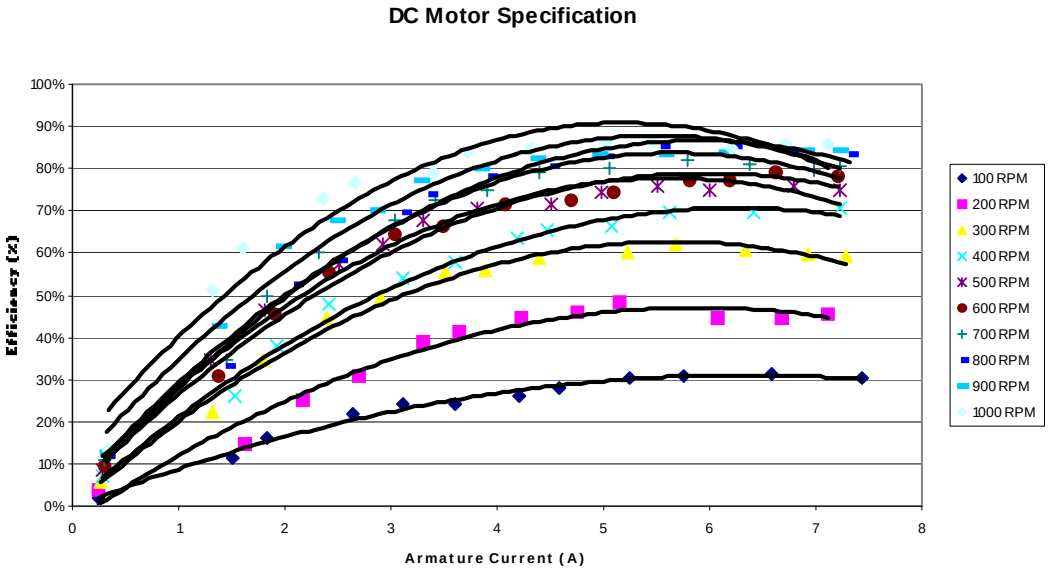

FIGURE 47
DC MOTOR I_A VS η CURVES

Figure 47 shows the plotted data with trendlines added to each set of results. All trend lines take the form of a polynomial of the second order.

$$y = x^2 + x + c$$

EQUATION 73

where c = a constant.

By plotting the trendlines an equation relating Armature current (I_A) and efficiency (η) for each rotational speed is found. In order to check the accuracy of the trendlines representation of the curves, the R-squared values can also be plotted. The lowest value for the R-squared value occurs at 1000 RPM and has an accuracy of 94%.

Using these equations relating the armature current (I_A) and efficiency the power output from the motor can be calculated, if the power input and armature current (I_A) are known.

The results from the testing and resulting equations can be found in Appendix 2.

9.1.4.3 Results from combining test data

By using the value of Kϕ obtained in section 9.1.4.1 and the armature current values obtained in section 9.1.4.2 a correlation of the validity of the results can be made.

DC Motor				kϕ * Ia		$N=\frac{V}{k\phi}-\frac{R_a}{(k\phi)^2}T$		Torque (Nm) * ω (rad/s)	Pout / Pin
Vf	**If**	**Va**	**Ia**	**Torque**	**Tdiff**	**N**	**N**	**Pout**	**η**
V	A	V	A	Nm	%	rad/s	RPM	W	%
220	0.31	11.7	0.25	0.272937	105.79%	10.1672	97.0895	2.8307	3.98%
219	0.3	13.7	1.5	1.63762	76.39%	9.25123	88.3427	16.9842	19.69%
219	0.3	14.2	1.83	1.997897	36.94%	8.98377	85.7887	20.5196	22.38%
219	0.3	16.4	2.64	2.882212	27.83%	9.21825	88.0278	30.3276	27.82%
219	0.3	19.3	3.12	3.406251	16.74%	10.8194	103.317	35.6702	28.33%
219	0.3	23.8	3.61	3.941207	10.06%	13.864	132.392	40.6769	26.83%
219	0.3	24.5	4.2	4.585337	8.04%	13.2082	126.129	47.5558	28.21%
219	0.3	24.3	4.59	5.011119	4.95%	12.1677	116.193	52.224	29.47%
218	0.3	24.6	5.25	5.731672	2.89%	10.9916	104.962	60.3105	31.00%
218	0.3	25.6	5.75	6.277545	0.70%	10.8084	103.212	65.7383	30.92%
219	0.29	27.2	6.59	7.194613	-1.37%	10.4273	99.5736	74.6174	30.74%
222	0.29	28.7	7.44	8.122598	2.07%	9.9327	94.8503	85.8775	30.90%

FIGURE 48
DC MOTOR THEORETICAL CALIBRATION

Figure 48 shows the table of results obtained if the derived value of the constant value kϕ is used to calculate the torque. The column Tdiff represents the difference in the calculated torque from the torque measured by the dynamometer. N is the value of the calculated value of rotational speed using equation 68. The output power is calculated using the rotational speed and the calculated value of torque then the efficiency is calculated with power output divided by power input.

The results shown are only for the 100RPM speed range but the results from the other rotational speeds follow the same generalised pattern. The results show that the values of torque have the greatest difference at low values of armature current (I_A) and have very similar values at high values. This then carries over to the efficiency column with the theoretical method giving higher values of efficiency at low armature currents. The reason behind this is although no loading is being exerted on the motor by the dynamometer, there are inherent inefficiencies and losses built into the motor. These losses will be small but at lower values of I_A they will have a

greater impact and will represent a higher percentage of I_A whereas at higher values the losses become insignificant.

The testing of the DC Motor has now provided two sets of results for the calibration that can be utilised when characterising the various generators tested in section 9.2.

9.2 Characterisation of Generators

This experimentation involved the use of the DC motor explained in section 9.1 to characterise a range of generators. In order to understand the process, the theory, experimental procedure and the processing of the results will be explained.

9.2.1 Generators

Generators are devices that convert mechanical energy to electrical energy. There are various types of generator available but they all work on the same basic principle of magnetism. The principle of coils and magnetic fields described in section 9.1.1 applies to generators as well, in generators though the mechanical force is applied and the electrical energy is produced.

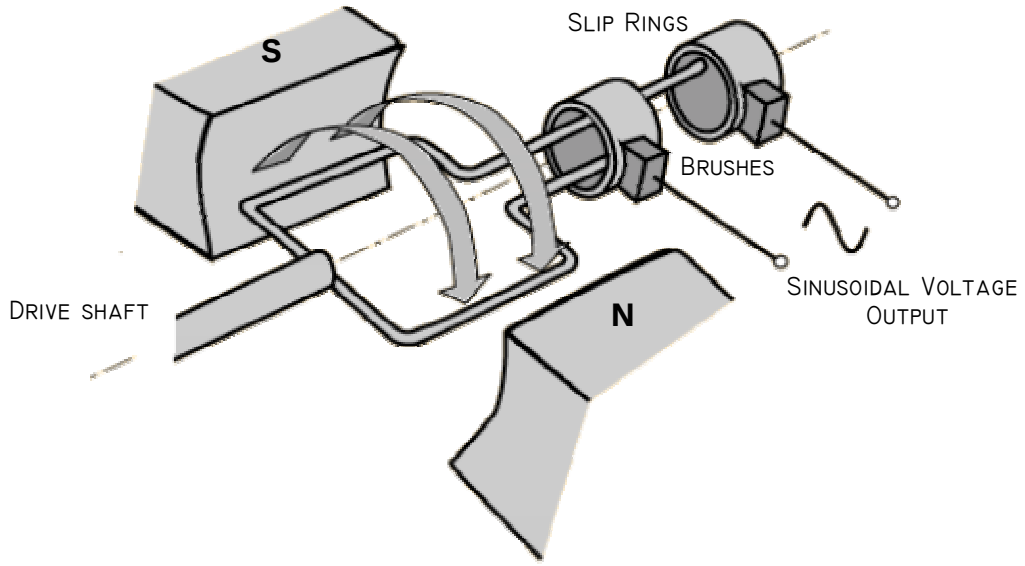

FIGURE 49 [17]
GENERATOR PRINCIPLE OF OPERATION

A charge moving through a magnetic field experiences a force. If the charge is inside a wire moving perpendicular to the magnetic field, the force will act along the wire and this force does work. Work per unit charge equals voltage. As seen in figure 49, if the wire movement is in the form of a rotating coil, the forces on opposite sides of the coil will summate the voltages. The force direction on each side of the coil is constantly varying depending upon the position in the axis of rotation, therefore the generated voltage is sinusoidal - AC (Alternating Current). As the drive shaft is continuously rotating the coils the voltage output has to be transferred to wiring without the wiring becoming twisted. This is where slip rings and brushes are used. The coil ends are attached to slip rings, which rotate with the coil and the brushes are normally carbon blocks that maintain contact with the slip ring to transmit the power to wiring. The frequency of the AC voltage is dependant upon the rotational speed of the coil within the magnetic field.

Figure 50 shows the output from a simple generator. Where the waveform undergoes one complete cycle for every revolution. The frequency of this waveform is 50Hz because one cycle (or the wave period) takes 20 milliseconds and the formula relating frequency and period is:

$$f = \frac{1}{t}$$

EQUATION 74

where f = frequency (Hz)
t = period (s)

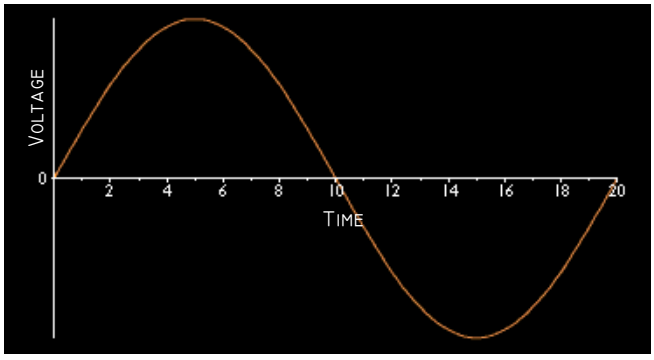

FIGURE 50
SINE WAVE

The theory discussed has only considered a basic generator with two poles. The poles are the polarity of the magnetic field shown on a magnet as north and south. A

magnet therefore has two poles. A generator can have many more poles if required, however there is always an equal number of poles as there can never be a north pole without a south pole. In figure 49 the angular distance between the poles is 180^o and this is a two pole machine, in order to create a four pole machine the angular distance is reduced to 90^o between poles, a 6 pole machine would be 60^o and so on. For a four pole machine the above waveform would have a period of 10ms instead of 20ms because there would be two cyclic period of the waveform for every revolution of the shaft.

Again figure 49 shows only a single coil but in reality a generator will have more than a single coil. In a 'single phase' generator it is possible to connect all the coils together to supply the same circuit because they all work together or are in phase with each other. Connecting coils together has exactly the same principle as connecting batteries together. By connecting in series the output voltage will be increased or by connecting in parallel the voltage will remain the same but a higher current output will be achieved.

A common practice in generator design is to produce '3-phase' machines. Here there are three sets of coils (each set can contain any number of coils) that produce the same voltage and frequency as each other but are out of phase with each other. The coils are distributed on the stator so that an angular distance of 120^o separates each set. Figure 51 shows the wave output from a 3-phase machine.

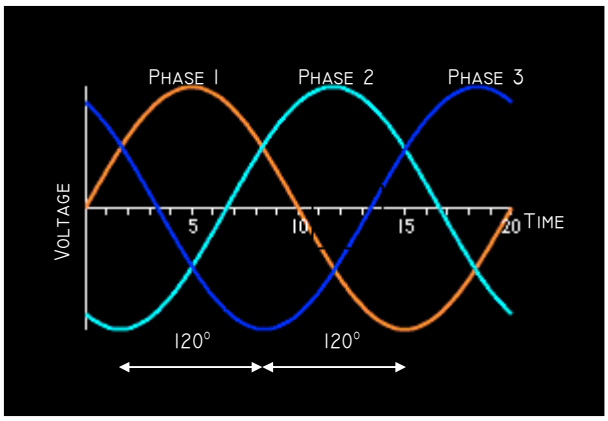

FIGURE 51
3-PHASE WAVEFORM

As can be seen the timings of the waveforms from each phase are different so cannot supply the same output circuit and each phase must supply its own circuit. The

outputs from each phase can be connected together but not in the common series or parallel connections due to the time delay between waveforms. There are two possible ways of connecting the coils together in a 3-phase machine.

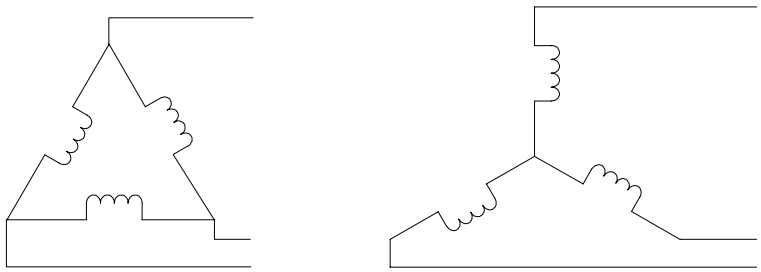

DELTA STAR

FIGURE 52
3-PHASE CONNECTIONS

The connection of each configuration has its own advantages and disadvantages, but suffice to say for a generator that 'star' connection will operate better at lower rotational speed but a 'delta' connection will produce a higher current at higher rotational speed.

There are reasons why 3-phase machines are preferred over single phase machines, in a three phase machine the space available is better utilised due to the layout of the windings. The output from a 3-phase machine is 'smoother' if the waveforms in figures 50 and 51 are compared it can be seen that the output from the single phase machines is pulsed whereas the 3-phase output is almost continuous.

In order to charge a battery using an AC generator the output power must be changed from AC to DC, a rectifier performs this change.

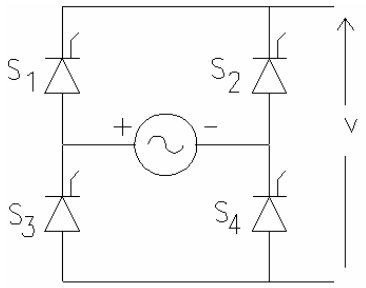

FIGURE 53
SINGLE PHASE RECTIFIER

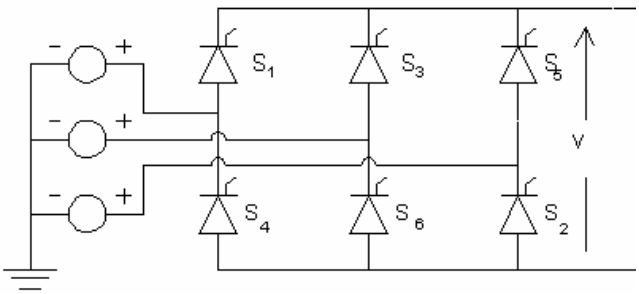

FIGURE 54
3-PHASE RECTIFIER

Figures 53 and 54 respectively show a bridge rectifier for a single and 3-phase connection. The output from each rectifier will produce a DC voltage.

If no load is connected to the output of the generator (whether AC or rectified DC) the voltage will continue to increase with rotational speed. When a load is connected and power is being drawn from the generator, a voltage drop will occur. This voltage drop is due to a number of factors including losses in the windings, changes in flux and the voltage of the battery. When charging a battery using a bridge rectifier the output from a phase has to pass through 2 diodes (or thyristors), which have an internal voltage drop of 0.7V each. Therefore in order to charge a 12V battery the output from the generator must be at 13.4V. Varying certain characteristics of the generator can change the output voltage. If the rotational speed, turns per coil or flux are altered this will alter the generator output voltage. (Increasing any of these will increase voltage output.)

In a generator electrical energy is created by moving a coil within a magnetic field, now it does not matter whether it is the coil that is moving or the magnets. There are also different types of generator that relate to the direction of the magnetic flux. The two types are axial field and radial field.

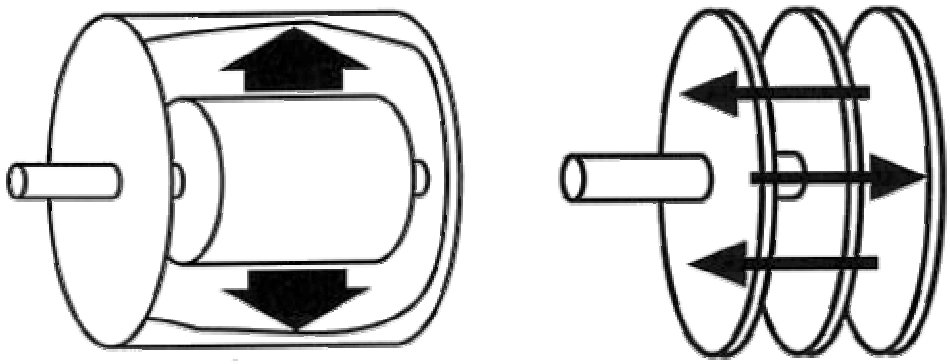

FIGURE 55 [19]
RADIAL AND AXIAL FIELDS

Figure 55 shows the difference in construction of axial and radial field machines. In the axial field machine the flux lines are parallel to the shaft and in a radial machine the flux lines are perpendicular to the shaft. It is often easy to tell by appearance what type of machine the generator will be. An axial field machine will often be thin but

have a large diameter (a pancake shape) whilst a radial field machine will have a longer body and often smaller diameter (a cylindrical shape).

In order to characterise the generators, the generators and DC motor are coupled together.

9.2.2 Generator Testing

9.2.2.1 Test Equipment

The equipment required for this test procedure is as follows.

Equipment	Quantity
DC motor (shunt connected)	1
Marlec 1-ph generator	1
Marlec 3-ph generator	1
Chinese generator	1
Multimeter	7

The DC motor characteristics are detailed in section 9.1.3.1.

The output connections from the generators are wires, 3 wires for the 3-phase devices and 2 for the single phase. The wires were connected to bridge rectifiers where 2 single phase bridge rectifiers were used to make a 3-phase rectifier. The same rectifiers were used for all generators to keep any losses in the rectifiers constant.

The details for each generator tested are as follows:

Marlec 1-ph

Rated power:	90W
Coil winding:	Single phase
Type:	Axial Field – permanent magnet

Marlec 3-ph

Rated power:	100W
Coil winding:	3-phase
Type:	Axial Field – permanent magnet

Chinese

Rated power:	300W
Coil winding:	3-phase
Type:	Radial Field – permanent magnet

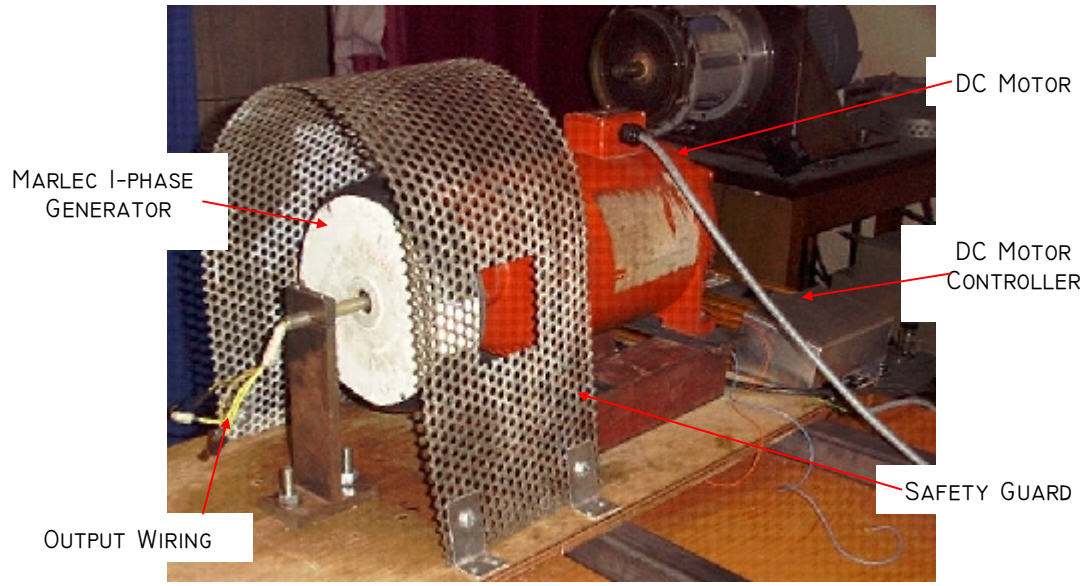

FIGURE 56
TEST SETUP

The seven multimeters are used to measure: Armature Voltage (V_A)
Armature Current (I_A)
Field Voltage (V_F)
Field Current (I_A)
Tachometer Voltage (V_{TACH})
Output Voltage (V_O)
Output Current (I_O)

It is essential when setting up equipment that the drive shafts of the motor and the generator are correctly aligned. If any misalignment occurs, permanent damage could be inflicted upon the generator by wearing out bearings and causing the coils and the magnets to rub together. Ensure that the alignment is correct by slowly rotating the generator by hand and checking for any sticky patches in the rotation. Once the alignment is correct proceed to testing of generator.

9.2.2.2 Test Procedure

9.2.2.2.1 No Load

Connect the output of the single phase Marlec generator to the AC terminals of the bridge rectifier.

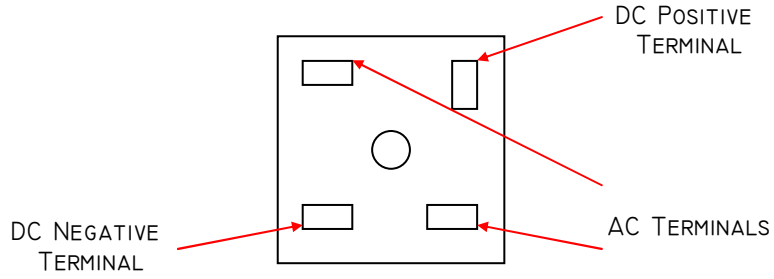

FIGURE 57
SINGLE PHASE BRIDGE RECTIFIER

The connections on a bridge rectifier are always as shown in figure 57 with the positive DC terminal perpendicular to all other terminals.

Connect multimeters to the Tachometer and the DC terminals of the rectifier.
Switch on the motor and run it at a speed of 100RPM. (Use figure 43 – Tachometer Speed/Voltage Table).
Note readings.
Increase speed to 200RPM and note readings.
Repeat procedure for speeds up to 1000RPM

Repeat the testing on all generators.

The connections to make 2 single phase rectifiers into a 3-phase rectifier are shown in figure 58.

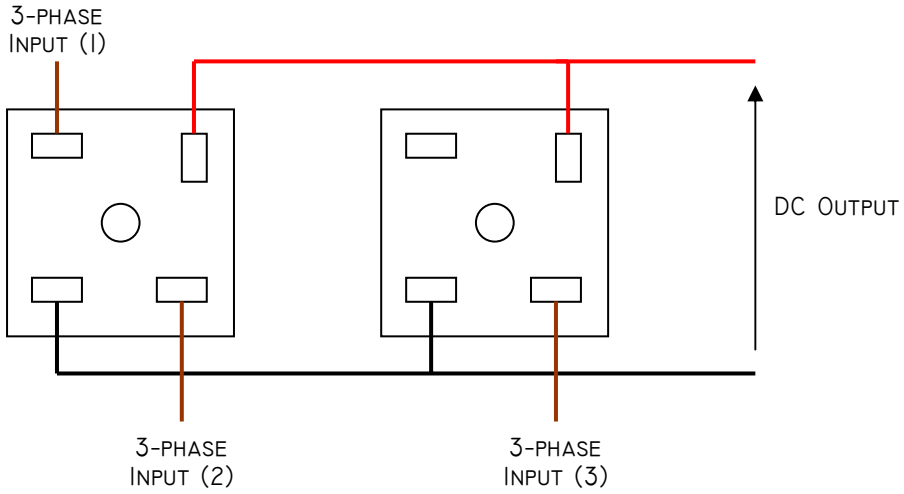

FIGURE 58
3-PHASE BRIDGE RECTIFIER

9.2.2.2.2 Resistive Loads

Connect the output of the single phase Marlec generator to the AC terminals of the bridge rectifier.
Connect the DC terminals of the bridge rectifier to the load.
Connect all seven mulitmeters to the connections in section 9.2.2.1
Switch on the motor and run it at a speed of 100RPM. (Use figure 43 – Tachometer Speed/Voltage Table).
Note readings on all multimeters.
Increase speed to 200RPM and note all readings.
Repeat procedure for speeds up to 1000RPM or until the power output exceeds the ratings on the resistive loads.
Change the resistive load and repeat testing.

Repeat the testing on all generators.

9.2.2.2.3 Battery Charging

Connect the output of the single phase Marlec generator to the AC terminals of the bridge rectifier.
Connect the DC terminals of the bridge rectifier to the generator.
Connect all seven mulitmeters to the connections in section 9.2.2.1.
Switch on the motor and run it at a speed of 100RPM. (Use figure 43 – Tachometer Speed/Voltage Table).
Note readings on all multimeters.
Increase speed to 200RPM and note all readings.
Repeat procedure for speeds up to 1000RPM or until the voltage of the battery exceeds 15V or the current limit on the multimeter is exceeded.

Repeat the testing on all generators.

9.2.3 Results

The results from the testing were entered into the software package Microsoft Excel where the data could be tabulated and graphed.

9.2.3.1 No Load Results.

The results from the testing under no load where the open circuit voltage could be graphed are shown in figure 59.

FIGURE 59
NO LOAD TEST RESULTS

Figure 59 shows that the Chinese generator produces the largest open circuit voltage with the 3-phase Marlec producing a higher voltage than the single phase. This is the expected result as a 3-phase machine is more efficient than a single phase machine and the Chinese generator has the highest power rating.

9.2.3.2 Resistive Load Results.

The testing of the generator using resistive loads was conducted using a combination of 3 x 10Ω - 100W resistors and a large variable resistor.

The loads used were: 3.3Ω, 4.7Ω, 5Ω, 8Ω, 10Ω, 25Ω, 50Ω and 100Ω.

The original testing did not measure the power input to the DC motor but did manage to give a characteristic for the generator performance against various loads.

Figures 60, 61 & 62 show the results for the 3 generator types.

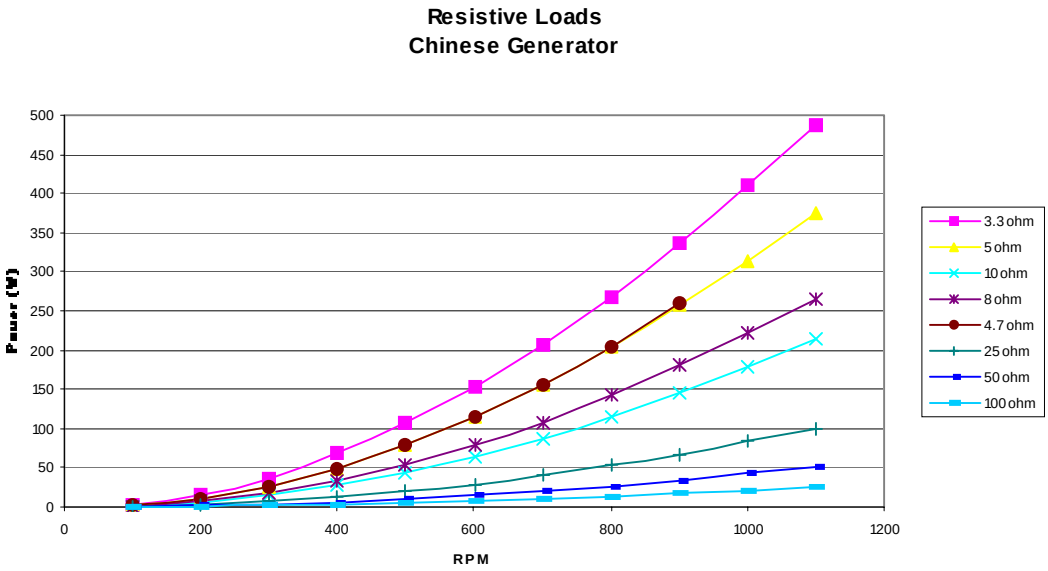

FIGURE 60
CHINESE GENERATOR RESISTIVE LOADS

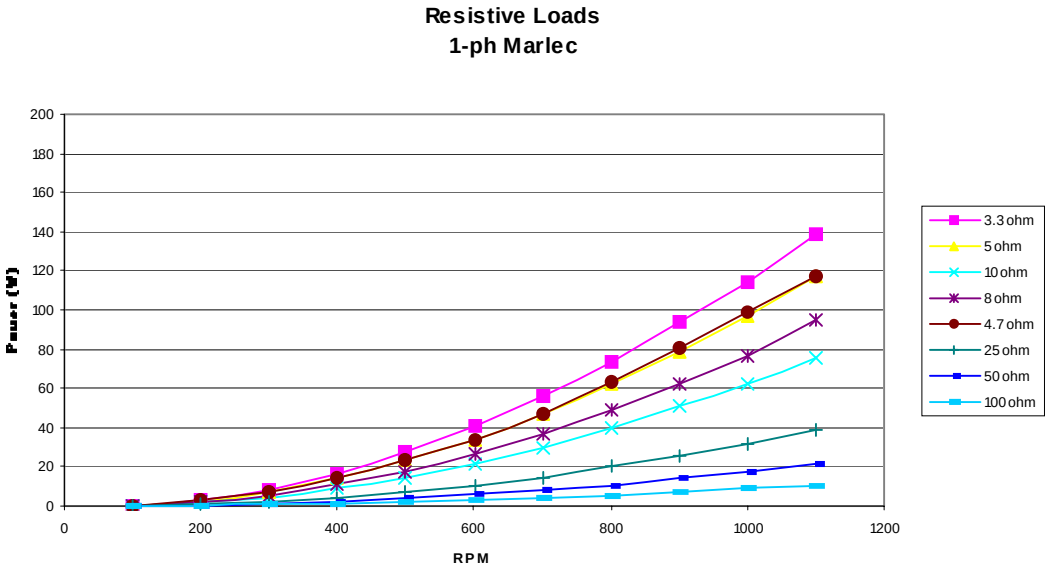

FIGURE 61
1-PH MARLEC RESISTIVE LOADS

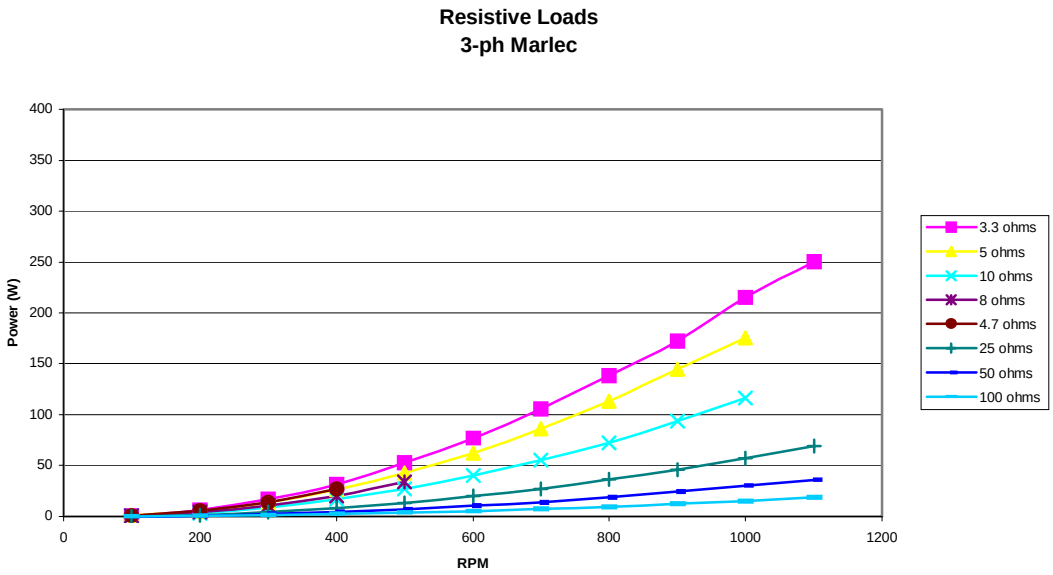

FIGURE 62
3-PH MARLEC RESISTIVE LOADS

The results show that the generators perform better whilst powering a low value resistance. This is as would be expected, as a lower resistance value provides an easier path for the current produced from the generator. If the current path is easier it allows for more current to be 'pushed' through the resistor and this will give a greater current due to the electrical law:

$$p = I^2 R$$

EQUATION 75

Therefore by doubling the current the power will increase four times.
These results show that the generators will supply the most current to a load with a low value of resistance.

9.2.3.3 Battery Charging Results

The results from the testing of the generators performance whilst charging a 12V, 75Ah lead acid battery are shown in figure 63.

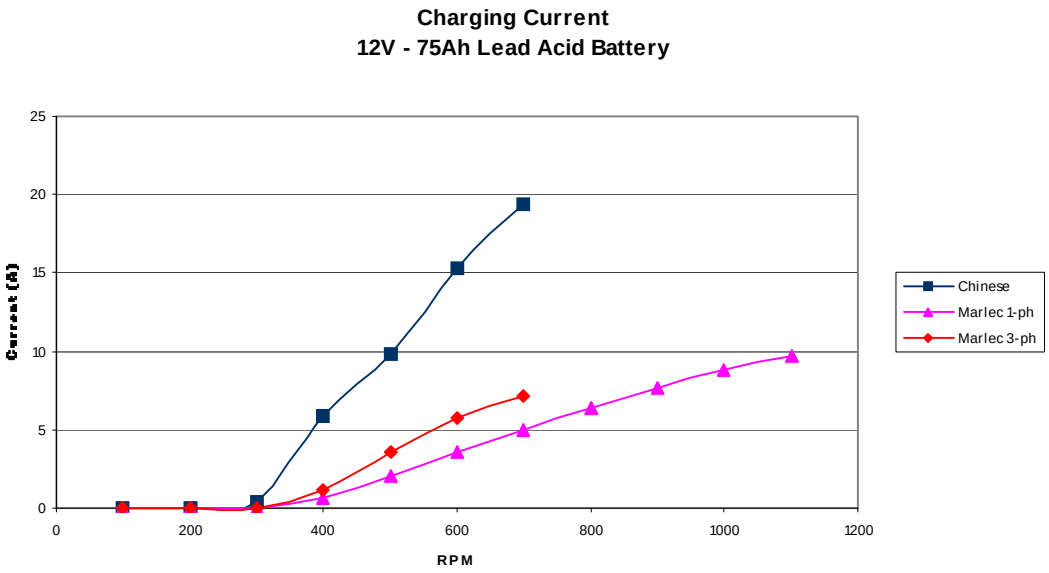

FIGURE 63
BATTERY CHARGING CURRENTS

The results shown in figure 63 are also as expected. The largest current produced is from the Chinese generator with the 3-ph and 1-ph Marlec in decreasing order. The power rating of the Chinese generator is the greatest of all the generators whilst the 3-ph winding of the 3-ph Marlec increases the power output compared to the 1-ph but it can be seen that they exhibit similar operating characteristics.

The figures from the spreadsheets used to create all charts can be found in Appendix 2.

9.3 Complete Generator Characterisation

The results from sections 9.1 and 9.2 have provided information regarding the operating characteristics of both the DC shunt motor and the 3 available generators, but this has not given the complete characteristics of the generators.

Using the results from testing on all devices it is possible to combine the results to provide a complete set of characteristics for the generators.

9.3.1 Combination Theory

In order to characterise the performance of the generators in full, the efficiency of the generators are required to be known. In order to calculate the efficiency of the generators the power inputs are required to be known.

$$\eta = \frac{P_{OUT}}{P_{IN}} \times 100\%$$

EQUATION 76

If the whole system is considered: The DC motor shaft is directly coupled to the shaft of the generator, so the power out from the motor will be the power into the generator. (Assuming no or negligible losses in the coupling.)

If the power output (or torque) from the DC Motor is known then this is also the input power to the generator. The torque value can be found due to the relationship with power and rotational speed.

$$p = \omega T$$

EQUATION 77

So by using the equations from the calibration of the DC motor the motor output power (generator input power) can be calculated, the power outputs from the generators are known so the generator efficiencies can be calculated and the required torque on the shaft can be found.

The results for each generator were plotted using both the measured torque values from the dynamometer that gave rise to the polynomial equations and also the theoretical values using the kϕ constant. On the charts the data marked (A) uses the polynomial equations whereas the data marked (B) uses the kϕ constant.

9.3.2 Chinese Generator Results

The results from the testing of the 300W Chinese radial field generator are detailed in this section.

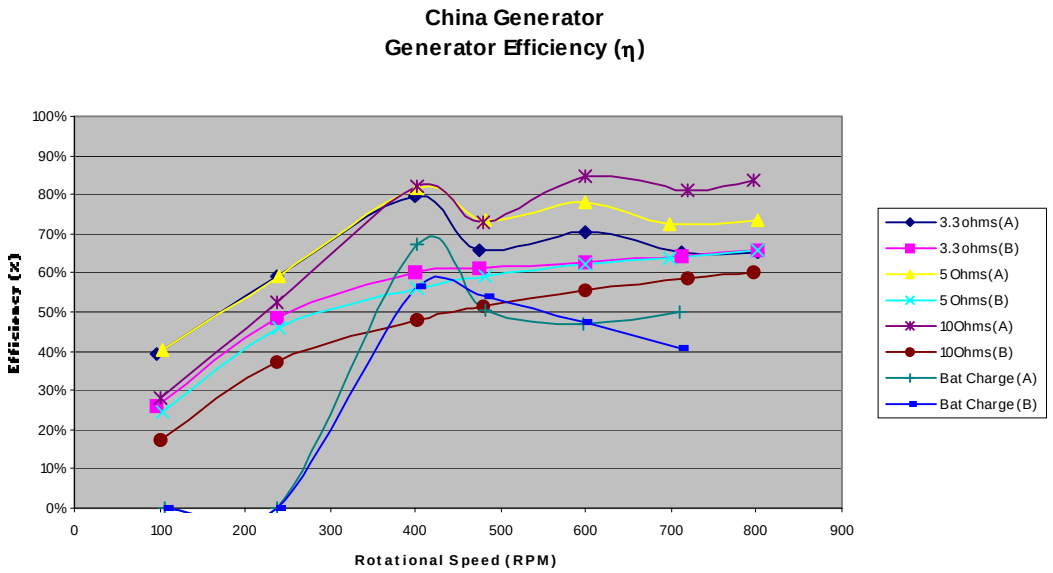

FIGURE 64
CHINA GENERATOR EFFICIENCY

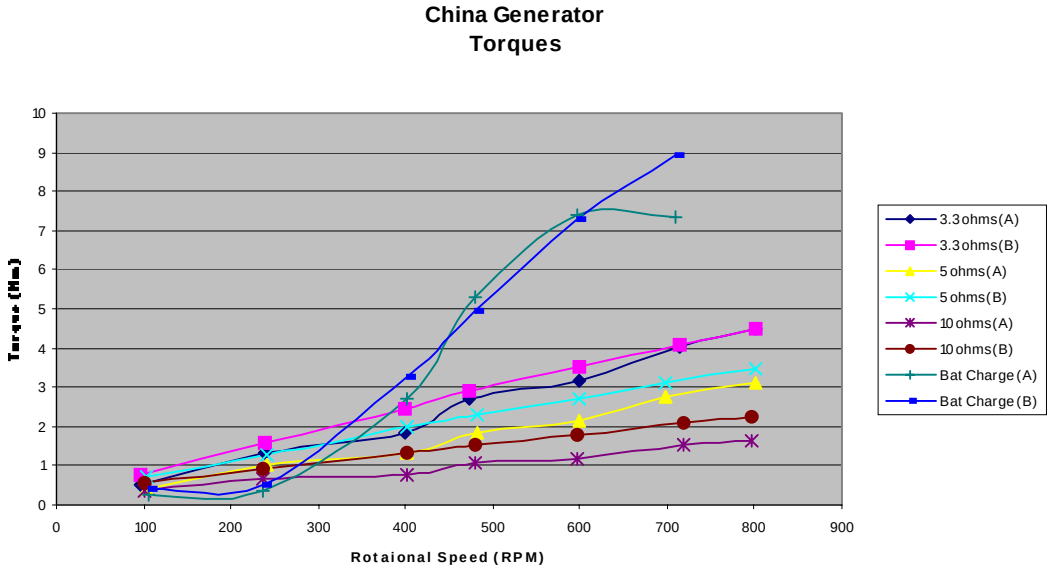

FIGURE 65
CHINA GENERATOR TORQUES

Figure 64 shows the efficiency of the Chinese generator, as mentioned the data marked (A) represents the polynomial efficiency curve method. The polynomial method provides results that provide greater efficiency and lower values of torque, as would be expected. The results are somewhat dubious though as they show that the generator reaches efficiencies of 85%. This is highly unlikely and a more reasonable value of efficiency would be in the 60 –70% range. (For the Marlec 3-ph generator the generator efficiency becomes greater than 100%, which is impossible.) It was

therefore decided that the method using the calculated value of kϕ would provide the most accurate information regarding the equipment.

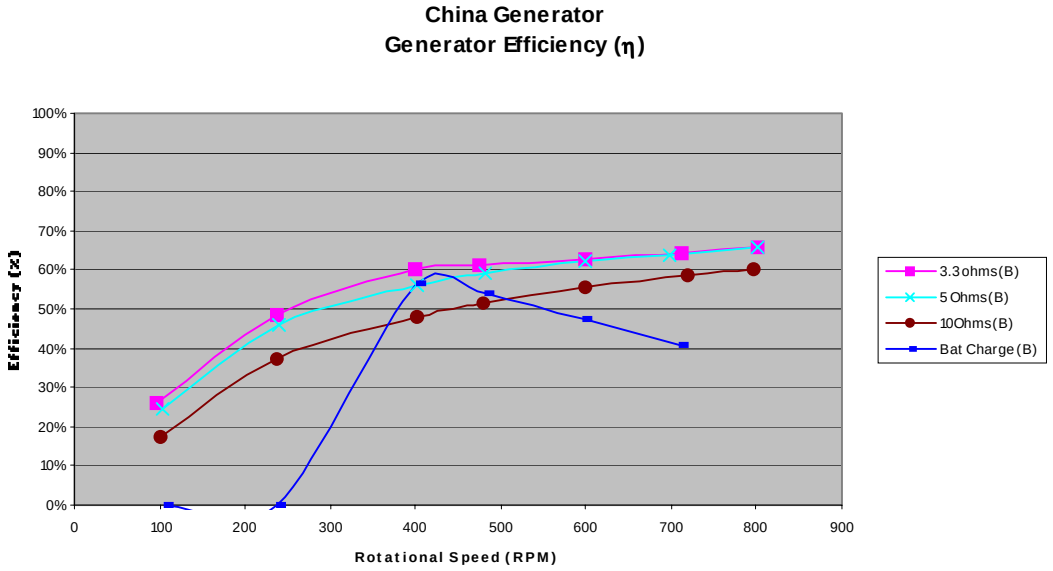

FIGURE 66
CHINA GENERATOR EFFICIENCY (Kϕ)

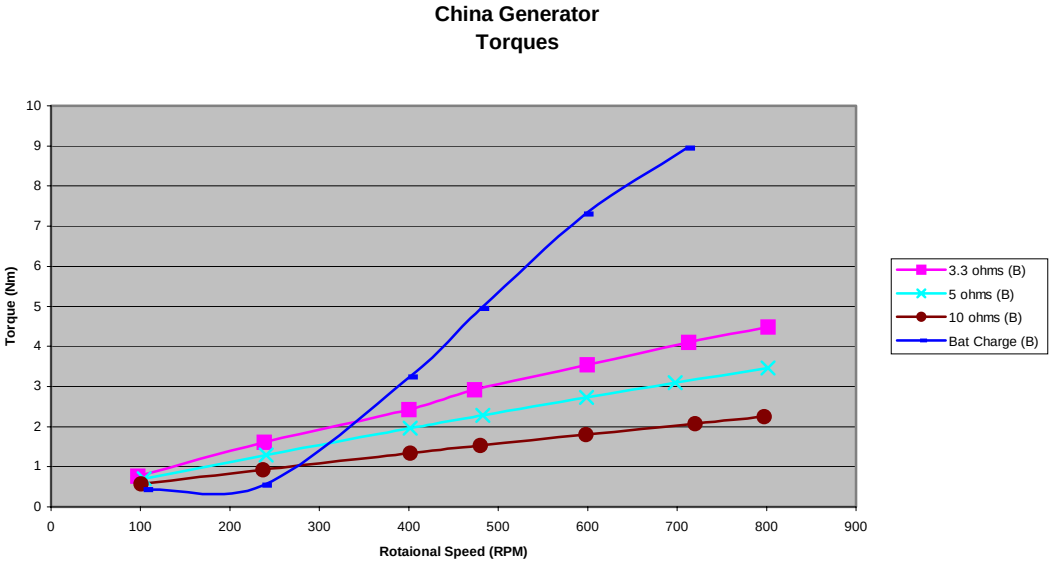

FIGURE 67
CHINA GENERATOR TORQUES (Kϕ)

The charts show results that would be expected. The lowest value of torque is required to rotate the highest value of resistance. Looking back at equation 75 it can be seen that to provide the same amount of power to a higher resistance would require a lower current, therefore less current being forced though the coils and less mechanical resistance, so less torque.

The largest torque is required when charging the 12V battery. As the charge in the battery increases it becomes increasingly more difficult to supply a charging current, and increasingly more difficult to supply larger currents through the windings. This has the effect of effectively lowering the value of resistance of the battery and therefore increasing the torque required to supply power to it.

Looking at the efficiency curves the battery charging mode has a very sharp rise and fall with a peak of approximately 60%, the sharp decrease is because of the relationships between torque, resistance and output current. The torque and output current exhibit a linear relationship as shown in figure 68 but the torque and resistance exhibit a power relationship (figure 69). So a decrease in resistance will make the torque value rise to the power of the relationship whereas the output current will only exhibit a linear increase. The efficiency curves for the resistive loads rise to approximately 65% and level out. This value of efficiency is approximately what would be expected. Using the data provided the generator coils do not reach a potential difference great enough to provide current to the battery until approximately 400RPM, this represents the cut in rotational speed of the generator. Correlating the data from the charts a torque of 3.35Nm is required before the generator will provide any power to the battery system.

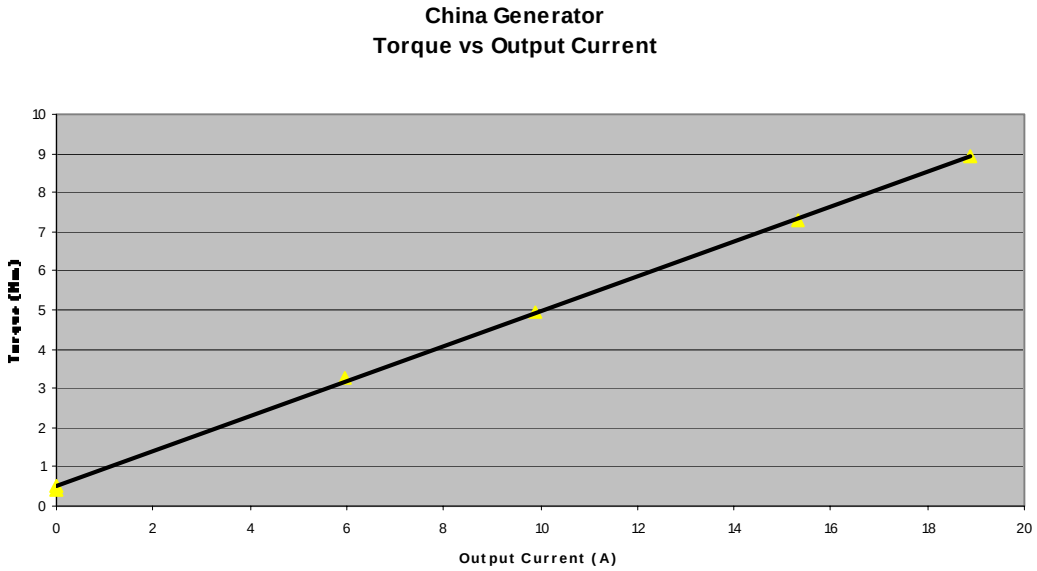

FIGURE 68
CHINA GENERATOR TORQUE VS OUTPUT CURRENT

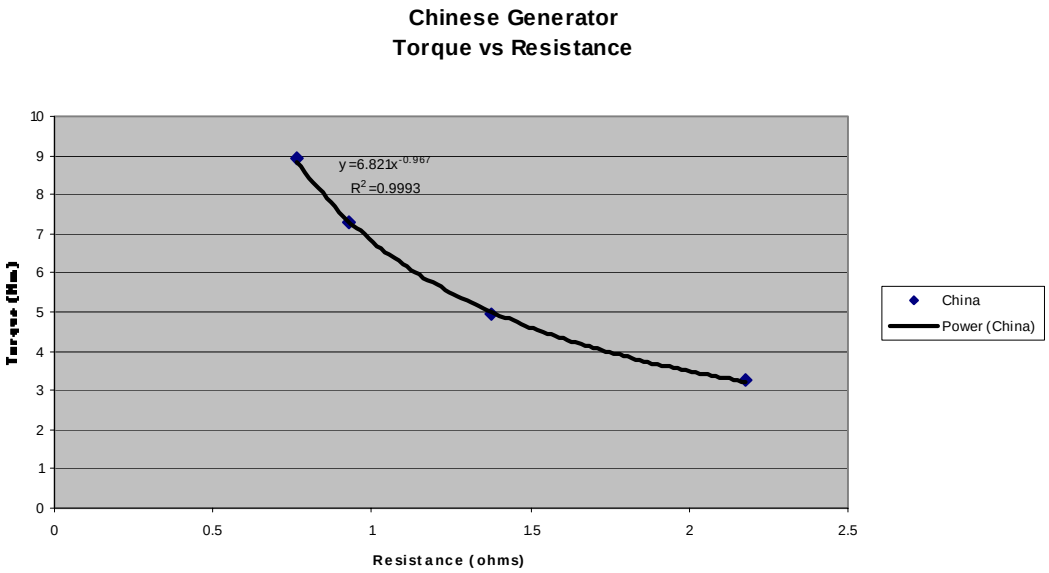

FIGURE 69
CHINA GENERATOR TORQUE VS RESISTANCE

9.3.3 Marlec 1-ph Generator Results

The results from the testing of the 90W Marlec single-phase axial field generator are detailed in this section and only contain the results from the correlation theory using the calculated kϕ value.

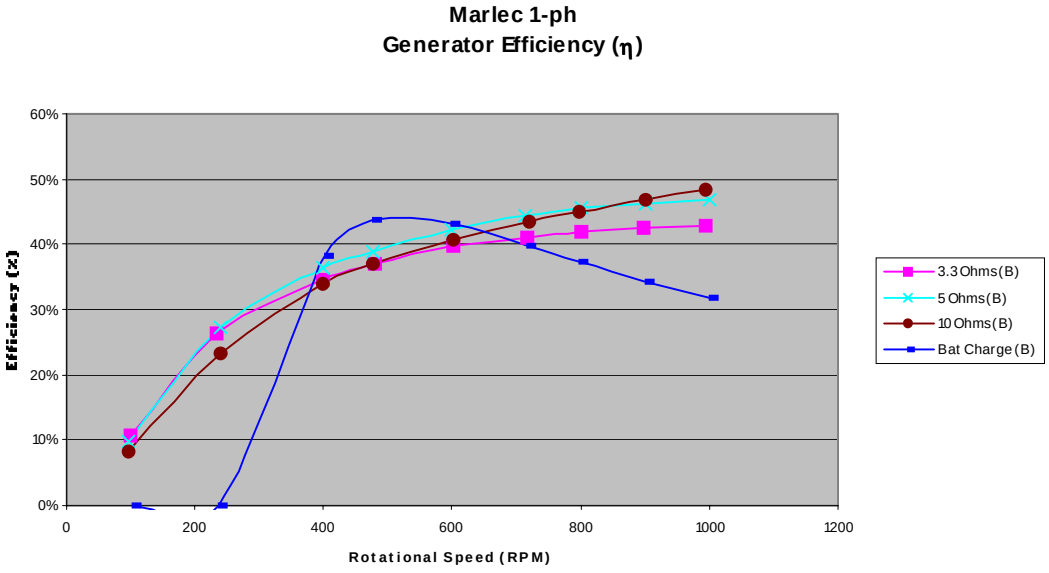

FIGURE 70
MARLEC 1-PH GENERATOR EFFICIENCY

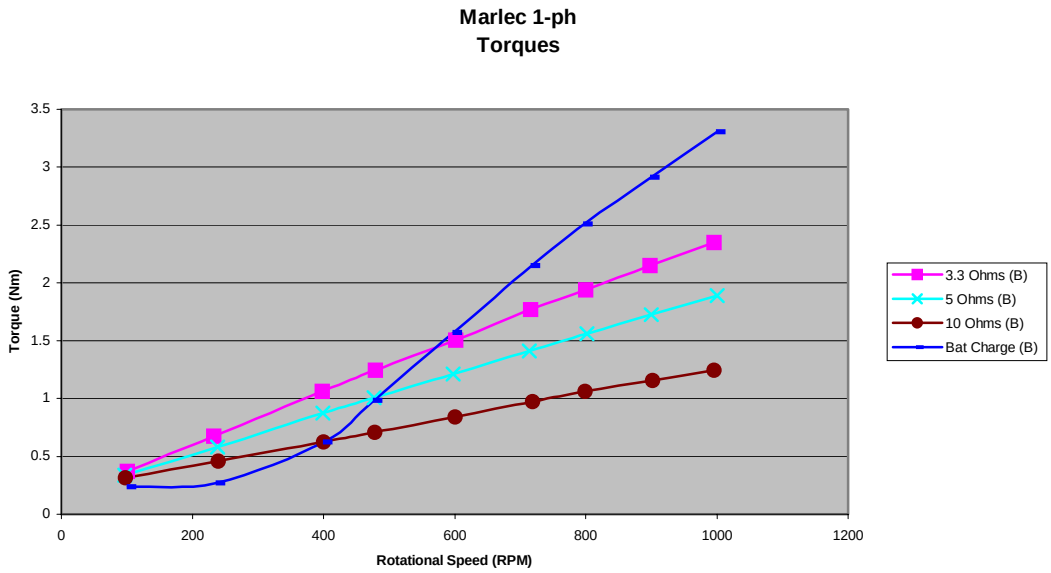

FIGURE 71
MARLEC 1-PH GENERATOR TORQUES

Again the charts show the same expected results as discussed for the Chinese generator, with the lowest torque for the highest resistance and the highest torque for the battery charging mode. Again a rotational speed of approximately 400RPM is required before the generator will start supplying a charging current to the battery and from the charts above this corresponds to a torque of 0.6Nm. The torque value increases linearly with output current and this is shown along with the other generator correlations in figure 77. The peak efficiency for the battery charging mode is approximately 400RPM (cut in speed) and the efficiency for the resistive loads rises to approximately 45%.

9.3.4 Marlec 3-ph Generator Results

The results from the testing of the 100W Marlec 3-phase axial field generator are detailed in this section and only contain the results from the correlation theory using the calculated $k\phi$ value.

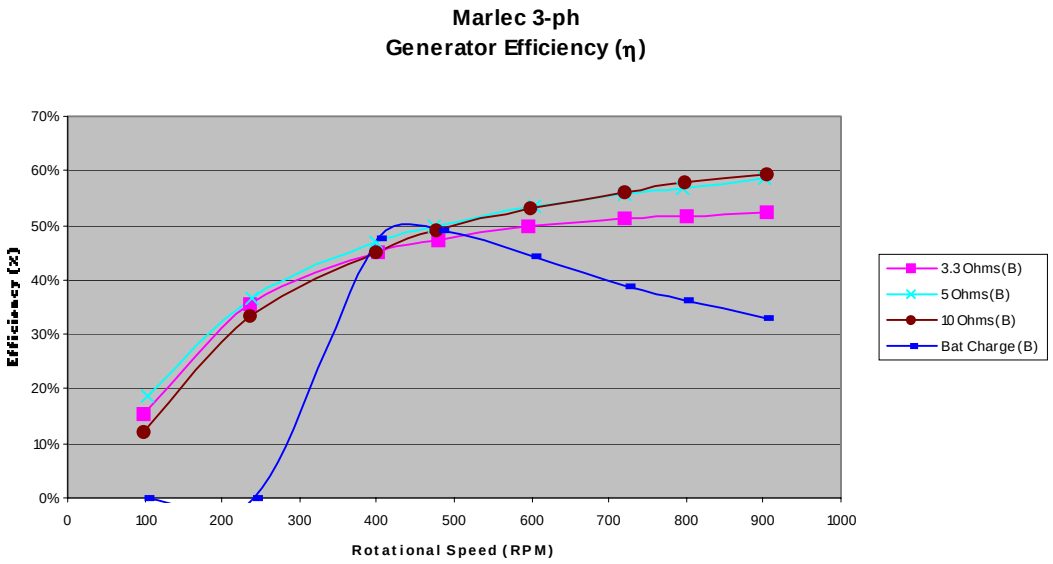

FIGURE 72
MARLEC 3-PH GENERATOR EFFICIENCY

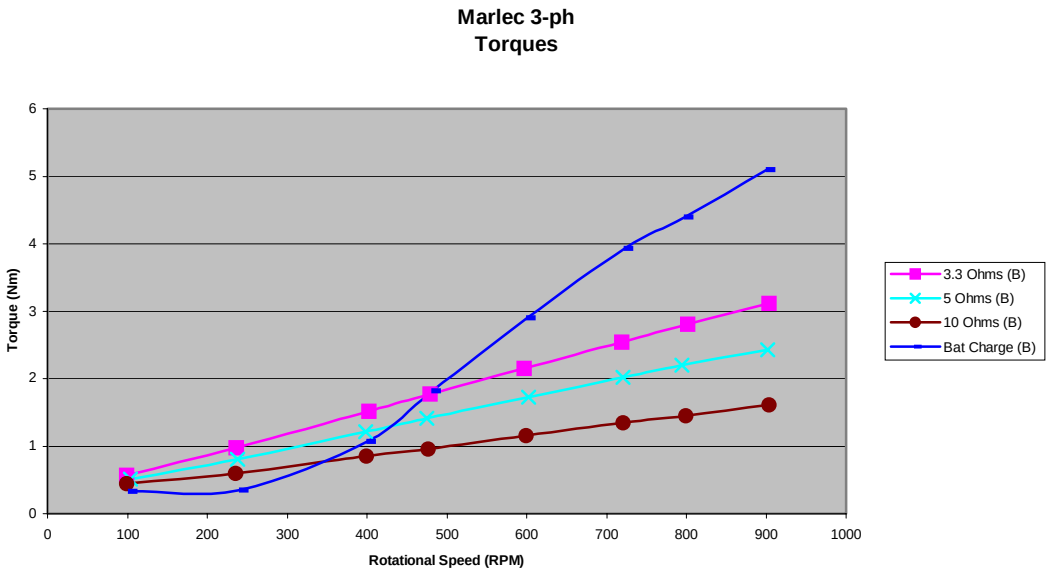

FIGURE 73
MARLEC 3-PH GENERATOR TORQUES

Figures 72 & 73 show the same expected results as discussed for the Chinese and Marlec 1-Ph generator, with the lowest torque for the highest resistance and the highest torque for the battery charging mode. Again a rotational speed of approximately 400RPM is required before the generator will start supplying a charging current to the battery and from the charts above this corresponds to a torque of 1.1Nm. The torque value increases linearly with generator output current and is shown with the other generator correlations in figure 89. The peak efficiency for the

battery charging mode is approximately 400RPM (cut in speed) and the efficiency for the resistive loads rises to approximately 50%.

9.3.5 All Results

The following charts aim to show a comparison of performance of the three generators tested.

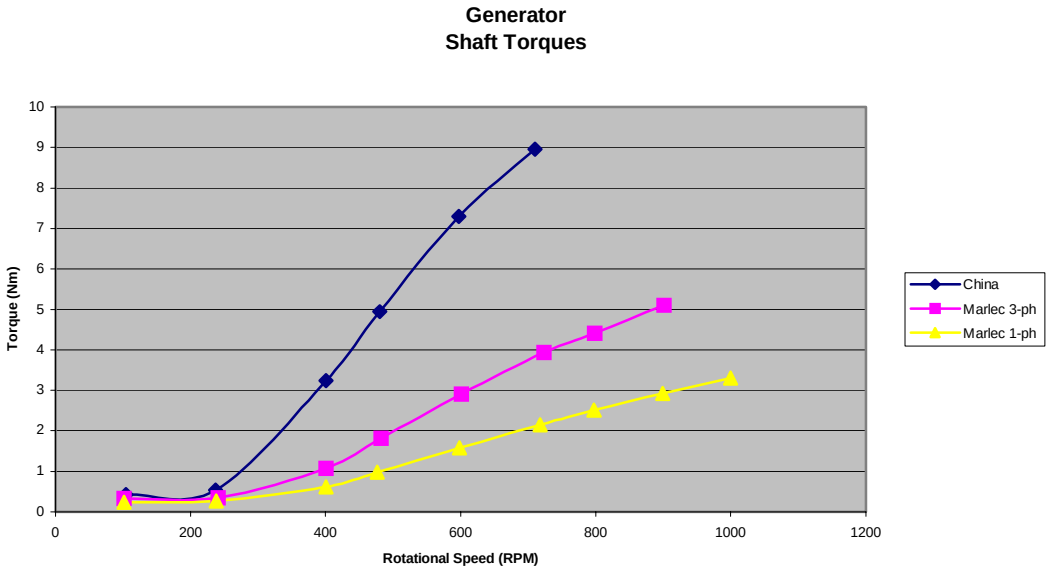

FIGURE 74
GENERATOR SHAFT TORQUES

The results shown indicate the torque required to rotate the shaft at the respective rotational speed, whilst charging the 12V lead acid battery. The greatest torque is required for the Chinese generator, as would be expected, because it is the highest rated generator so trying to induce more current in coils will require a greater input power to rotate shaft. The least torque is required for the Marlec 1-ph generator as this is the lowest rated generator and single phase so the power output is not as smooth and continuous, therefore the shaft torque is reduced from that of the 3-phase Marlec.

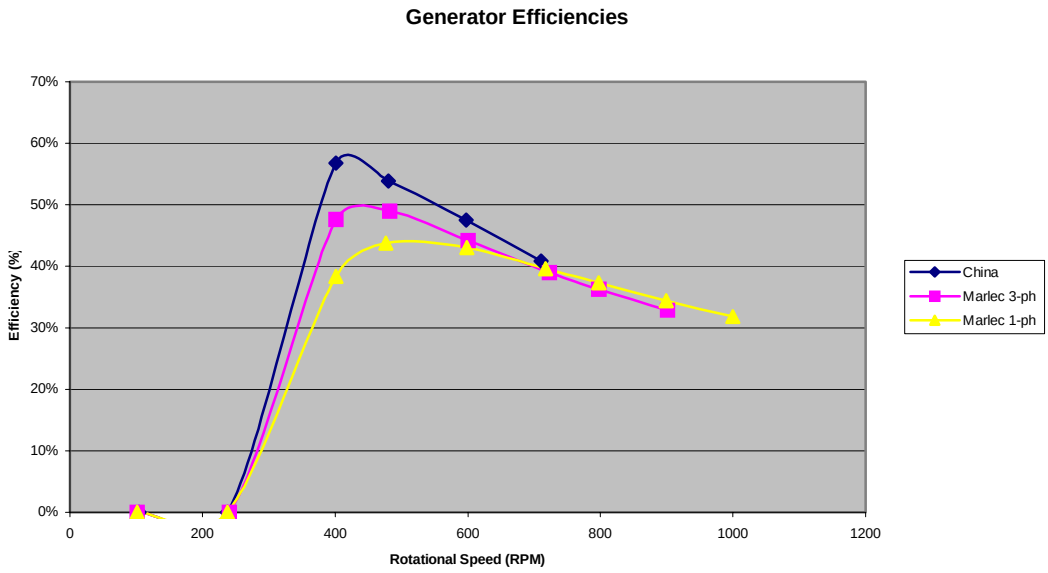

FIGURE 75
GENERATOR EFFICIENCIES

The efficiency of the generators, when charging the battery are shown in figure 75. The efficiencies peak at a relatively low rotational speed of around 400RPM (cut in speed). As expected the Marlec 3-ph generator has a greater efficiency that the single phase. This is a common advantage of 3-ph machines over 1-ph machines and why Marlec will have changed the device from 1-ph to 3ph. The reason is because of the smoother more continuous AC output the generator provides. The rates of efficiency decrease after the cut in speed vary, with the Chinese generator experiencing the steepest decrease and the single-phase Marlec experiencing the shallowest decrease. The reason for this difference in efficiency decrease rate is because of the currents each generator are trying to 'force' into the battery. As the Chinese generator is trying to supply the greatest current the apparent resistance of the battery will decrease the fastest with the single phase Marlec decreasing the slowest. Figure 76 shows the change in torque and resistance when each generator was used to charge the battery. As can be seen the resistance of the battery when starting to charge using the single phase Marlec is approximately 14Ω whereas when the Chinese generator is used the value is approximately 2Ω. So the curve of the Chinese generator is starting closer to the steepest part of the slope and hence will experience the greatest rate of efficiency reduction. The battery used in the testing was close to full charge, but if the battery was nearly empty the resistance torque relationship would still exist

with the same power relationship, except the resistance value would start at a much greater value.

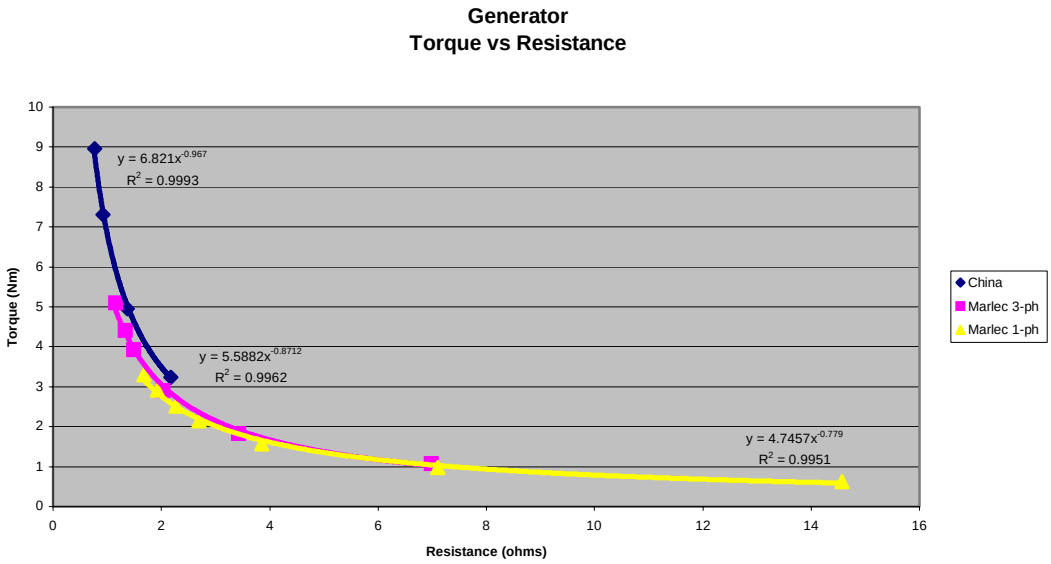

FIGURE 76
GENERATOR TORQUE / RESISTANCE RELATIONSHIPS

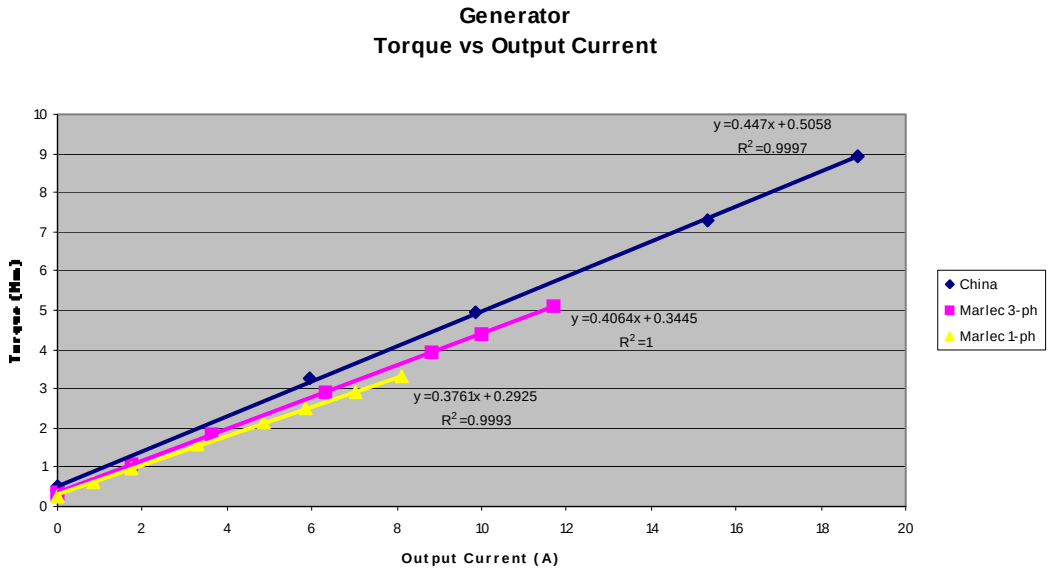

FIGURE 77
GENERATOR TORQUE / CURRENT RELATIONSHIPS

Figure 77 shows the generator torque values versus the output current values and it can be seen that the Chinese generator exhibits the steepest slope. This indicates that out of the three generators, an increase in output current will require the greatest increase in torque on the Chinese generator.

Figure 78 shows a table of data for the three generators at the various rotational speeds. The table allows a comparison of performance to be made for the generators. If the 400RPM speed is considered the Chinese generator requires 5.22 times more torque than the single phase Marlec but provides 7.18 times more current output. Tables of comparison are available for the various resistive loads in the Appendix.

Rotational Speed	Generator	Torque (Nm)	Efficiency (η)	Vout (V)	Iout (A)	Resistance (Ω)
100 RPM	Chinese	0.43	0	11.96	0	N/A
	Marlec 3-ph	0.33	0	12.05	0	N/A
	Marlec 1-ph	0.24	0	11.89	0	N/A
240 RPM	Chinese	0.53	0	11.96	0	N/A
	Marlec 3-ph	0.35	0	12.05	0	N/A
	Marlec 1-ph	0.27	0	11.89	0	N/A
400 RPM	Chinese	3.24	56.8%	12.98	5.96	2.18
	Marlec 3-ph	1.07	47.6%	12.22	1.75	6.98
	Marlec 1-ph	0.62	38.4%	12.09	0.83	14.57
480 RPM	Chinese	4.95	53.9%	13.58	9.88	1.37
	Marlec 3-ph	1.82	49.0%	12.43	3.63	3.42
	Marlec 1-ph	0.98	43.8%	12.36	1.74	7.10
600 RPM	Chinese	7.30	47.6%	14.18	15.32	0.93
	Marlec 3-ph	2.90	44.2%	12.8	6.31	2.03
	Marlec 1-ph	1.57	43.1%	12.78	3.32	3.85
720 RPM	Chinese	8.95	40.9%	14.42	18.88	0.76
	Marlec 3-ph	3.93	39.0%	13.16	8.81	1.49
	Marlec 1-ph	2.15	39.7%	13.14	4.88	2.69
800 RPM	Chinese					
	Marlec 3-ph	4.40	36.3%	13.34	10	1.33
	Marlec 1-ph	2.51	37.3%	13.34	5.87	2.27
900 RPM	Chinese					
	Marlec 3-ph	5.10	32.9%	13.54	11.69	1.16
	Marlec 1-ph	2.91	34.4%	13.47	7.01	1.92
1000 RPM	Chinese					
	Marlec 3-ph					
	Marlec 1-ph	3.31	31.8%	13.59	8.1	1.68

FIGURE 78
GENERATOR CHARACTERISTICS - BATTERY CHARGING

10.0 Field Testing of Marlec Generator

In order to characterise the performance of the readily available 3-phase Marlec generator a purpose built structure was erected to mount the turbine and to house data logging equipment.

The structure used to mount the turbine was a triangular pillar construction designed by W K McMillan Steel Fabricators as a mounting assembly for banners to be displayed. The design was altered to allow a turbine to be mounted at the top and the normal banners were replaced by UV (ultraviolet light) sensitive banners. In the middle of the structure UV lights were used as a load for the system and to illuminate the banners. The structure is shown in figure 79.

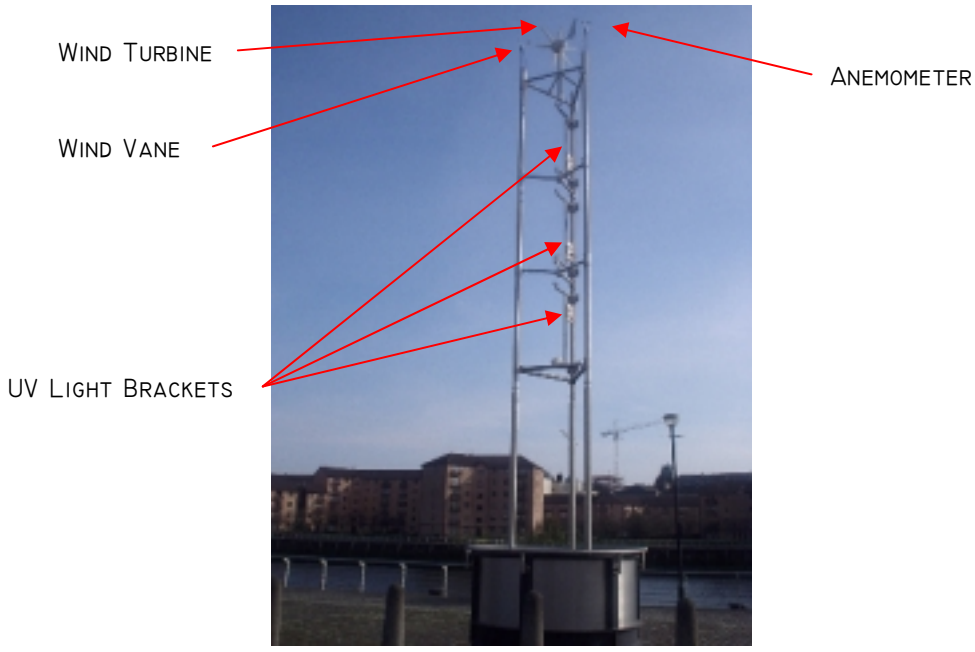

FIGURE 79
TOBLERONE STRUCTURE

In order to utilise and monitor the turbine system properly a control circuit is required.

10.1 Control Circuit

In order to properly exploit renewable energy it is important to have a control system in place to monitor the installation. When using batteries as the power storage medium it is imperative that they are properly maintained. Any battery has upper and lower limits of where the voltage should sit without causing damage to the battery itself. Values often taken for the upper and lower voltage levels on a 12V battery are 14.4V and 10.8V. A control circuit is therefore required that will monitor the voltage level of the battery and automatically maintain this safe working region.

In order to prevent the voltage rising above 14.4V a 'dump' load can be attached that will utilise any excess power generation and prevent the voltage level rising, at the other end a battery charging system can be attached to charge the battery when the voltage level has become too low. Figure 80 shows how the control system should operate, the red line represents the battery charger operation and the blue line represents the dump load operation.

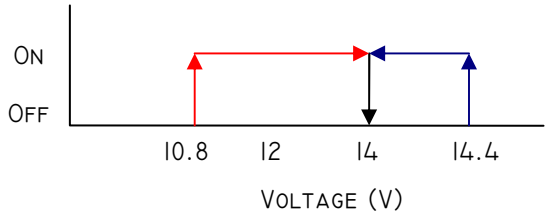

FIGURE 80
CONTROL SYSTEM OPERATIONS

This automatic switching requires the design and construction of two separate controllers. Each controller must have adjustable set points, which can control the switching on and off limits.

10.1.1 Dump Load Controller

The dump load controller circuit diagram is shown in figure 81. Near the left hand side of the controller are two potentiometers that control the switching levels of the circuit. Turning clockwise increases the switching voltage and turning anti-clockwise decreases the switching voltage. There are two switches incorporated onto the circuit board. The top switch is a 'Test' switch that can be used to check that the switching

action turns on the dump load. The switch is non-latching so has to be held down for the duration of the testing. The other switch is a reset button. Pressing the reset button will switch off the Dump Load as long as the button is held down, once the button is released the dump load will remain off as long as the voltage level is below the turn on threshold voltage.

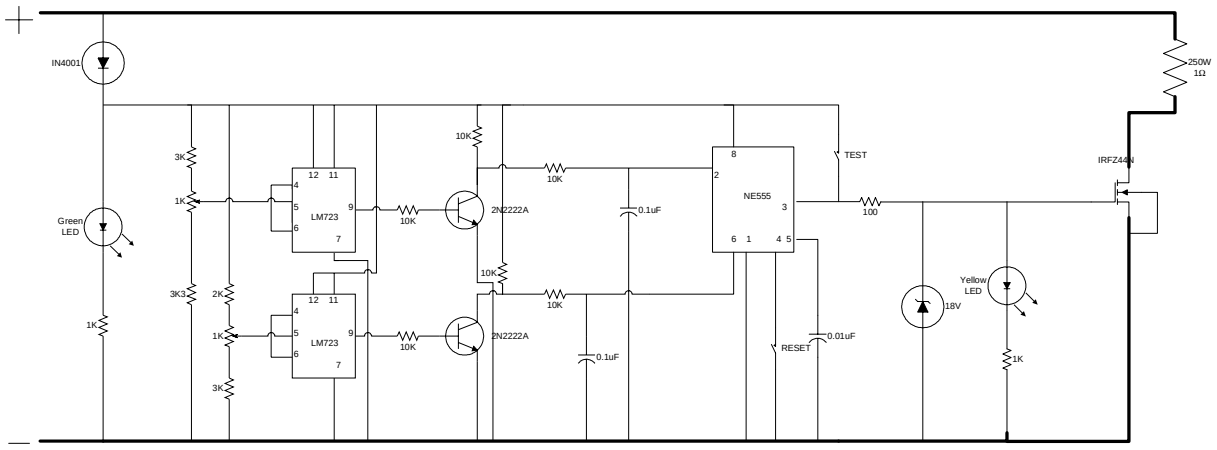

FIGURE 81
DUMP LOAD CONTROLLER - CIRCUIT DIAGRAM

The controller operates by using a voltage divider circuit with variable resistor to determine the on-off points. The output from the divider then goes into pin 5 of the LM723 voltage regulator. This IC (integrated circuit) operates by comparing the input from the divider with its reference voltage, once the input exceeds the reference, the series bypass transistor switches on and Vz (pin 9) goes high. The output from this is put through a resistor to provide 0.69V to operate the transistor and induce the input (pin 2) of the 555 timer chip to go to zero volts. The 555 timer works in the following way: when input (pin 2) drops below reference voltage (pin 5) the output (pin 3) goes high (12V). Pin 3 then stays high until the value of pin 6 rises above pin 5. The input to pin 6 uses another voltage divider and LM723 voltage regulator but has a lower activation voltage. Once pin 3 of the 555 timer is at 12V, the power Mosfet activates and connects the negative terminal to the battery, switching on the dump load. The two LEDs are to inform the user of the status, the green LED shows that there is power in the controller and the yellow LED shows that the dump load is on.

The power required for the dump load is determined by the output from the turbine and the maximum current value that it would have to absorb to prevent the batteries charging. Figure 82 shows a graph of the charging current into a 12V battery under various wind speeds. The wind speeds are measured in knots. (Figure 16 showed that 1knot = 0.514m/s.) It shows that a current of 18A will flow at wind speed of 38knots (19.532m/s) therefore a value can be calculated for the required dump load.

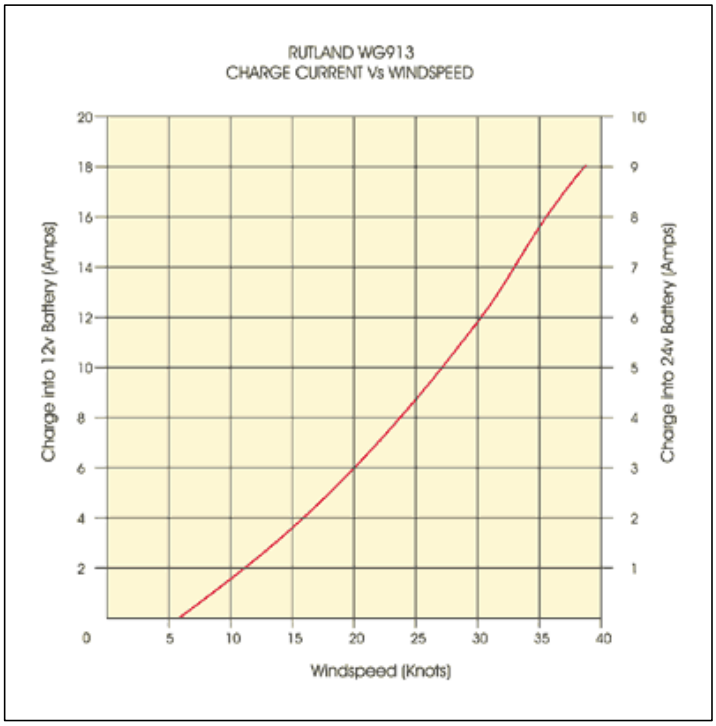

FIGURE 82 [20]
MARLEC GENERATOR - POWER OUTPUT

The power output can be calculated from equation 78.

$$p = IV$$
$$p = 18 \times 12$$
$$p = 216W$$

EQUATION 78

Using the power value calculated in equation 78 the resistor value for the dump load can be calculated from equation 75.

$$p = I^2 R$$
$$216 = 18^2 \times R$$
$$\therefore R = \frac{216}{18^2} = 0.666\Omega$$

A resistor value of 0.666Ω with a power rating of 216W is required. Unfortunately an exact match cannot be found (and in most cases is unlikely to be found) so an alternative is required. A resistor of value 1Ω with a power rating of 250W is selected and by re-arranging equation 75 the current it will absorb can be found.

$$p = I^2 R$$
$$250 = I^2 \times 1$$
$$\therefore I = \sqrt{250} = 15.811A$$

This resistor will absorb 15A, which should be more than enough for this application.

10.1.2 Battery Backup Controller

Figure 83 shows the battery backup controller circuit diagram. The layout of the circuit is almost identical to that of the dump load controller. Again at the left hand side of the controller are two potentiometers that control the switching levels of the circuit. The two switches are again incorporated with the 'test' and 'reset' switches. (Sometimes when turning battery power on the circuit sees a rise in voltage, so the initial voltage seen is below the desired level and switches on the charger, if the level then does not rise above the turn off voltage the charger will stay on, even though the battery voltage is within desired limits.) Pressing the reset button returns the control circuit switch to the off position.

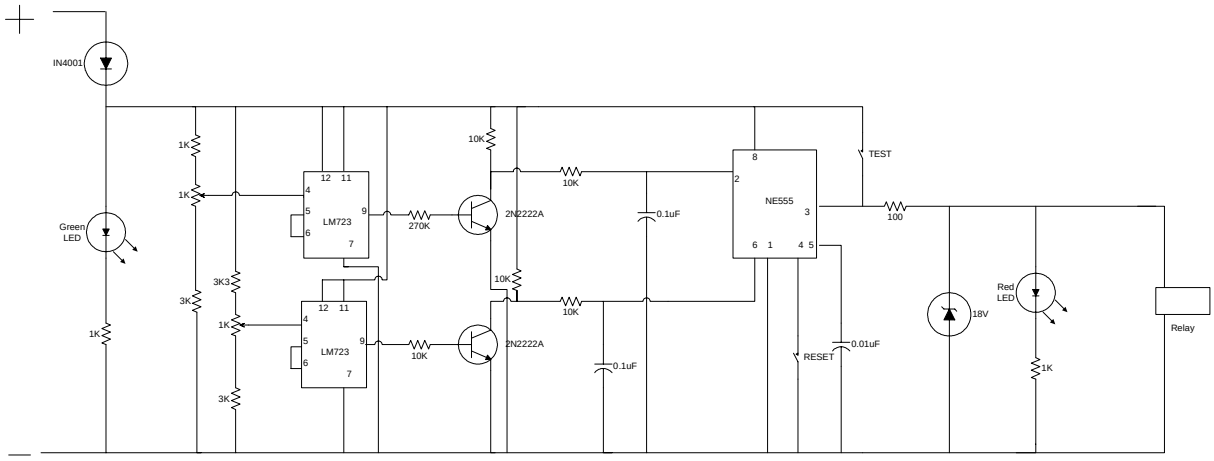

FIGURE 83
BATTERY BACKUP CONTROLLER - CIRCUIT DIAGRAM

The controller operates in exactly the same way as the Dump Load Controller except for one slight difference. The output from the voltage divider circuit goes into pin 4 (inverting input) instead of pin 5 (non-inverting input) of the LM723 voltage regulator, this means that the output (pin 9) goes high when the input voltage drops below the reference voltage. The LED showing that the circuit has switched on the battery charger is red this time.

A relay is used on the output of the control circuit this time instead of the power Mosfet utilised for the dump load controller. The relay connections are shown in figure 84.

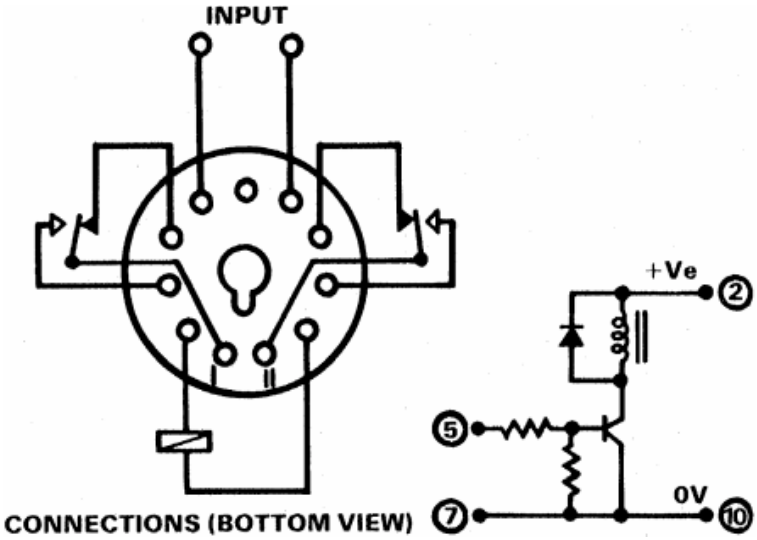

FIGURE 84 [21]
BATTERY BACKUP CONTROLLER - RELAY

The output from the control circuit is connected to pins 5 & 7 of the relay, which when high will turn on the transistor allowing the power to flow between pins 2 & 10 operating the relay switch. The relay has 2 switching channels with input pins 1 & 11 and output pins 3 & 9 (normally open) and output pins 4 & 8 (normally closed). The positive line of the battery charger is connected to pin 1 and the output to pin 3.

The above sections have shown the control elements of the circuit but in order to monitor and control the performance of the system other elements including fuses and indicator dials are required.

10.1.3 Control Circuit Wiring Diagram

The wiring diagram for the control circuit is shown in figure 85. It includes wiring for the 230Vac connections as well as the 12Vdc connections. The connections shown using heavy lines require cable of at least 2.5mm^2. The thin lines are low current cable and 1mm^2 will be sufficient.

The two DPST (Double Pole Single Throw) switches are used to isolate the 12Vdc and 240Vac supplies. The DPDT (Double Pole Double Throw) switch is used to toggle the power from the generator to either the batteries or directly to the dump load. The use of the diode is to ensure that when the generator is connected to the dump, no current can flow back up the cable to the +ve busbar and make the system live.

Control Circuit Wiring Diagram

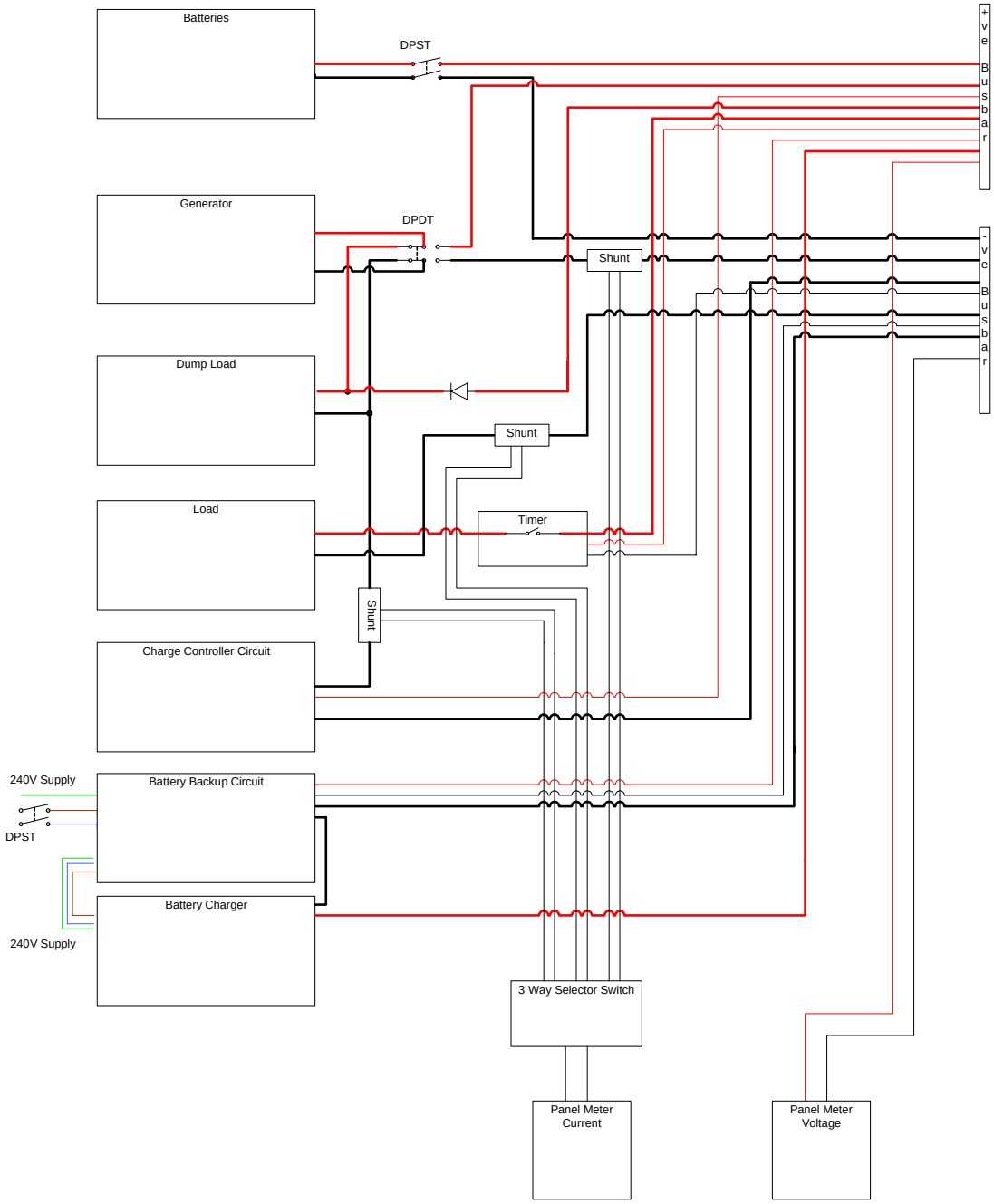

FIGURE 85
CONTROL CIRCUIT WIRING DIAGRAM

The current shunts are connected to a panel meter, which displays the current flow in the respective shunt depending upon the location of the selector switch.

The control circuit has been created to allow control and monitoring of the turbine installation but in order to record the data requires the use of a data logger.

10.2 Data Logger

A record of the various values of voltage and current from each device requires the use of data logging equipment. The equipment used for logging will be a 'Delta-T Logger' produced by 'Delta-T Devices LTD' in Cambridge, London. The Delta-T logger is a programmable data logging device that is capable of taking, and storing, readings from a wide range of devices. The device is independently powered powered by either a 12Vdc power supply or six AA batteries. Computer software supplied by the company is required to configure the logger to the user's desired combination of sensors and sampling strategy. After the logger has recorded the required data it can be downloaded to a computer for analysis.

The logger shall be configured to record data on all desired channels every five seconds and then compress these values over a one minute period. The outputted data will only show a reading every minute but the actual value will be the average of all readings taken during that minute. The data logger is able to measure values of voltage but not current, so the current value is recorded as a voltage value with the use of a shunt resistor. The maximum input voltage allowed by the data logger is two volts and this is why a voltage divider circuit (figure 86) is required when recording values of battery voltage.

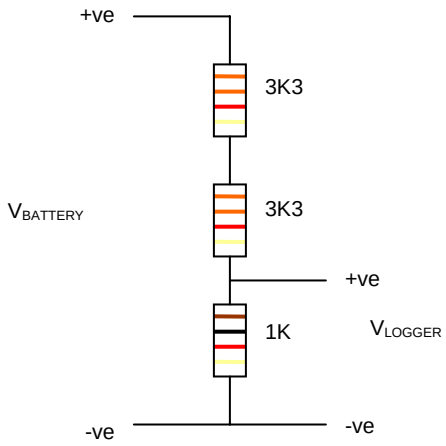

FIGURE 86
VOLTAGE DIVIDER CIRCUIT

Equation 79 shows how the voltage divider circuit reduced the voltage to be recorded on the logger.

$$V_{LOGGER} = V_{BATTERY} \times \frac{R_1}{R_T}$$
$$V_{LOGGER} = V_{BATTERY} \times \frac{1}{7.6}$$
$$V_{LOGGER} = \frac{V_{BATTERY}}{7.6}$$

EQUATION 79

If the maximum voltage of the battery is 15V, the maximum voltage registered on the logger will be:

$$V_{LOGGER} = \frac{15}{7.6}$$
$$V_{LOGGER} = 1.973V$$

The voltage divider circuit has therefore reduced the voltage enough to be recorded on the logger. The recorded values are imported into the software package Microsoft Excel where the data is processed to produce meaningful values. In Excel the recorded value of voltage for the battery is multiplied by 7.6 to show the true battery voltage level. (The logger records in mV so the value is also divided by 1000 to show volts.)

The current values recorded use a current shunt rated at 75mV, 30A. This gives a resistance of 0.0025Ω (equation 81). In order to show the true current flows in the system the values of voltage recorded across the current shunts are divided by 0.0025. (re-arrange equation 80 to get current)

$$V = I \times R$$
$$R = \frac{V}{I}$$
$$R = \frac{0.075}{30}$$
$$R = 0.0025\Omega$$

EQUATION 80

All values of voltage and current from the system can now be recorded but the values of wind speed and wind direction must also be recorded.

10.2.1 Anemometer

As previously mentioned in section 4.2.1 the anemometer utilised in this project is an A100L2 Anemometer produced by Vector Instruments. The output from the anemometer is a voltage of 0-2.5Vdc for a wind range of 0-150 knots. This wind speed is equivalent to 77m/s or 172mph, which is very unlikely to be seen so no voltage reduction is required and the anemometer output can be connected straight to the data logger.

In order to process the voltage values recorded the correlation between voltage and wind speed has to be known. If the 2.5V is divided by 150knots the correlation seen is: 16.67mV/knots. In Excel the recorded value of voltage is divided by 16.67 to show the wind speed in knots and then multiplied by 0.5144444 to show wind speed in m/s.

10.2.2 Wind Vane

As previously mentioned in section 4.2.2 the wind vane utilised in this project is a W200P wind vane produced by Vector Instruments. The W200P utilises a potentiometer with a 1kΩ resistance, where the resistance changes depending upon the wind direction. To record the wind direction a voltage is applied across the end terminals of the potentiometer and the voltage across one terminal and the vane wiper is recorded to show the wind direction. Figures 87 – 88 show the theory.

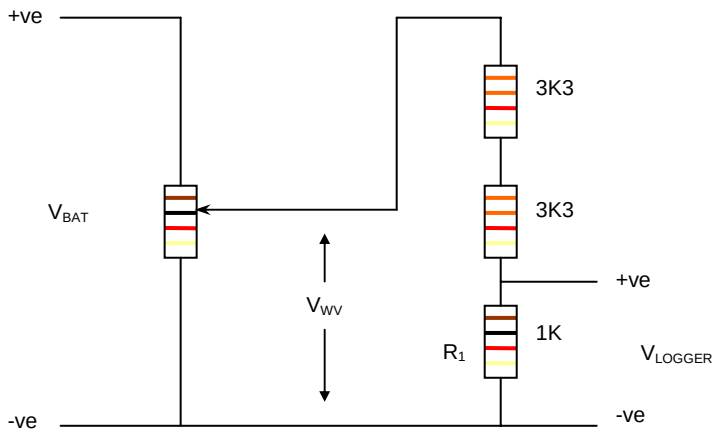

FIGURE 87
WIND VANE WIRING CIRCUIT

To analyse the circuit it is easier to split into two parts then recombine.

The right-hand side of the circuit is identical to the voltage divider circuit in figure 86 and the theory is the same.

$$V_{LOGGER} = V_{WV} \times \frac{R_1}{R_T}$$

$$V_{LOGGER} = \frac{V_{WV}}{7.6}$$

$$V_{WV} = V_{LOGGER} \times 7.6$$

EQUATION 81

The left hand side of the circuit is the actual potentiometer of the windvane and is shown in figure 88.

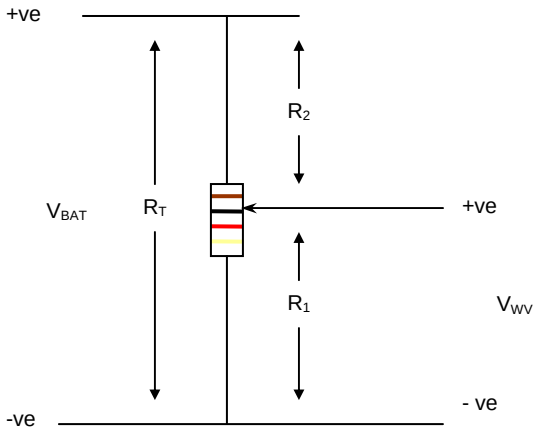

FIGURE 88
WIND VANE POTENTIOMETER CIRCUIT

$$V_{WV} = V_{BAT} \times \frac{R_1}{R_T}$$

$$\frac{V_{WV}}{V_{BAT}} = \frac{R_1}{R_T}$$

$$R_1 = \frac{V_{WV}}{V_{BAT}} \times R_T$$

$$R_1 = \frac{V_{WV}}{V_{BAT}} \times 1000$$

EQUATION 82

If the two circuits are now recombined, the value of V_{wv} can be substituted to give equation 83.

$$R_1 = \frac{V_{LOGGER} \times 7.6}{V_{BAT}} \times 1000$$

EQUATION 83

As the battery voltage has already been logged and the voltage from the windvane is being logged, Excel can execute equation 84 to show the resistance value of the potentiometer. The resistance indicates the position around the track that the variable arm is, hence indicates the direction of the wind. As the potentiometer has a small gap giving an electrical continuity angle of 357.7°, there are 2.796Ω per degree, therefore to calculate the angle of the wind equation 84 is used.

$$\theta = \frac{R_1}{2.796}$$

EQUATION 84

In order to record the wind angle as a standard metrological direction, figure 89 shows the separation angles and an 'IF' statement is used in Excel to show the angle as a direction.

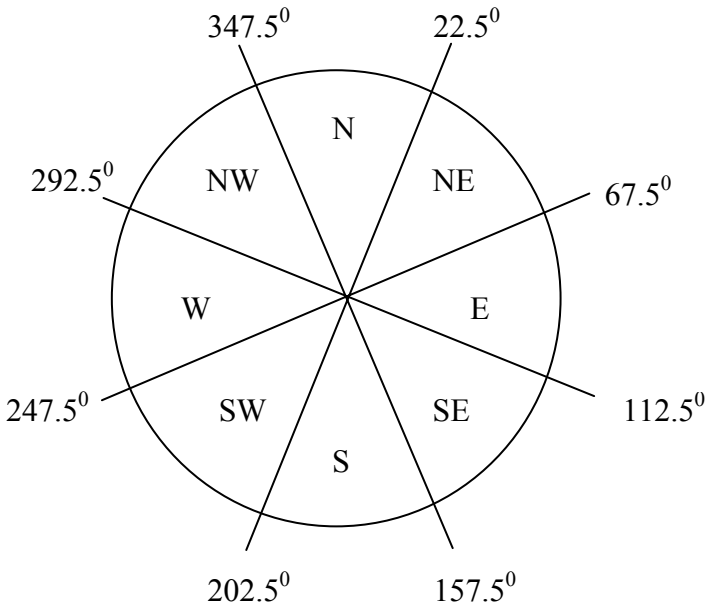

FIGURE 89
WIND VANE METROLOGICAL DIRECTIONS

As all values are now able to be recorded the readings can be analysed to produce results of the generator performance.

10.3 Results

The readings from the data recordings on the data logger were first transferred into Microsoft Excel so that the recorded values could be translated into meaningful results. Only after the readings have been transferred can the results be analysed.

Channel number	2	3	6	7				
Sensor code	VLT	VLT	VLT	VLT				
Label	I Gen	I Load	V Bat	Gen	**I Gen (A)**	**I Load (A)**	**V Bat (V)**	**V Gen (V)**
Unit	mV	mV	mV	mV				
01/03/2003 00:00	1.175	0.004	1600	1671.2	**0.47**	**0.002**	**12.16**	**12.7**
01/03/2003 00:01	0.141	0.004	1585.7	1454.6	**0.056**	**0.002**	**12.05**	**11.05**
01/03/2003 00:02	0.076	0.004	1581.1	1426.4	**0.03**	**0.002**	**12.02**	**10.84**
01/03/2003 00:03	0.079	0.004	1578.5	1391.6	**0.032**	**0.002**	**12**	**10.58**
01/03/2003 00:04	0.194	0.004	1578.5	1527.8	**0.078**	**0.002**	**12**	**11.61**
01/03/2003 00:05	0.472	0.004	1581.1	1576.4	**0.189**	**0.002**	**12.02**	**11.98**
01/03/2003 00:06	0.327	0.004	1582.1	1567.7	**0.131**	**0.002**	**12.02**	**11.91**
01/03/2003 00:07	0.403	0.004	1580	1653.2	**0.161**	**0.002**	**12.01**	**12.56**
01/03/2003 00:08	1.309	0.003	1588.7	1681.9	**0.524**	**0.001**	**12.07**	**12.78**
01/03/2003 00:09	0.725	0.004	1590.8	1660.4	**0.29**	**0.002**	**12.09**	**12.62**
01/03/2003 00:10	0.235	0.004	1581.1	1617.4	**0.094**	**0.002**	**12.02**	**12.29**

FIGURE 90
DATA LOGGER VALUES - TURBINE VARIABLES

Figure 90 shows a small portion of a spreadsheet with data recorded on 01 March 2003 where the recorded values on each channel are converted into actual real values of current and voltage. Figure 91 shows where the anemometer and windvane recorded values are converted into speeds and directions.

Channel number	8	9								
Sensor code	VLT	VLT								
Label	W Speed	W Dir	**V supply (V)**	**V read (V)**	**Resistance (ohms)**	**Angle (deg)**	**Direction (N,E,S,W)**		**W Speed (Knots)**	**W Speed (m/s)**
Unit	mV	mV								
01/03/2003 00:00	105.86	1106.9	**12.16**	**1.1069**	**691.8125**	**247.429**	**SW**	**225**	**6.35033**	**3.266892**
01/03/2003 00:01	62.34	1090	**12.05132**	**1.09**	**687.39358**	**245.849**	**SW**	**225**	**3.739652**	**1.923843**
01/03/2003 00:02	56.13	987.1	**12.01636**	**0.9871**	**624.312188**	**223.288**	**SW**	**225**	**3.367127**	**1.732199**
01/03/2003 00:03	63.17	1026.6	**11.9966**	**1.0266**	**650.36427**	**232.605**	**SW**	**225**	**3.789442**	**1.949457**
01/03/2003 00:04	60.86	1038.8	**11.9966**	**1.0388**	**658.093126**	**235.37**	**SW**	**225**	**3.65087**	**1.87817**
01/03/2003 00:05	68.1	1042.4	**12.01636**	**1.0424**	**659.287838**	**235.797**	**SW**	**225**	**4.085183**	**2.101599**
01/03/2003 00:06	69.25	1013.8	**12.02396**	**1.0138**	**640.793882**	**229.182**	**SW**	**225**	**4.154169**	**2.137089**
01/03/2003 00:07	87.36	1103.9	**12.008**	**1.1039**	**698.670886**	**249.882**	**W**	**270**	**5.240552**	**2.695973**
01/03/2003 00:08	92.35	1017.3	**12.07412**	**1.0173**	**640.334865**	**229.018**	**SW**	**225**	**5.539892**	**2.849966**
01/03/2003 00:09	98.62	1078.3	**12.09008**	**1.0783**	**677.835052**	**242.43**	**SW**	**225**	**5.916017**	**3.043462**
01/03/2003 00:10	73.47	1030.7	**12.01636**	**1.0307**	**651.887926**	**233.15**	**SW**	**225**	**4.407319**	**2.26732**

FIGURE 91
DATA LOGGER VALUES - WIND VARIABLES

The calculations performed by Excel are the same as those detailed in section 10.2 and the results can be used to model the performance of the turbine.

The results can be used to see how closely the performance of the turbine matches the manufacturers data. Figure 92 shows the performance curve of the Marlec generator at various windspeeds when charging a 12V battery, since this is what is effectively being done here the plots can be compared against each other.

The first stage was to note values from the manufacturers curve and plot a representation in Excel to provide an equation to represent the curve. The equation that was found to represent the curve is shown in equation 85.

$$I = 0.0077w^2 + 0.2001w - 1.0984$$
$$\left(R^2 = 0.999\right)$$

EQUATION 85

where I = current (A)
w = wind speed (knots)

Using equation 86 in conjunction with the recorded values of windspeed the validity of the manufacturers performance data can be analysed.

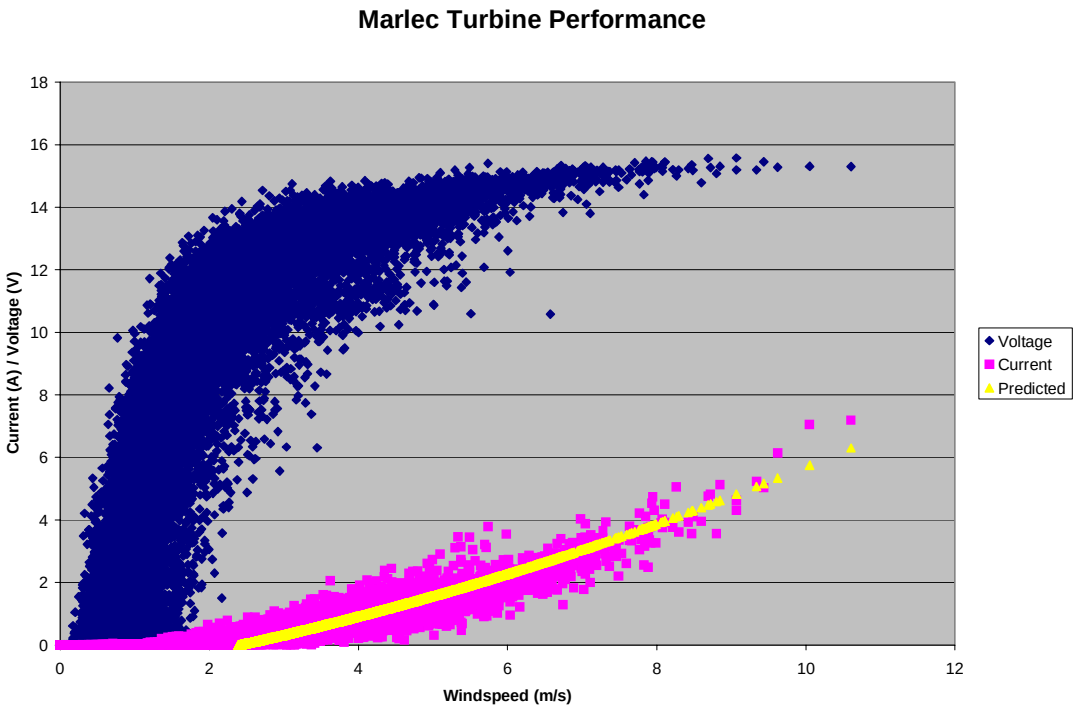

FIGURE 92
MARLEC PERFORMANCE VALIDITY

Figure 92 shows the performance of the Marlec turbine under test conditions. The yellow line represents the predicted current output using equation 85, the pink scatter represents the current output recorded by the logger and the blue scatter represents the voltage across the coils of the turbine. (Note: equation 85 uses knots as the unit for wind speed but the graph has plotted in m/s.)

The curve of both the yellow and pink plots follow near enough the same path and so allowing for discrepancies in recorded data due to turbulent wind in an urban environment and gusts altering the current output it can be said that the performance curve provided by the manufacturer provides a reasonably accurate measure of performance of the machine.

Figure 82 shows that the turbine is not expected to provide any generating current for a 12V battery until approximately 6knots (this can be seen in figure 92 also where the yellow curve starts at approximately 3m/s.) This can be accounted for in figure 92 where the voltage across the coils of the turbine does not reach 12V until approximately 3m/s (again allowing for discrepancies). So the turbine cannot force any charging current into the battery before the coils has reached the appropriate potential difference and it does not achieve this until it has reached the appropriate speed of rotation, which equates to approximately 3m/s.

In order to characterise the turbine further the characteristics of Tip Speed Ratio (TSR) and Coefficient of Performance (Cp) are required. The TSR is found using equation 7 and the Cp is found from equation 5 or by rearranging equation 6.

The results in figure 92 show that the performance data provided by the manufacturer can be taken to be accurate and so is used to show current output versus wind speed. Results from section 9 also provide current outputs at different rotational speeds. If both these values are plotted with current on the x-axis it is possible to read the corresponding wind speeds and rotational speeds. If both these are known it is then possible to use equation 7 to calculate the corresponding Tip Speed Ratio.

As the wind speed and current output are known and the turbine is used to charge a 12V battery the output power from the turbine can be found. Using this data and rearranging equation 6 the Coefficient of Performance can be found.

Figure 93 shows the spreadsheet used to perform these calculations and shows average values for the TSR and Cp.

The calculated values of the TSR range from 5.05 to 2.92 with the average value measured being 3.47. These values are consistent with a small multi-bladed turbine. The Cp values peak at 0.41 and range down to 0.15 with an average value of 0.27. The values all appear to be in an acceptable range.

[R] Blade Radius (m)	**0.455**
[A] Swept Area (m^2)	**0.65**
[ρ] Air Density (kg/m^3)	**1.225**

$$\lambda = \frac{\Omega R}{V}$$

$$P = C_p \frac{1}{2} \rho A V^3$$

$$\therefore C_p = \frac{2P}{\rho A V^3}$$

Marlec		Generator Bench Test												
Wind Speed (m/s)	Current (A)	Rotational Speed (RPM)	Rotational Speed (rad/s)	Current (A)	Current (A)	Wind Speed (Knots)	[V] Wind Speed (m/s)	[Ω] Rotational Speed (rad/s)	[λ] Tip Speed Ratio	Battery Voltage (V)	Power (W)	Cp
5	0	99.52	10.42	0	0.2	5.95	3.06	34	5.05	12.00	2.40	0.21
7.5	1	198.08	20.74	0	0.4	6.49	3.34	36	4.91	12.00	4.80	0.32
10	1.5	299.52	31.37	0	0.6	7.02	3.61	38	4.79	12.00	7.20	0.38
12.5	2.7	397.12	41.59	1.19	0.8	7.55	3.88	39	4.57	12.00	9.60	0.41
15	3.8	498.56	52.21	3.51	1.0	8.07	4.15	40.5	4.44	12.00	12.00	0.42
17.5	4.7	598.08	62.63	5.74	1.2	8.59	4.42	41.7	4.29	12.00	14.40	0.42
20	6	697.12	73.00	7.09	1.4	9.11	4.69	43	4.18	12.00	16.80	0.41
22.5	7.2				1.6	9.62	4.95	44	4.05	12.00	19.20	0.40
25	8.7				1.8	10.13	5.21	44.8	3.91	12.00	21.60	0.38
27.5	10				2.0	10.63	5.47	45.7	3.80	12.00	24.00	0.37
30	12				2.2	11.13	5.73	46.5	3.69	12.00	26.40	0.35
32.5	13.5				2.4	11.63	5.98	47.4	3.61	12.00	28.80	0.34
35	15.7				2.6	12.12	6.23	48.2	3.52	12.00	31.20	0.32
37.5	17				2.8	12.61	6.49	49	3.44	12.00	33.60	0.31
					3.0	13.09	6.73	50	3.38	12.00	36.00	0.30
					3.2	13.57	6.98	50.9	3.32	12.00	38.40	0.28
					3.4	14.05	7.23	51.9	3.27	12.00	40.80	0.27
					3.6	14.52	7.47	52.7	3.21	12.00	43.20	0.26
					3.8	14.98	7.71	53.5	3.16	12.00	45.60	0.25
					4.0	15.45	7.95	53.4	3.06	12.00	48.00	0.24
					4.2	15.91	8.18	55.2	3.07	12.00	50.40	0.23
					4.4	16.36	8.42	56.2	3.04	12.00	52.80	0.22
					4.6	16.81	8.65	57	3.00	12.00	55.20	0.21
					4.8	17.26	8.88	58	2.97	12.00	57.60	0.21
					5.0	17.70	9.11	59	2.95	12.00	60.00	0.20
					5.2	18.14	9.33	60	2.93	12.00	62.40	0.19
					5.4	18.57	9.55	61	2.90	12.00	64.80	0.19
					5.6	19.00	9.78	62	2.89	12.00	67.20	0.18
					5.8	19.43	10.00	63	2.87	12.00	69.60	0.18
					6.0	19.85	10.21	64.2	2.86	12.00	72.00	0.17
					6.2	20.27	10.43	65.8	2.87	12.00	74.40	0.16
					6.4	20.68	10.64	67.1	2.87	12.00	76.80	0.16
					6.6	21.09	10.85	69	2.89	12.00	79.20	0.16
					6.8	21.50	11.06	70.8	2.91	12.00	81.60	0.15
					7.0	21.90	11.27	72.2	2.92	12.00	84.00	0.15
					Average λ				3.47	Average Cp		0.27

FIGURE 93
MARLEC TSR AND CP CALCULATIONS

Figure 26 showed that the values of TSR and Cp are often plotted against each other and provide different plots depending upon the style of turbine used. Figure 94 shows the plot for the results in figure 93.

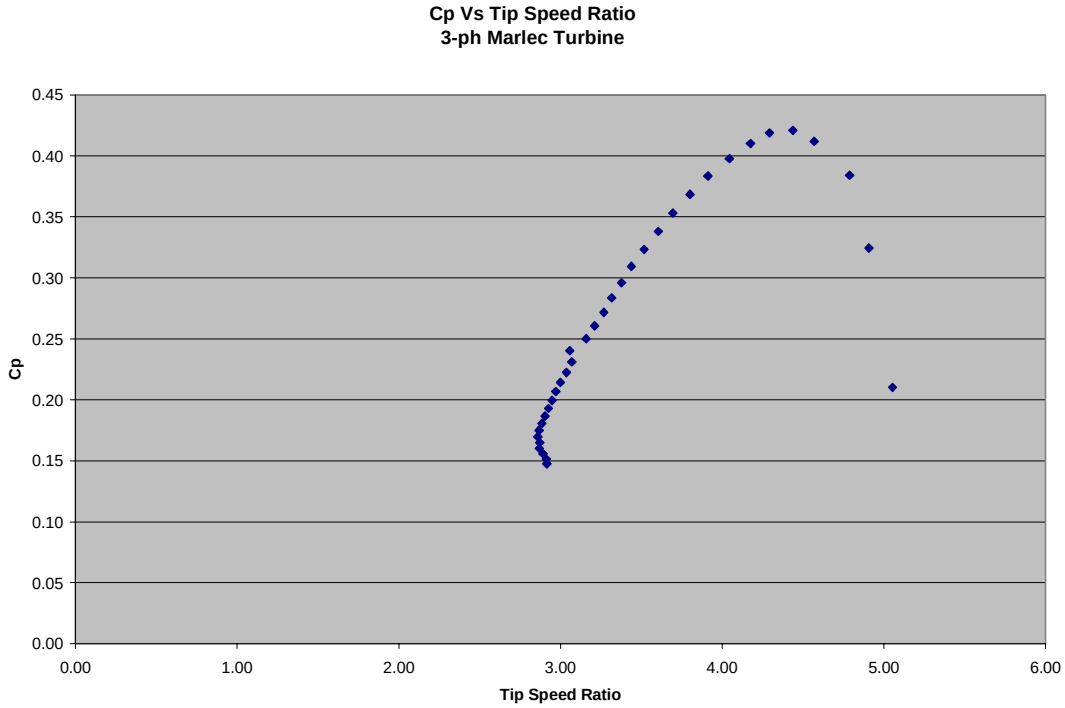

FIGURE 94
MARLEC CP VS TSR CHART

The plot shows that the correct relationship does exist between the resultant values of Cp and TSR. The plot is consistent in size and shape to those already existing in figure 26 and so the results can be taken as correct and represent the characterisation of the turbine including results in figure 92.

All data recorded is available on CD where the unprocessed data files are available, subsequent Excel files are available and data has been sorted into monthly charts. Met Office information on wind speed and direction are added to a spreadsheet to enable comparisons between recorded values and the Met Office values. The results showed that the Met Office values of wind speed were consistently higher than the locally recorded ones, this is as expected as the Met Office recording location is in an open rural environment and the local recordings were in an urbanised area. The recorded wind directions were the same a large percentage of the time and the most predominant directions recorded were South and Westerly winds, typical for the west of Scotland.

11.0 Discussion

The work carried out over the duration of the project was to investigate the Ducted Wind Turbine Devices and progress the development towards a commercial product. This report details the theory behind conventional wind turbine devices and then develops in the more specialist theory of the DWT, which indicates performance may be available that is an improvement on the Betz limit of conventional turbines.

The energy produced from any DWT will be part of an embedded generation system and the options available for embedded generation have been detailed and discussed with the option of a grid interfaced system, shown in figure 37, having been decided as the best option to utilise in the development of the product. At this moment the only viable option for storage of the generated power is to use batteries and the theory of lead acid batteries has been shown to allow any installation to get the maximum performance from the batteries.

A major part of the project was the characterisation of the available generators to help produce the most efficient turbine for the Ducted Turbines. The results from section 9.1.4.1 gave a consistent value of the theoretical value of $k\phi$ from which the average was utilised as the value of $k\phi$ for the DC motor. As the values were consistent over a range of testing the value was assumed to be correct and therefore suitable to be utilised with the recorded values of armature current (I_A) when characterising the generators.

The use of the dynamometer enabled specific loads to be placed upon the DC motor and record the operating characteristics. The results were then plotted using Microsoft Excel and equations relating armature current to motor efficiency were derived. The equations have inaccuracies because of the nature of a ‘best fit’ curve that Excel provides, however the data was best represented by a polynomial expression but as explained in section 9.1.4.2 the efficiency would not drop off as in a polynomial curve but rather stay at a constant value until the motor began to stall. The data recorded in this testing was then combined with the calculated $k\phi$ value to allow the theoretical method to be utilised. The results showed that the values of

torque recorded for each method differed greatly at low values of armature current but were almost identical at higher values. The reason for the difference at the low values is due to inefficiencies and internal resistance of the motor. These values will be small but make a greater impact on the results at low values of armature current, as they will represent a greater percentage of the loading on the motor.

The testing of the DC Motor provided two sets of results that could be utilised in the complete characterising of the generators.

The testing of the generators provided characteristics that were expected from each generator. The most effective resistive load to power was 3.3Ω load, which was the lowest value of resistance available. Out of all the generators the Chinese supplied the most power, as expected since it was the highest rated but they all exhibited similar operating characteristics. This is since they are all constructed using the same theory of permanent magnet fields. Even though the Chinese generator is a radial field and the Marlec generators are axial field, the same basic construction and principles apply. Although the Chinese generator has the greatest rating, it may not have been the most efficient. However the 3-phase Marlec was expected to be more efficient than the single-phase due to the inherent advantages of 3-phase operation.

The results obtained by combining the theory from both sets of testing showed that the equations obtained in section 9.1.4.2 were not accurate and had to be disregarded because they underestimated the efficiency of the DC motor, which gave rise to the efficiencies of the generators appearing greater than they actually are and even showed that the 3-phase Marlec was over 100% efficient, which is impossible. Knowing this, the theoretical method using the kϕ value was utilised. The results confirmed expectations of performance, and provided values to assign. For each generator the highest value of resistance required the lowest torque and the battery charging operation required the greatest input torque. The relationships between output current torque and apparent resistance of the battery enabled the drop in efficiency of the generators to be explained. When comparing the results of the three the Chinese generator was the most efficient with the 3-ph Marlec second and the 1-ph Marlec least efficient, as expected. The Chinese Generator however requires the largest amount of torque to rotate the shaft with the 1-ph Marlec requiring the least.

A comparison of performance shows that to rotate the Chinese generator at 400RPM requires 5.22 times the torque of the 1-ph Marlec but provides 7.18 times more current, and 3 times the torque of the 3-ph Marlec but provides 3.4 times more current.

An external test rig was fabricated to allow the performance of the 3-ph Marlec generator to be monitored in 'real life' conditions. This required the design and construction of a control system. A suitable control system was produced and utilised in the test rig. The system was extensively tested inside laboratory conditions and in an external rig, where it was found to work effectively.

The test rig also provided the results for the 3-ph Marlec performance which showed that the manufacturers performance characteristics were accurate. The calculated relationship between the Tip Speed Ratio and the Coefficient of Performance was found to be consistent with that of other turbines and hence deemed to be correct.

12.0 Future Work

In order for the development of the Ducted Wind Turbine to progress, further work in addition to the work contained within in this report will have to be carried out. Some suggestions and ideas for the further development work required will now be mentioned and discussed.

In order to fully utilise the results from the testing of the generators in section 9, a full set of characteristics will have to be found for a range of available rotor configurations. The testing here will want to characterise rotors utilising different numbers of blades on the hub and different pitch angles within a controlled wind tunnel testing arrangement. The results here will be able to be combined with the generator characteristics to produce the most efficient combination of generator and blades. A design for a simple tapered test tunnel has been produced and is available in AutoCAD 2004 and PDF format on CD.

A new shape for the DWT has been discussed and it is believed that this will provide better performance characteristics than that of the existing model. The new design is a simple cylinder with the turbine in the centre, rather than the contoured inlet of the current design. The device will still be located at the roof edge but angled to intercept the wind. Fabrication of a prototype will be required with investigation into the size of the device and the optimal angle to intercept the most wind. This testing will provide results than can be analysed to verify if the new design is an improvement, provide the optimal angle of inclination and see the best location in the cylinder for the turbine. Figure 95 shows a basic drawing of the new design with the turbine located in the middle of the cylinder.

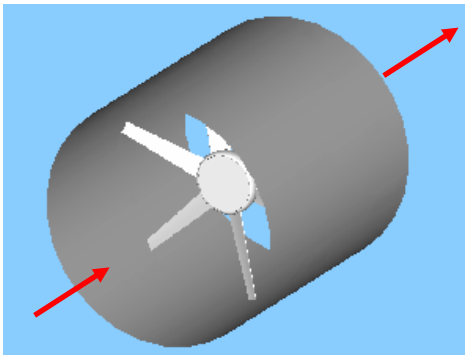

FIGURE 95
PROTOTYPE DWT DESIGN

13.0 Conclusion

The aim of this report was to investigate and progress the design and production of a novel building integrated Ducted Wind Turbine module (DWT) towards a commercial product.

The design and theory of the devices has been investigated with different options presented for the way the generated energy can be utilised. The control system is a major progression as it is an essential component in any installation of the devices and exists with reproduction possible for further testing. The results from the generator testing provided a set of performance characteristics to be utilised when designing the final device. Although the Chinese generator is the most efficient at converting energy, it may not be the most suitable generator for the ducted turbine. The large torques required to rotate the generator may be outwith the range of torques that the blade configurations can provide. No decision on the correct generator to use can be made until there is an understanding of the available turbine rotors and their characteristics. Only once these are known can the two components be effectively matched together.

The project can be deemed to be successful as it has achieved in its aim of aiding the progression of the Ducted Wind Turbine towards a commercial product. With the detailed theory, the generator characteristics, the control circuit and the ideas for future work detailed within, the project should provide invaluable information to whoever is next employed in the development stage of the devices.

14.0 References

[1] http://www.cogreenpower.org

[2] http://www.oldenbrau.com

[3] http://www.ssec.wisc.edu

[4] http://geology.csupomana.edu

[5] http://www.usatoday.com/weather

[6] http://www.sciencenorth.om.ca

[7] http://www.windspeed.co.uk

[8] http://www.hemmworkshops.com

[9] http://www.bwea.com

[10] http://www.fluid.mech.ntua.gr/wind/G/genuvp.html

[11] http://www.eere.energy.gov

[12] University of Strathclyde – Fluid Mechanics course notes

[13] http://www.dkonline.co.uk

[14] http://www.grahics.cornell.edu

[15] http://www.esru.strath.ac.uk

[16] http://www.hepi.com/basics/ph.htm

[17] http://hyperphysics.phy-astr.gsu.edu/hbase/hframe.html

[18] http://www.tokyometer.co.jp

[19] Windpower Workshop – Hugh Piggott

[20] http://www.marlec.co.uk

[21] http://www.rswww.com

15.0 Bibliography

Wind energy explained: theory design and application
J.F. Manwell, J.G. McGowan, A.L. Rogers
Wiley, 2002

Wind energy: handbook
Tony Burton
Wiley, 2001

Wind energy conversion systems
L.L. Freris
Prentice Hall, 1990

Wind energy
Tom Kovarik, Charles Pipher, John Hurst
Domus Books, 1979

Embedded generation
Nick Jenkins
Institution of Electrical Engineers, 2000

Power electronics
C.W. Lander
McGraw Hill, 1993

Small scale wind power
D. McGuigan
Prism press, 1978

Windpower Workshop
Hugh Pigott
Centre for Alternative Technology Publications, 1997

Websites

www.windpower.org
www.windsun.com
www.bp.com/centres/energy/index.asp
www.tpub.com
www.eere.energy.gov
www.metoffice.gov.uk
www.ofgem.gov.uk
www.windstuffnow.com
www.energy.iastate.edu
www.awea.com